uOttawa

L'Université canadienne
Canada's university

**FACULTÉ DES ÉTUDES SUPÉRIEURES ET POSTOCTORALES**

uOttawa

L'Université canadienne
Canada's university

**FACULTY OF GRADUATE AND POSDOCTORAL STUDIES**

Danya Alhyari
AUTEUR DE LA THÈSE / AUTHOR OF THESIS

M.Sc. (Cellular and Molecular Medicine)
GRADE / DEGREE

Department of Cellular and Molecular Medicine
FACULTÉ, ÉCOLE, DÉPARTEMENT / FACULTY, SCHOOL, DEPARTMENT

*DSLMAP* is a Component of the Developing Heart Tube and may Interact with *Slit/Robo* pathway in *Drosophila*

TITRE DE LA THÈSE / TITLE OF THESIS

Balwant Tuana
DIRECTEUR (DIRECTRICE) DE LA THÈSE / THESIS SUPERVISOR

CO-DIRECTEUR (CO-DIRECTRICE) DE LA THÈSE / THESIS CO-SUPERVISOR

Antonia Colavita

Marc Ekkee

Gary W. Slater
Le Doyen de la Faculté des études supérieures et postdoctorales / Dean of the Faculty of Graduate and Postdoctoral Studies

# *DSLMAP* is a component of the developing heart tube and may interact with *Slit/Robo* pathway in *Drosophila*

By
**Danya H. Alhyari**

Department of Cellular and Molecular Medicine
Faculty of Medicine
University of Ottawa
Ottawa, Ontario,Canada
January 19,2010

**This thesis is submitted as a partial fulfilment of the M.Sc.degree program in the**

**Department of Cellular and Molecular Medicine**

*Your file Votre référence*
*ISBN:* 978-0-494-73830-6
*Our file Notre référence*
*ISBN:* 978-0-494-73830-6

# ACKNOWLEDGMENTS

It is a pleasure to acknowledge my supervisor Dr. Balwant Tuana for his continuous support, and help during this project, and my co-supervisor Dr. Margaret Sonnenfeld who has given me constant advice, I owe a dept of gratitude to Momena Dawood for her helpful advices and her continuous support which made a difference in this project.

I would like also to thanks my colleagues; Helina Tadesse, Jennifer Rugers, Mysoon Salih , Puneet Singh, Moni Nader, Tatiana Morozova, Omar hawari for their continous support during my graduated studies.

I want to thank University of Petra Amman-Jordan, for giving me a scholarship to finish my Master degree.

Finally, I would like to thank my parents, for their continuous support, encouragement, and prayers through my academic research, Special thanks to my husband Moath who helped me and supported me through my graduated studies, and my two sons, Sa'ad and Abdualrahman who always put a smile on my face. Special thanks to all my brothers and sisters for their continuous support.

# ABSTRACT

The *Drosophila* heart is composed of cardioblasts (CBs) and pericardial cells. Together, these cells form a linear heart tube that resembles the early vertebrate heart. Many genes involved in heart development are conserved from fruit flies to mammals. For example, the *Drosophila* homeobox gene Tinman and its vertebrate homologue Nkx2.5 are both critical for heart development. The secreted protein Slit and its receptor Roundabout (Robo) contribute to heart tube formation by guiding cardioblast alignment and adhesion. Slit null mutant showed severe alignment and migration defects, which include delays, gaps in the heart tube, and failure of lumen formation. Robo loss of function mutant also had severe defects which include, twisted heart tube, missing parts of the heart tube, and aggregation of the CBs. The Slit/Robo complex appears to serve conserved roles across species and in different systems by influencing cell guidance and migration. Previous studies have shown that sarcolemmal membrane associated protein (SLMAP) is expressed early during mammalian cardiac development and it may play role in cardiac function at the level of membrane biology and signal transduction. *SLMAP* and its homolog in *Drosophila DSLMAP* have similar structural features which include, a C-terminus transmembrane domain, a coiled-coil region, and a fork head associated domain at the N-terminus. *DSLMAP* and its mammalian homologue share 28.6% identity over 721 amino acid residues; a higher percentage identity was noted in the forkhead-associated domain (55.9%). Further more, *DSLMAP* were found to genetically interact with Slit/Robo pathway in the developing nervous system. Here, we show that *DSLMAP* is expressed in both the CBs and the pericardial cells at early stages of *Drosophila* heart development. Alterations in *DSLMAP* expression in the CBs, and the pericardial cells,

using a UAS-*DSLMAP*-RNAi transgene causes a delay in migration of CBs and PCs, and misalignment of the cardiac cells. The up-regulation of *DSLMAP* in the CBs and the pericardial cells led to delay in migration of the cardiac cells, and to CBs aggregation. Down-regulation of DSLMAP has similar phenotypes to *Robo* down-regulation in both the CBs and the pericardial cells. In addition, over-expression of DSLMAP or

Slit have the same phenotypes in the two cell types. Delayed migration defects are reduced by pericardial expression of UAS-*DSLMAP* RNAi in Robo down-regulated embryos. Myocardial expression of UAS-DSLMAP transgene suppresses the delayed migration defects seen in Slit over-expression. DSLMAP over-expression in the CBs significantly reduced the phenotypes seen in $slit^2$ loss of function mutant. Over-expression of DSLMAP in the CBs of $robo^{189}$ heterozygous background showed a significant reduction in the phenotypes observed in $robo^{189}$ alone. DSLMAP down-regulation in the pericardial cells of $slit^2$ heterozygous background, or $robo^{189}$ heterozygous background led to a significant decrease in defective embryos and the heart tube was seem to be properly organised. The data suggests that *DSLMAP* is expressed early in cells that form the *Drosophila* heart, and its regulated levels are critical for normal heart tube formation. Data also suggests that DSLMAP may genetically interact with the Slit/Robo pathway to ensure proper heart tube formation.

# Table of contents

# LIST OF FIGURES

# LIST OF TABLES

# LIST OF ABBREVIATIONS

| | |
|---|---|
| BMP | Bone morphogentic protein |
| CBs | Cardioblasts |
| CNS | Central nervous system |
| Dpp | Decapentaplgic |
| *DSLMAP* | *Drosophila* sarcolemmal membrane associated protein |
| E-C | Excitation-Contraction |
| FGF | Fibroblast growth factor |
| FHA | Forkhead associated domain |
| IR | Inverted repeats |
| M1 | 1$^{st}$ initiating methionine |
| M2 | 2$^{nd}$ initiating methionine |
| PUAST | Upstream activating sequence transformation vector |
| pWIZ | white intron zipper motif |
| PCs | pericardial cells |
| Robo | Roundabout |
| RNAi | RNA interference |
| SLMAP | Sarcolemmal membrane associated protein |
| TMD | Trans membrane domain |
| UAS | Upstream activating sequence |
| Wt | Wild type |

# Introduction

## 1.1. *Drosophila* as a model organism

*Drosophila* (fruit fly) is one of the most widely studied model organisms in developmental biology. It has been used for more than a century now, for genetic studies; because it is easy to handle, low in cost, and has a very short life cycle (Fig.1) (Tompkins, 1994; Flannery, 1997). The fruit fly has evolved to being an excellent tool for genetic studies, and has provided a wealth of information regarding cell fate and organogenesis. The *Drosophila* genome has been sequenced resulting in the identification of over 13,000 genes and providing a very useful source for developmental biologists: http://www.pitt.edu /~biohome/Dept/Frame/drosophila.htm.

The functions of many *Drosophila* genes have been recognized, due to the ease of creating mutants and performing gain or loss of function experiments. Although *Drosophila* has fewer genes than humans, *Drosophila* genes and human genes have a very close relationship, since the sequence of many recently discovered genes can usually be matched against their *Drosophila* counterparts. Among these genes, it is the disease causing genes that are of most interest. The studies of these relationships will help in discovering the function of analogous genes in humans - which may eventually help in the development of efficient drugs (http://genome.wellcome ac.uk/ doc_WTD020807.htm).

The *Drosophila* heart tube is similar to the early vertebrates' heart, and this similarity makes it a good model to study the early events in mammalian heart development. Recently, *Drosophila* has been used to study the genes that are involved in specifying heart formation and the genes that are implicated in cardiac function (Bier and

## Figure 1. Life cycle of the fruit flies

*Drosophila* starts it is life span as an embryo in an egg. The embryo stays in the egg for about one day. During this time, the embryo develops into a larva. The first instar larva hatches out of the egg, after a day, the first instar larva molts and becomes the second instar larva. After two days in this stage, the larva molts again to become the third instar larva. After three days the larva crawls out of the food source and molts again. Following this molt, the larva stops moving and forms a pupa. Drosophila stays in the pupa for about five days. During this time, the metamorphosis from larva to adult is occurring, and adult structures, like wings, legs, and eyes develop (adapted from http/:www.fly move .com)

# The life cycle of *Drosophila melanogaster*

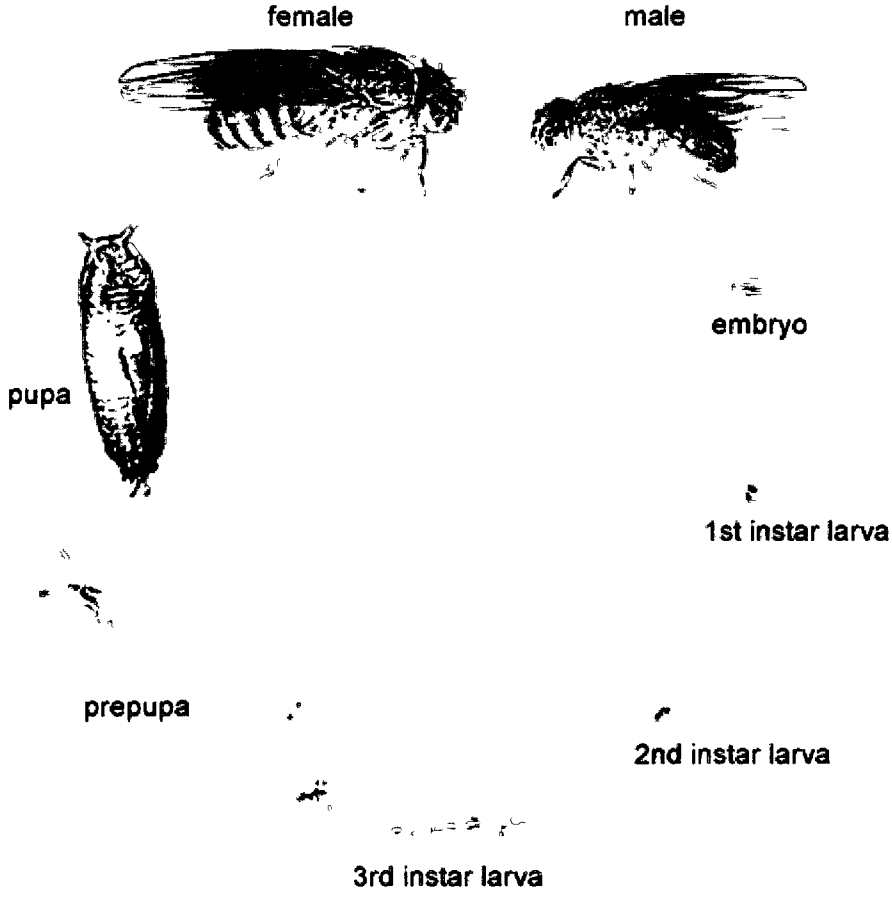

Bodmer, 2007). The data strongly supports the view that genetic programming in heart formation and function in *Drosophila* is highly conserved across species, and that further studies defining functional roles for genes would have direct relevance across species.

## 1.2. Heart development in *Drosophila* and vertebrates

The Drosophila circulatory system - which is similar to all other insects - consists of a dorsomedial muscular tube called the heart or the dorsal vessel (Wigglesworth, 1984; Cripps and Olson, 2002). This simple linear heart tube shares distinguished similarities with the more complicated vertebrate heart at early stage of heart development (Bodmer and Venkatesh, 1998). Heart cells in both are derived from cardiac precursor cells that originate from the dorsal mesoderm. Heart cells in both systems assemble in two rows of cells forming a heart tube; the only difference that these cells are merged at the dorsal midline in *Drosophila*, while in the vertebrates they are merged at the ventral midline. There is a clear change in terms of the reversal of the dorsal-ventral axis between vertebrates and invertebrates (Bodmer and Frasch, 1999).

Dorsal mesoderm is specified through genetically regulated networks and signalling pathways that are conserved from fruit flies to vertebrates (Ocorr *et al.,* 2007). The *Drosophila* heart consists of two types of cells: the inner cardioblasts (CBs) that have contractile muscle property that pumps the hemolymph in an open circulatory system and the outer pericardial cells (PCs) that flank the CBs on each side (Bodmer and Venkatesh, 1998; Bodmer and Frasch, 1999). The latter may have a role in filtering and detoxifying the hemolymph of the fly (Miller, 1950) (Fig 2, 3). The two cells are connected to one another by adherence junctions, and they align in two rows that fuse at the dorsal midline forming a heart tube where the hemolymph flows from posterior to anterior.

**Figure 2. Morphogenesis of the heart tube at different stages.**

The dorsal vessel is derived from the ventral mesoderm layer (yellow color) which is developed at stage 5. By stage 9 this layer will spread laterally to form a dorsal mesoderm (yellow). At stage 11, precursor cells are being specified which in turn are differentiated to cardioblasts at stage 12 (red), at stage 13-14 the cardioblasts will be aligned in two rows of cells, which will migrate dorsally, and form a complete heart tube by stage 17. Adapted from (Cripps and Olson, 2002; Sorrentino, Gajewski and Schulz, 2005; Tao and Schulz, 2007).

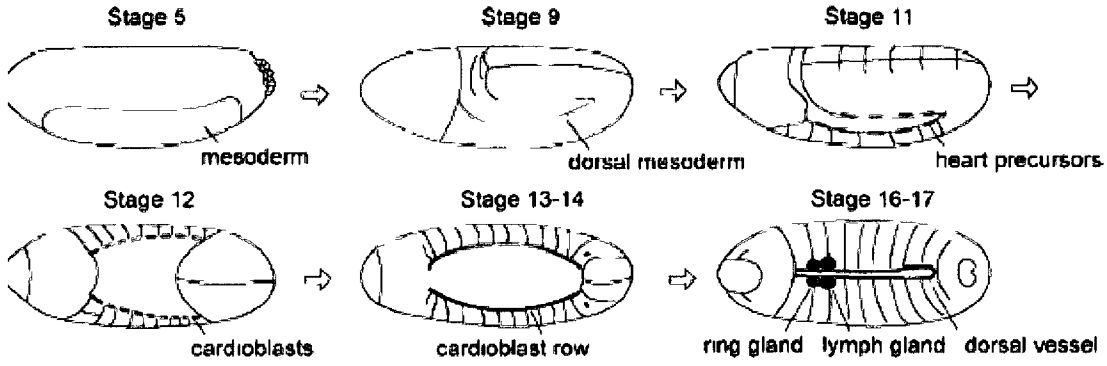
Stage 5
Stage 9
Stage 11
mesoderm
dorsal mesoderm
heart precursors
Stage 12
Stage 13-14
Stage 16-17
cardioblasts
cardioblast row
ring gland
lymph gland
dorsal vessel

This process the same as blood flow in a vertebrate's heart (Rugendorff, 1994; Bodmer and Venkatesh, 1998). Each row of the heart tube is composed of 52 CBs surrounded by 22 PCs (Bodmer and Frasch, 1999; Miller, 1950). *Drosophila* heart has anterior/posterior polarity, which leads to morphological variety along the length of the heart tube. The anterior part is called the aorta, while the posterior part is called the heart. The aorta and the heart are separated by the cardiovascular valve, which is composed of a pair of cells (Rizki, 1978; Molina and Cripps, 2001; Tao and Schulz, 2007).The hemolymph enters the circulation through the ostia, which is located in the heart, during the embryonic and larval stages (Rizki, 1978; Molina and Cripps, 2001).

*Drosophila* heart is composed of 11 segments. The heart cells extend along these segments from the second larval thoracic segment T2 to the eighth abdominal segment A8 (Fig. 3) (Bodmer and Frasch, 1999; Tao and Schulz, 2007). Most of the segments are composed of six pairs of cardiac cells. Two of them have smaller nuclei than the other, and express the receptor gene *seven-up* (Bodmer and Frasch, 1999); while the other four express the homeobox gene *Tinman* (Bodmer, 1993; Azpiazu and Frasch, 1993). In addition, two of these cells also express another homeobox gene (*ladybird).* One expresses *ladybird-early*, and the other expresses *ladybird-late* (Fig. 2) (Jagla *et al., 1997*). Less PCs are seen in the anterior segments, but there is a cluster of cells expressing PC markers called the lymph gland (Rizki, 1978; Lanot *et al.,* 2001) and another rounded structure called the ring gland - which is an endocrine organ (Fig. 3) (Rugendorff, 1994). The similarities between *Drosophila* and vertebrate hearts are limited to the early stages of heart development in vertebrates, when a linear heart tube is formed.

## Figure 3. *Drosophila* heart

*Drosophila* heart consists of 11 segments from T2 – A8; the anterior part is the aorta (a) the posterior part is the heart (h). The confocal microscopy shows the cells that compose the *Drosophila* heart; it has two types of cells: PCs (pc) and cardioblasts (cb). At the anterior front of PCs, there is the lymph gland (lg); and there is another rounded structure called the ring gland. The heart is surrounded by alary muscles (am). (Adapted from Tao and Schulz, 2007).

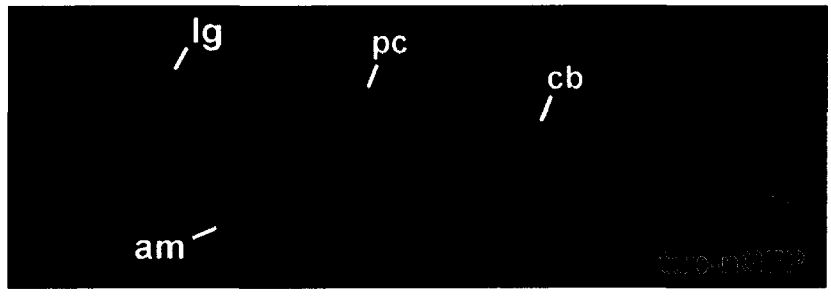


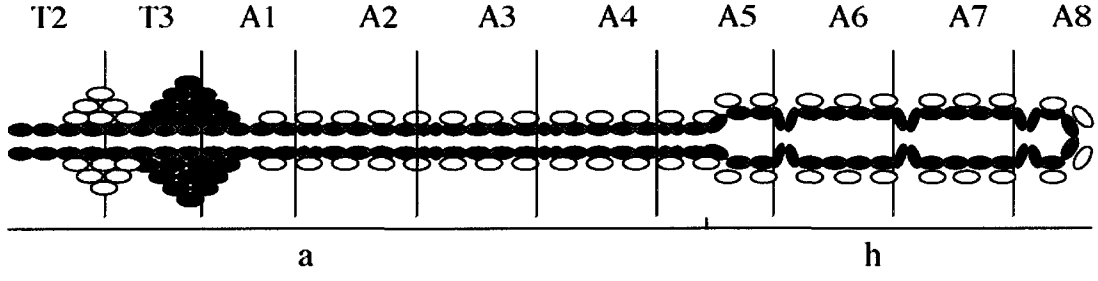


○ Ring gland cell ● Lymph gland cell ● Cardioblast ○ Pericardial cell

The embryonic vertebrate's heart starts developing from a flat disc called the heart field which is composed of thin layers of epithelial cells. Later on, the flat heart field will be converted into a linear heart tube that resembles the *Drosophila* heart (Fig. 4) (Zaffran and Frasch, 2002).

The principal question is: How is this flat heart field converted into a linear heart tube? Studies on zebrafish embryos showed that the left heart field acts differently from the right heart field. The right heart field cells form a kind of a leading edge and move as a group beneath the cells of the left heart field, by rolling beneath them. In this way, the right heart field will be rolling inward on its own axis. Accordingly, the right heart field will shape the ventral floor of the heart tube; while the left heart field will form the roof (http://www.sciencedaily.com/ releases /2008.02/080206153309.htm).

The vertebrates' heart develops in the same way as in *Drosophila.* The cells migrate dorsally, to form a bilateral row of cells forming the heart tube. Afterwards, the cells will merge anteriorly, to form the "cardiac crescent" (Cripps and Olson, 2002). The initiated heart tube is formed from two layers: the inner endocardial layer and the outer myocardial layer (Redkar *et al.*, 2001). This linear heart tube will then undergo a looping process to form a chambered heart. During this process, double outflow tract will be shaped, in addition to the left and right ventricles and sinus venosus (Anderson, *et al.*, 1978; Moorman *et al.*, 1994).

How does this linear heart tube then give rise to a multi chambered heart? Heart development of the zebrafish and its' vascular system shares a lot with the human heart (Shin, 2004). Two main genes are responsible for the formation of the atria ventricle (AV) valve in the chambered heart of the zebrafish: *foxn4* and *tbx2b*.

**Figure 4. Drosophila heart compared to vertebrate heart.**

(A) In *Drosophila,* the dorsal vessel is formed from two rows of cells that converge at the dorsal midline forming a linear tube (Semeriva *et al.*, 2002). Similarly in *zebrafish,* a linear heart tube is initially formed at the ventral midline from two rows of converging cells. This zebrafish heart begins as a simple vessel containing endocrinal cells in (green), CBs in (red), and epicardial cells in (blue). Epicardial cells are not found in *Drosophila.* The zebrafish heart resembles the dorsal vessel in fruit flies at this stage. (*B*) After expression of *foxn4*, which activates *tbx2b* expression, the endocardial cells move inward, forming the AV canal, and a valve; resulting in a conduction delay, that is required for setting up a unidirectional circulation. (*C*) Finally, the mature two-chambered heart with mature valves can circulate blood with high efficiency, in a closed system (Cohen and Morrisey, 2008).

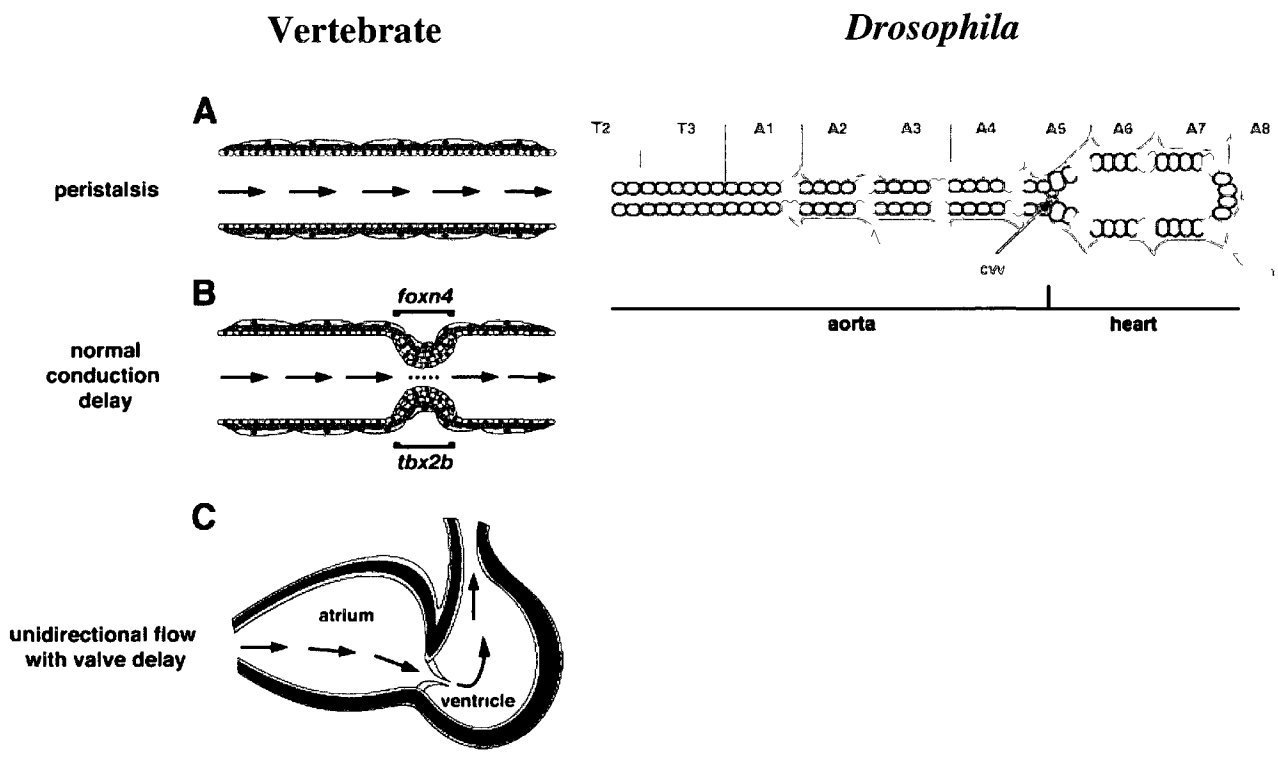
Vertebrate
Drosophila
A
peristalsis
B
foxn4
normal
conduction
delay
tbx2b
C
unidirectional flow
with valve delay
atrium
ventricle
T2
T3
A1
A2
A3
A4
A5
A6
A7
A8
CVV
aorta
heart

*Foxn4* is one member of the large FOX (Fork Head Box) family of transcription factors. *Foxn4* has a major role in the regulation of cell proliferation and specification during development. *Tbx2b* is a transcription factor member of the TBX2 family, and it has been shown to be required for the specification of the midline mesoderm (Cohen and Morrisey, 2008). *Tbx2b* is required for outflow tract, and AV canal development in the mouse (Harrelson *et al.*, 2004). Conserved binding sites for *foxn4* and *tbx5* - another member of T-box family - are present on the *tbx2b* promoter. When *foxn4* is expressed, it activates the expression of tbx2 at locus q122qdb. Endocardial cells then ingress inward, leading to the formation of the AV canal, which will divide the linear heart into chambers (Fig. 4) (Cohen and Morrissey, 2008). Different aspects are responsible for the formation of the heart tube in both *Drosophila* and vertebrates, including signalling pathways, transcription factors and regulating genes.

## 1.3. The signals required for heart tube development are conserved from *Drosophila* to the vertebrates

### 1.3.1 Decapentaplegic (DPP) and Bone Morphogenetic Proteins (BMPs) signaling

Cells of the dorsal mesoderm in *Drosophila* receive Dpp signalling in addition to other signals from the adjacent ectoderm where it is being secreted (Haag, 1999). Dpp is a member of the transforming growth factor-beta TGFβ superfamily. It is involved in many developmental processes, including the dorsal closure of the embryo, and the subdivision of the embryonic mesodermal layer (Affolter, 2001). Dpp activates the expression of the

*tinman* gene - which plays an important role in the heart and visceral mesoderm development - in the dorsal mesoderm (Yin and Frasch, 1998).

How does Dpp signalling activate *tinman*? There is a specific binding site located downstream from *tinman*, called smad. The activation of these sites through mad and medea effectors that are found in Dpp signalling lead to the activation of *tinman,* but this binding is not enough to drive the expression of *tinman.* Therefore *tinman* itself works together with smad, in order to express *tinman* in the dorsal mesoderm (Yin *et al.*, 1997; Xu *et al.*, 1998). Dpp signal is therefore very important for dorsal vessel morphogenesis. In *Drosophila* embryo lacking this signal, there is failure of both dorsal vessel formation, and progenitor cells (Frasch, 1995). A similar signal is found in the vertebrates' bone morphogenetic proteins (BMPs) which are considered the largest family of the TGFβ superfamily (Ashe, 2005).

There are more than six members of the BMPs being expressed in the heart, from early stages until late stages of development. BMPs are implicated in diverse biological processes including cell migration, differentiation, cellular proliferation, and play an important role in the formation of the anterior–posterior axis (Dale *et al.*, 1992; Shinsuk *et al.*, e 2009). Inhibitors of BMP signalling were used to prove its inductive activity in the heart. Some of these inhibitors were inhibitory SMAD6 and BMP inhibitor noggin (Schultheiss, 1997; Walters, 2001). These studies showed that BMPs were required for cardiogenic mesoderm differentiation, and were also found to be necessary for the maintenance of transcription factors *NKx2.5* (homologue of *tinman*) and *gata* transcription factor expression. Similar to Dpp and *tinman* the mouse *NKx2.5* is also regulated by activating sequences that include SMAD binding sites (Reiter, 2001;

Liberatore, 2002; Lien, 2002). Accordingly, Dpp and BMP are very important signalling mechanisms for the heart, since they are responsible for the activation of *tinman/NKx2.5.* As both of these genes are considered the corner stone in heart formation, without them there would be no heart formed.

### 1.3.2 Wnt/ wingless signaling

DPP or BMP signalling is not enough for cardiogenic mesoderm specification in both *Drosophila* and vertebrates. Another signal is required for cardiac cell specification and heart development, known as wingless (wg) signalling. It is expressed early in both the ectoderm and the mesoderm, and secreted from transverse stripes that are located in ectodermal cells. These stripes intersect with the dorsally located dpp expression domain Wg performs its action in two ways: either directly in the mesoderm or it passes from the ectoderm to the mesoderm, in order to activate the specification of cardiogenic mesoderm from the dorsal mesoderm.

In *Drosophila,* the wg loss-of-function embryos failed to form progenitors of the dorsal vessel; which indicates the importance of wg signalling in heart development (Lawrence1 *et al.*, 1995; Zaffran and Frasch, 2002; Tao and Schulz, 2007). Pangolin (Pan/dTCF/LEF-1) is a downstream transcriptional regulator of wg signalling (Park, 1996, 1998). When Pan is activated by wg, it affects three target genes. All of them are forkhead domain transcription factor genes, that are required for heart specification, known as *sloppy-paired-1* and *-2* (*slp-1* and *slp-2*), and *even-skipped* (*eve) (*Lee and Frasch, 2000; Halfon, 2000; Knirr and Frasch, 2001). *Slp* is considered a very important mediator of wg signalling, since loss of its activity will lead to a complete loss of cardiogenic precursors (Zaffran and Frasch, 2002). In the mesoderm, *slp* has two main activities: first is the

suppression of bagpipe (bap) which is an important transcription factor that is involved in subdividing the mesoderm and determining the fate of the cells in the dorsal mesoderm (Azpiazu and Frasch, 1993). Second, *slp* sustains the expression of wg in the ectoderm, which is essential for wg to perform its function in heart development (Jagla *et al.*, 1997). Several binding sites for Pan/TCF (Wingless effector) have been recognized in pericardial enhancer elements of even-skipped, which in addition to Tin and Smad maintain the expression of eve ( Halfon *et al.*, 2000; Knirr *et al.*, 2001).

On the other hand, vertebrate studies have shown that wnt signalling is involved in blocking cardiac development. In the frog embryo for example, over-expression of Wnt3a and Wnt8 prevents the expression of *Nkx2.5* and *Tbx5*, in addition to blocking cardiac differentiation. Similarly, in a chick embryo, when the mesoderm from the heart field was exposed to Wnt3a and Wnt-1, the expression of *Nkx2-5* and *Tbx5* was blocked. Wnt signalling has endogenous inhibitory factors: Crescent and Dkk-1 which can inhibit Wnt3a and Wnt-8, in addition to other Wnt ligands. (Marvin, 2001; Schneider and Mercola, 2001).

These different members of Wnt signalling, which act through β-catenin - its main transducer - have suppressing activity in heart development. In other words, cardiogenesis is inhibited by the canonical Wnt/β-catenin signalling (Marvin *et al.*, 2001; Schneider and Mercola, 2001). Other contrary studies have shown that Wnt signalling also has a positive effect, through the non-canonical Wnt11/JNK signalling - which induces cardiogenesis in later stages of development (Eisenberg and Eisenberg, 1999, 2006; Pandur *et al.*, 2002; Terami *et al.*,, 2004).

Consequently, this pathway has different functions throughout the different stages of heart development, through the activation of particular downstream effectors. In Xenopus embryo, Wnt6 was found to be expressed endogenously within the developing heart. Wnt6 loss-of-function experiments revealed that Wnt6 is required to prevent cardiac hypertrophy. Gain-of-function experiments showed that Wnt6 prevents heart muscle development at late stages of development; so Wnt6 is not needed during gastrulation but it is needed for later stages of development, during organogenesis, just before the cells differentiate into myocardium (Lavery *et al.*, 2008).

### 1.3.3 Fibroblast growth factor signalling

Fibroblast growth factor (FGF) signalling controls the spread of the mesodermal layer during heart development, in both the vertebrates and the invertebrates (Wilson *et al.*, 2005). There are 22 genes of the FGF family found in humans, all structurally related. Three genes are found in fruit flies: *branchless*, *pyramus* and *thisb* (Itoh and Ornitz, 2004). FGF are implicated in embryonic morphogenesis in both vertebrates and invertebrates, and are involved in many cellular processes, including cell migration and differentiation. FGFs act through activation of their receptors (FGFRs) with tyrosine kinase domains (Bottcher and Niehrs, 2005).

Heartless *(htl)* encodes an FGF receptor in *Drosophila.* Studies on heartless mutant embryos have shown that the mesodermal layer was unable to go through dorsolateral migration, and the dorsal vessel was lost (Gisselbrecht *et al.*, 1996; Shishido *et al.*, 1997). Two other mutations that lead to failure of dorsal mesoderm spreading are: the *sugarless* and *sulfaless* genes - which are important for the synthesis of the co-factor heparin proteoglycan of FGF signalling (Ling *et al.*,, 1999).

FGF signalling is required for the formation and migration of the mesodermal layer and without this signal it is hard for a dorsal vessel to be formed. Inhibition of FGF in mice leads to impairment in hearing function and raises the risk of heart failure (Murakami *et al.,* 2008).

FGF16, which is a member of the FGF9 subfamily, was found to be involved in embryonic cardiac development in mice. Deletion of FGF16 led to embryonic death, and heart defects were seen in FGF16 null heart by day 10.5(E10.5), including dilation in the chamber and reduced thickness of the arterial and ventricular walls (Yan, *et al., 2008*).

In zebrafish, FGF8 is expressed early in the heart, in FGF8 mutant embryos known as *acerebellar,* show strong cardiac defects and absence of ventricular structures. In addition, there was an obvious reduction of *Nkx2-5* and *Gata4* observed from the start of their expression. Inhibition of the FGF receptor with Fgfr1 SU5402 inhibitor blocked the expression of *Nkx2-5 (*Reifers *et al.*, 2000). Altogether, FGF is not only involved in heart development, but it is also required for the activation of different cardiogenic transcription factors.

### 1.3.3 Notch signalling

Notch signalling is a very important signalling pathway, which plays a vital role during the early stages of heart development in both drosophila and vertebrates. Notch signalling has two main components: the transmembrane receptor and transmembrane ligand.

In *Drosophila,* there is a single notch receptor and two ligands: Delta and Serrate (Langdon *et al.*, 1999). Mammals have four type I transmembrane receptors (Notch1 to Notch4) and five type I transmembrane ligands: Delta-like (Dll)1, Dll3, and Dll4, Jagged1, and Jagged2; all together referred to as the DSL (Delta/Serrate/Lag-2) family

(Fleming *et al.*, 1998). Notch signalling during *Drosophila* heart development has two main functions: one is lateral inhibition, which is considered cell-cell interaction between Notch and its ligands. This takes place in a group of cells which has the same destination in the process of the heart progenitor's development. In response to this shared inhibition, Notch signalling will be inactivated by one cell of an equivalence group that allows it to be a heart progenitor (Mumm *et al.*,, 2000). The second function of Notch signalling is involved in its ability to specify the destination of heart precursor cells. In *Drosophila,* the heart precursor cells' fate is determined by two types of cell division: symmetric and asymmetric (Ward *et al.,* 2000). This signalling works in an asymmetric manner, in order to control the specification of CBs from distinct heart precursors (Han and Bodmer, 2003). A study done on a Notch mutant embryo showed that, asymmetric division was influenced by this mutation which led to the formation of two daughter cells of similar identity. Accordingly, in this mutant embryo, CBs were formed, but PCs were absent, which point to the importance of Notch signalling in *Drosophila* heart development (Ward *et al., 2000*).

In vertebrates, Notch signalling plays an important role in cell fate determination, in addition to other functions. The genes that are considered a direct target for notch signalling are members of the HRT family of basic helix-loop-helix proteins. All of them are involved in cardiac development (Nakagawa *et al.*, 2000). These genes of the Hrt family are considered direct targets of notch signalling. They include three genes discovered by different groups and thus given different names: *Hrt, Hey, Hesr, Herp and CHF* (Nakagawa *et al.*, 2000; Iso *et al.,* 2003).

They are expressed in the vascular smooth muscle and the endothelial cells in the developing cardiovascular system (Kokubo *et al.*, *1999*; Leimeister *et al.*, 2000). Severe cardiac defects were seen in *Hrt2* knockout mice, including cardiomyopathy, AV valve dysfunction, ventricular enlargement and other defects that led to high rates of postnatal lethality (Donovan *et al.*, 2002; Sakata *et al.*, *2002*; Kokubo *et al.*, 2004). Alternatively, knockout of the genes *Hrt1* and *Hrt3* does not cause obvious cardiac defects (Fischer *et al.*, 2004; Kokubo *et al.*, 2005). Notch signalling is an important signal in both *Drosophila* and vertebrates, and loss of this signal will lead to abnormal heart tube formation.

## 1.4. Transcription factors and heart development

### 1.4.1Tinman and its homologue *Nkx gene*

*Tinman* was the first gene discovered to control heart development in *Drosophila*. *Tinman* is a homeodomain containing transcription factor (Bodmer *et al.*, 1990, Bodmer 1993; Azpiazu and Frasch, 1993).

*Tinman* is expressed in both CBs and PCs, in addition to somatic muscles. It is initially expressed in the presumptive mesoderm, but after gastrulation, its expression is limited to the dorsal portion of the mesoderm - this gives rise to the gut muscles, some dorsal skeletal muscles, and the heart. *Tinman* divides the mesoderm and the dorsal mesoderm into small sections, with the capability to form the heart (Bodmer *et al.*, 1997; Bodmer and Frasch, 1998; Yin and Frasch, 1998). Knockout of *tinman* led to a complete loss of the heart, which indicates the importance of this gene in heart development (Bodmer *et al.*, *1993*).

*NKx-2.5* is the vertebrates' homologue of *tinman.* In both mouse and xenopus, this gene was found to be expressed early in the heart (Komuro and Izumo, 1993; Lints *et al.*, 1993; Tonissen *et al.,* 1994). *Nkx-2.5* is important for the specification and maintenance of cells' fate that originate from the mesoderm, subsequent to gastrulation (Chen and Fishman, 1996; Cleaver *et al.*, 1996). The knockdown mouse of this gene led to altered expression of the gene and abnormal heart development, this is in addition to death of the embryos between 8 and 9.5 dpc (Lyons *et al.*, 1995; Tanaka *et al.*, 1999). Altogether, NKx2.5 is extremely vital for heart development, just as *tinman,* and performs similar function during heart morphogenesis.

### 1.4.2 MEF2 and DMEF2

*Tinman* is not the only transcription factor that is involved in heart development. Dmef2 is a member of myocyte enhancing factors, which belong to the MAD box family. Dmef2 and its homologue in vertebrates MEF2 play a critical role in heart cell differentiation and specification in both systems (Bour *et al.*, 1995; Lilly *et al.*, 1995; Ranganayakulu *et al.*, 1995). There are four members of this gene family in mice and they are expressed in different cell types, but mainly in the precursors of cardiac, smooth and skeletal muscle. Mice which had a mutation in the *MEF2C* gene showed defects in heart development and other defects similar to NKX2.5 mutants (Lin, *et al., 1997*).

Fruit flies have only one gene - *Dmef2* - that is expressed in the heart precursor cells. In *Dmef2* mutant embryos, heart cells were not differentiated, and failed to express contractile protein genes (Bour *et al.*, 1995; Lilly *et al.*, 1995; Ranganayakulu *et al.*, 1995). These defects mean that *dmef2* controls the later stages of heart development, in contrast to *tinman. Dmef2* was found to be a direct target of *tinman,* since two binding

sites were discovered in the cardiac enhancer of *Dmef2* that are necessary for promoting the function of cardiac muscle cells (Gajewski *et al.*, 1997).

## 1.5. Slit ligand and its Robo receptor

The epidermal growth factor (EGF) slit is a large multi domain leucine-rich repeat (LRR) ligand. Slit is involved in different functions, including heart morphogenesis, angiogenesis, and tumor metastasis (Taskonas *et al.*, 1990).

Slits are ligands for the Robo (Roundabout) receptors, which belong to the immunoglobulin (Ig) super family of transmembrane signalling molecules (Frenandis and Ganju, 2001). Slit is a secreted protein that is expressed by glial cells and neurons (Rothberg, 1990) and by the CBs in *Drosophila* heart (Li *et al.*, 2005). In vertebrates, slit consists of a family of three genes: *Slit1*, *Slit2*, and *Slit3*; while in *Drosophila,* there is only one *Slit* (Frenandis and Ganju, 2001). Slit proteins have four leucine-rich repeats (LRRs) at the N-terminus, known as D1–D4. This is followed by six epidermal growth factor (EGF) repeats, then a laminin G-like domain, and a cysteine knot at the C-terminus (Hohenester, 2008) (Fig. 5).

Robo receptor proteins which are highly conserved from *Drosophila* to mammals consist of five immunoglobulin (Ig) repeats and three fibronectin type III repeats in the ectodomain and polyproline stretch (Fig.5). In *Drosophila,* there are three genes: *Robo, Robo2*, and *Robo3*; but the vertebrates possess four receptors: they are Robo1, Robo2, Robo3, and Robo4 (Tear *et al.*, 1998; Cisholm and Lavigne, 1999; Hohenester, 2008). Slit and Robo induce a signal when Slit LRRs bind to the Ig domains of Robo. LRRs are considered the most important domain in Slit protein, since they are responsible for neuronal migration and axon projection (Chen *et al.*, 2001; Morlot, 2007).

**Figure 5. Structural features of Slit ligand and Robo receptor.**

Slit ligand consist of: four leucine-rich domains, from D1-D4 at the N-terminus, five epidermal growth factor (EGF), and laminin globulin domain( G), and a cysteine knot at the C-terminus. While the robo receptors consist of five immunoglobulin(Ig) repeats and three fibronectin type III repeats in the ectodomain and polyproline stretch (adapted from Hohenester, 2008).

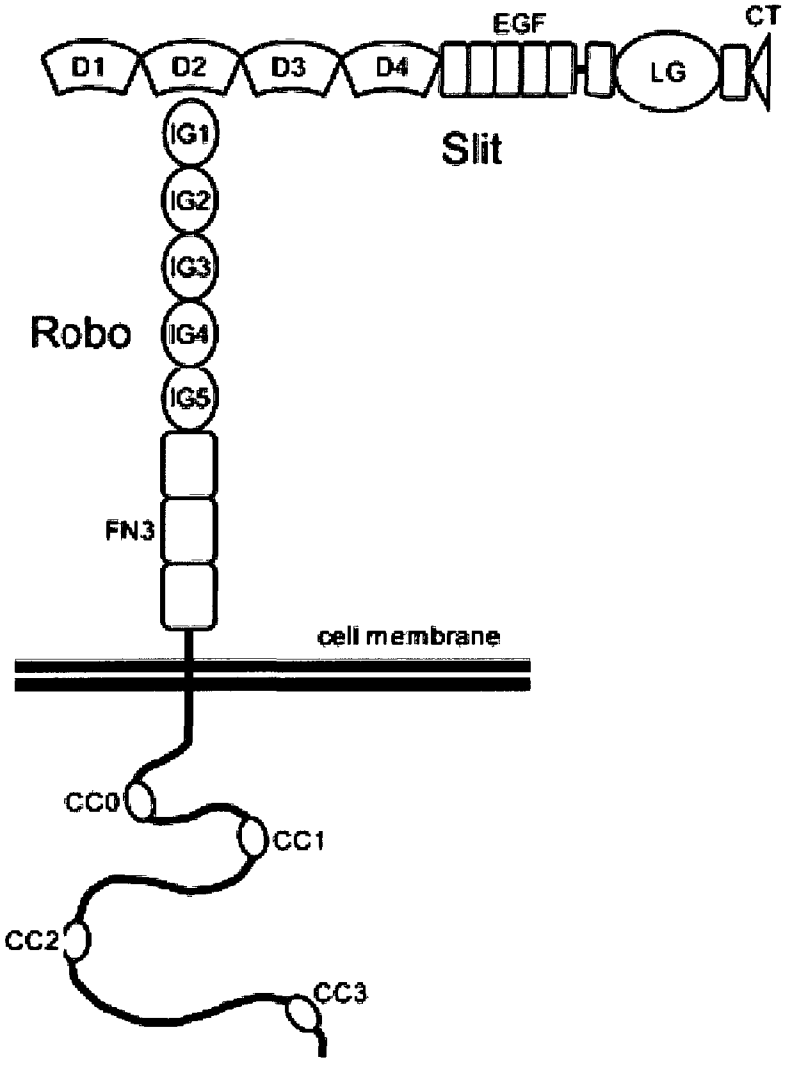
EGF
CT
D1
D2
D3
D4
LG
Slit
IG1
IG2
IG3
Robo
IG4
IG5
FN3
cell membrane
CC0
CC1
CC2
CC3

The Slit/Robo complex regulates the growth of axons and their projections to certain regions of the brain. In addition it acts as a repellent to prevent the axons from crossing non-target areas (Rao, 1999; Fernandis and Ganju, 2001).

*Drosophila* heart tube formation needs Slit-Robo signal, to ensure proper cardiac tube assembly and lumen formation. (Li *et a*l., 2005; MacMullin and Jacobs, 2006; Santiago-Martinez et al., 2006). In addition the Slit/Robo complex act as a repulsive signal to antagonize Shotgun/E-cadherin mediated cell adhesion. It was found that Shg/E-cad gain-of-function or Robo loss-of-function had similar phenotypes in which the lumen formation was prevented due to improper CBs adhesion. The Shg/E-cad loss-of-function or Robo gain-of-function the lumen formation was also prevented because the CBs adhesion was lost. Accordingly, Slit and Robo signal may be a repulsive signal, and it is required for normal lumen formation (Santiago-Martinez *et al.*, 2008). *Slit3* is the only member of *Slit* family genes that is expressed in the developing atrial walls of the murine heart. In addition, *Slit3* deficient mice resulted in abnormal heart formation including an apparent enlargement of the right ventricle (Liu *et al.*, 2003).

## 1.6 Common defects observed during *Drosophila* heart development in Slit and Robo mutants

Altering the expression of Slit or Robo in *Drosophila* results in different types of defects, and the severity of these defects depends on the type of the mutation in each gene. For instance, *slit* null mutant and *robo* double mutant causes severe migration defects in *Drosophila* heart tube compared to the wild type at the same stage (Fig.6 A-J). Delayed migration is one of the most common defects in *slit* null mutant embryo; in this defect the cells were not able to migrate dorsally as in a control embryo to form an organized heart

tube. Instead it is formed in an irregular manner (Fig.6 B, D asterisk) ( MacMullin and Jacobs, 2006). Another defect that is seen in both *slit* and *robo* double mutant, are large gaps, in which part of the heart tube totally disappeared (Fig .6 D, f, J arrow). In addition, a twisted heart tube is also seen in *slit* null and *robo* double mutant, in which crossed lines of the CBs is seen, compared to the control embryo at stage 17 of embryonic development (Fig.6 B diamond, J arrow) (Li et al., 2005; Macmullin and Jacobs, 2006). Another defect that is detected at different stages of embryonic heart development is formation of double rows of cells or clustering of 2-3 cells as seen in stage 15 of Slit null mutant embryo (Fig.6, H arrow) (Li et al., 2005).

## 1.7. Sarcolemmal Membrane Associated Proteins SLMAPs

The Tail-anchored (TA) membrane protein family are distinguished by a hydrophobic transmembrane domain at the C-terminus (Wattenberg and Lithgow, 2001). They have a major role in membrane fusion and are implicated in different cellular events such as neurosecretion and cell death (Cory and Adams, 2002). SLMAP is a member of this family which has two alternatively spliced tail anchors (TA1 and TA2) (Guzzo *et al.*, 2004). SLMAP consists of alpha helical coiled regions containing two leucine rich motifs and a transmembrane (TA) at the C- terminus (Wigle *et al.*, *1997*; Guzzo *et al.*, 2004). There are three isoforms of SLMAP: two cardiac muscle specific variants (SLMAP1, SLMAP2) and a ubiquitously expressed isoform (SLMAP3) (Wigle *et al.*, 1997) SLMAP3 is recognized by its forkhead associated domain (FHA) at the N-terminus that is not found in the other isoforms, and two transmembrane domain at the N-terminus (TA1 and TA2) (Guzzo *et al.*, 2004). SLMAP3 and *Drosophila* SLMAP (*D*SLMAP) have similar structural features.

## Figure 6. Cardiac defects observed in *Drosophila* heart caused by *slit* and *robo* mutants

Different types of defects were detected in Slit and Robo mutants. (A-J) Embryos are at dorsal view anterior to the left.(A-D) the cardioblasts are stained with Cardial cells are labeled with the B2-3-20 enhancer trap,(E-J) the cardioblasts are labeled with Dmef2 antibody. (A) Control embryo, at stage 17 shows normal cardioblasts alignment. (B) *slit* null mutant embryo, at stage 17 shows several migration defects in the same embryo which include delayed migration (asterisk), twist or crossed line (diamond) and blisters (arrowhead). (C) Control embryo, at stage 14 has aligned cardioblasts. (D) *slit* null mutant embryo, at stage 14, two defects are seen in the embryo delayed migration (asterisk), and a gap (arrow). (E) Wild type embryo, at stage 17, shows organized heart tube (arrow). (F) *slit* null mutant embryo, at stage 17, shows crooked lines of the cardioblasts and misaligned cardioblasts (arrows). (G) Control embryo at stage 15, shows aligned cardioblast. (H) Slit null mutant embryo, at stage 15 shows double rows of the cardioblasts (arrow), and a gap (star). (I) control embryo, stage 17 shows normal cardiac cells alignment. (J) *robo* double mutant embryo, at stage 17, shows gaps, delays and twisted heart tube (arrows). (Fig. A-D, adapted from: MacMullin and Jacobs, 2006, Fig. E-J, adapted from: Li et al., 2005)

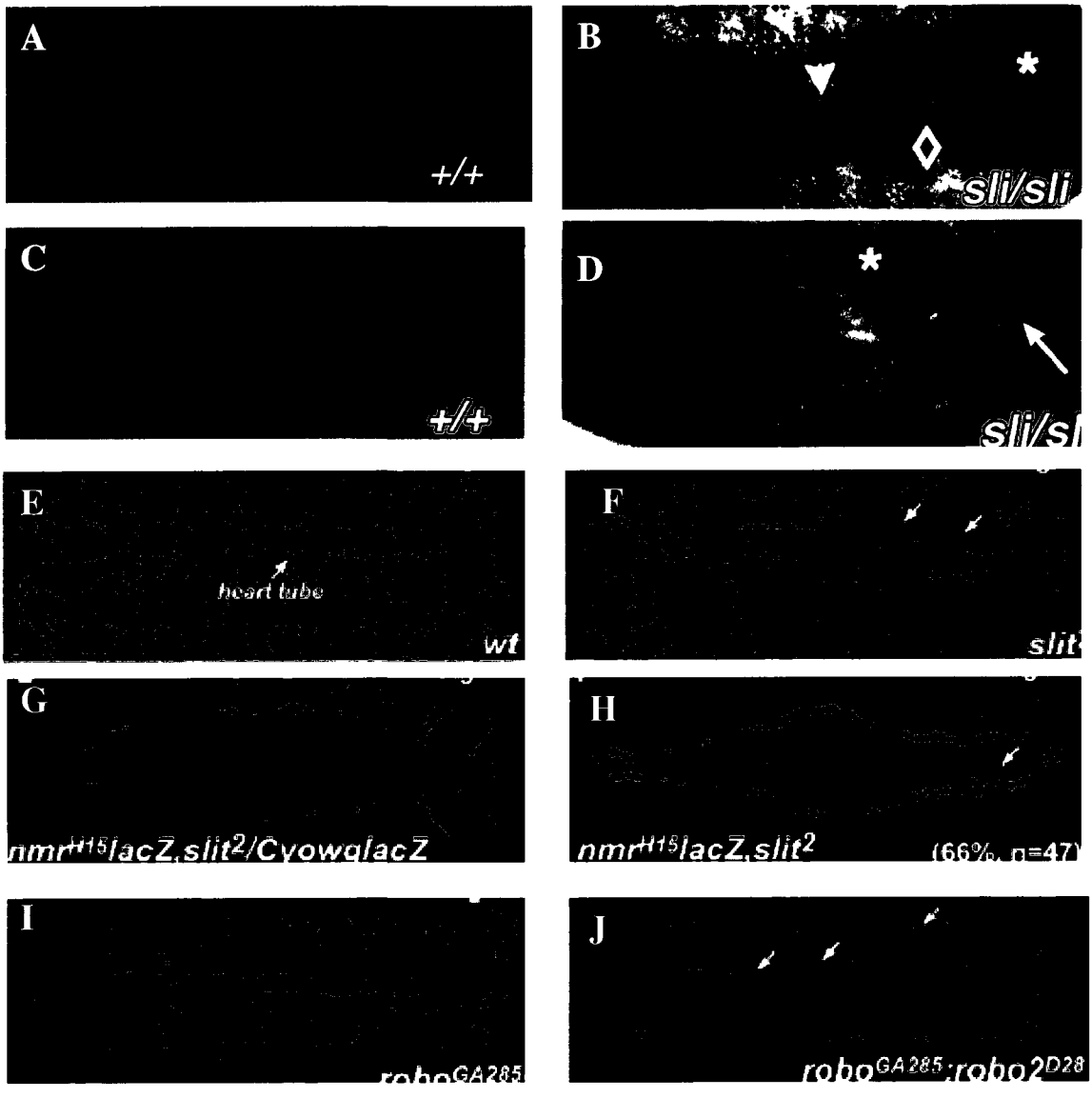
A
+/+
B
sli/sli
C
+/+
D
E
heart tube
wt
F
G
nmr^H15lacZ,slit^2/CyowglacZ
H
nmr^H15lacZ,slit^2
(66%, n=47)
I
roboGA285
J
roboGA285;robo2D28

**Figure 7. Structural features of *Drosophila* SLMAP and its mammalian homologue.**

*D*SLMAP resembles the mammalian SLMAP. Both of them possess a fork head associated domain (FHA), a coiled-coil region, and a TM domain. A 55.9% identity was identified in FHA domain, and 25% identity was identified in the TM domain, and the % identity for overall sequence is 28.6% (Adapted from M'omena Dawood thesis, 2006; Guzzo *et al.*, 2003).

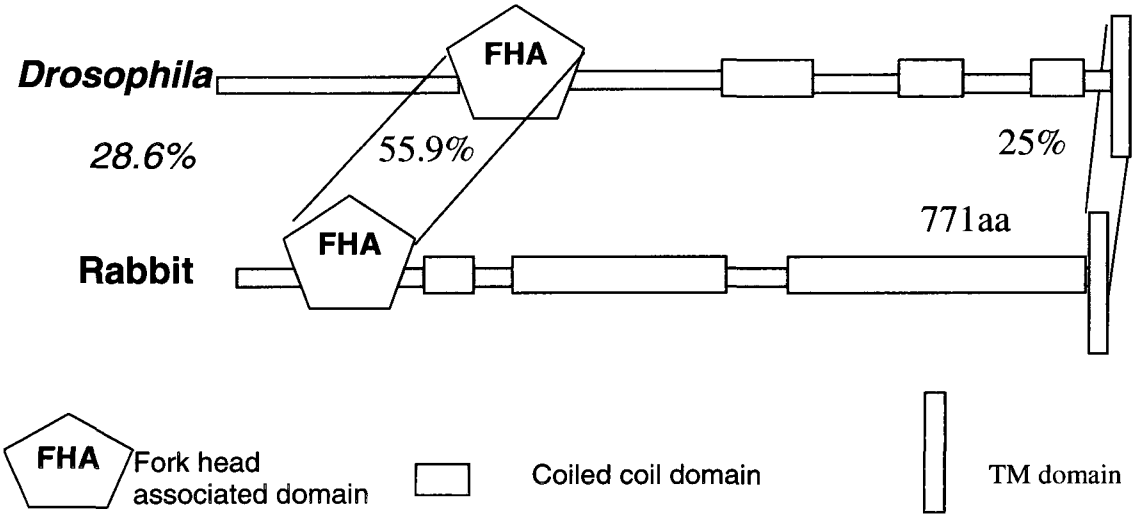
Drosophila
28.6%
FHA
55.9%
25%
771aa
FHA
Rabbit
FHA
Fork head associated domain
Coiled coil domain
TM domain

DSLMAP and its mammalian homologue share 28.6% identity over 721 amino acid residues with the SLMAP3 isoform; a higher percentage identity was noted in the forkhead-associated domain (55.9%) (M'omena Dawood thesis, 2006) (Fig.7).Each domain in (SLMAP) has its own function. The presence of leucine-rich coiled coil regions in SLMAP is essential for SLMAP oligomerization and also to mediate SLMAP-SLMAP interaction (Guzzo *et al.*, 2004).

Coiled-coil domains are extensively used in extracellular matrix molecules to join subunits in oligomeric proteins and maintain protein stability by directing subunit oligomerization (Procopio *et al.*, 1999). Another domain that is found in *D*SLMAP and the mammalian SLMAP is the FHA domain, which plays an important role in different cellular events including DNA repair and cell cycle progression (Pike *et al.*, 2001). The TA domains targets the SLMAP to reticular structures while TA2 targets SLMAP to the mitochondria (Guzzo *et al.*, 2004) and may have a role in the function of this organelle (Byers *et al.*, 2009).

SLMAP was found to be expressed in different systems, including early expression in the heart at nine days post coitum (d.p.c) (Guzzo *et al.*, 2004), skeletal muscles, and in the rat (during neurogenesiss) in the neonatal hippocampus and neonatal migratory neurons (Wigle *et al.*, 1997). Studies on SLMAP have shown that it plays an important role in myoblast fusion during myogenesis. SLMAP is involved in the membrane biology of excitation-contraction (E-C) coupling in the developing muscles (Guzzo *et al.*, 2004). Moreover, it was found that SLMAP in the mouse heart is implicated in the remodelling of E-C coupling components and that its elevated levels in cardiomyocytes are essential to guarantee a proper organization of subcellular compartments (Nader *et al.*, 2008).

Recent work in our lab showed that *DSLMAP* is ubiquitously expressed at different stages of embryonic development in *Drosophila*, and was found to be expressed early in the CNS. Over-expression and down-regulation of DSLMAP in glia and neurons led to defects during neuronal development in the embryonic CNS and it was found that critical levels of DSLMAP is required for proper neuronal development (M'omena Dawood thesis, 2006).In addition different genetic interactions of *D*SLMAP with the Slit/Robo pathway indicated a role for DSLMAP in the CNS (M'omena Dawood, 2007).

## 1.8 Rationale and statement of the problem

SLMAP was found to be expressed early in the mammalian heart development, and data suggests that it may play a role in cardiac function at the level of membrane biology and signal transduction. SLMAP and its *Drosophila* homologue DSLMAP are highly conserved in terms of structural motifs including the presence of a C-terminal membrane anchor, a central coiled-coil region and a N-terminal FHA domain. *D*SLMAP was shown to be ubiquitously expressed during the embryonic development of *Drosophila*, and to interact genetically with the Slit/Robo pathway in the developing nervous system. In view of the ubiquitous expression of *D*SLMAP during embryonic development here we have studied expression of DSLMAP in the developing *Drosophila* heart tube. We have used a targeted approach to de-regulate DSLMAP levels in cardiac cells to define any potential contribution of this protein to heart tube formation. Further, we have also studied any potential genetic interactions of DSLMAP with the Slit/Robo pathway which is known to be a critical player in the normal development of the *Drosophila* heart.

## 1.9 Hypothesis

*DSLMAP* is expressed early in cardiac cells and its levels play a critical role in

developing the *Drosophila* heart tube. Further, in view of the role of Slit/Robo pathway in heart tube formation, we propose that DSLMAP interacts with these proteins to ensure proper heart development.

## 1.10 Objectives

A- To determine mRNA expression of *DSLMAP* during heart development.

B-To investigate the role of *DSLMAP* in *Drosophila* heart by:

1- Targeted down regulation of *DSLMAP* in *Drosophila* heart cells using RNAi.

2- Targeted up regulation of *DSLMAP* in *Drosophila* heart cells.

C- To characterize any genetic interactions between *DSLMAP* and Slit/Robo pathway in *Drosophila* heart by:

1. Targeted over-expression of *DSLMAP* in the CBs of $slit^2$ and $robo^{189}$ mutant heterozygous background.
2. Targeted down-regulation of *DSLMAP* in the PCs of $slit^2$ and $robo^{189}$ mutant heterozygous background.
3. Targeted over-expression of *DSLMAP* in the CBs of UAS-*Slit* transgene.
4. Targeted over-expression of *DSLMAP* in the CBs of UAS-*Robo*-RNAi transgene.
5. Targeted down-regulation of *DSLMAP* in the PCs of UAS-*Slit* transgene.
6. Targeted down-regulation of *DSLMAP* in the PCs of UAS-*Robo*-RNAi transgene

# Materials and Methods

## 2.1Fly Stocks and Genetics

Flies were raised on corn cornmeal molasses/ agar /yeast medium with both proprionic acid and Tegosept at room temperature.

Stocks were obtained from Bloomington *Drosophila* Stock Center at Indiana University:

1. $w^{118}$ white eye wild type
2. Paired-GAL4 driver
3. UAS Slit, UAS Robo RNAi
4. $slit^{2}$ and $robo^{189}$ loss of function mutants

Heart drivers were obtained from Ralf Bodmer lab, university of Michigan:

TincΔ 4-GAL4 specific for CBs; Prc-GAL4 specific for PCs

## 2.2 *D*SLMAP RNAi construct

The UAS DSLMAP RNAi line was generated in the lab, by the use of pWIZ vector. *DSLMAP* inverted repeat was subcloned in this vector to generate RNAi construct (M'omena Dawood thesis, 2006).as illustrated in (Fig. 8). This construct was sent for injection at Drosophila Transgenic Services in Sudbury, MA, USA.

## 2.3 *D*SLMAP HA tagged over-expression construct

A pUAST-Dros-SLMAP-2X HA construct was used to generate the over-expression lines. Briefly the generation of the construct was done by amplifying the full length DSLMAP cDNA (LD47843) from pOT2 vector. The amplified fragment was inserted into pCR-4 TOPO vector and then shuttled in frame from pCR-4 into EagI site of the Drosophila transformation plasmid pUAST (Brand and Perrimon, 1993). The colony with

## Figure 8. Structure of the RNAi construct

The RNAi construct was generated using white intron zipper pWIZ vector (Lee and Carthew, 2003). Panel A shows a schematic representation of the pWIZ vector. This vector was made by inserting the 374-bp second intron of the white gene into the pUAST transformation vector (Lee and Carthew, 2003). Cloning was facilitated by several specific cloning sites on the 5' and 3' ends that flank the intron. Panel B, the RNAi construct generated using pWIZ vector. (Adapted and modified from M'omena Dawood thesis, 2006|)

**A.**

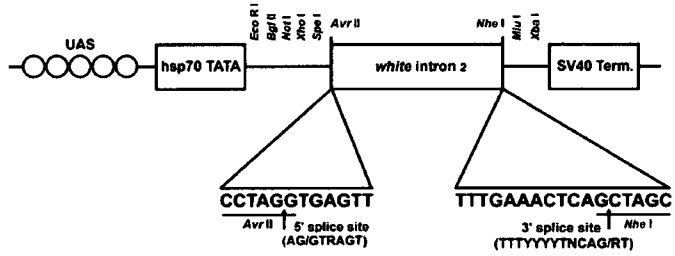


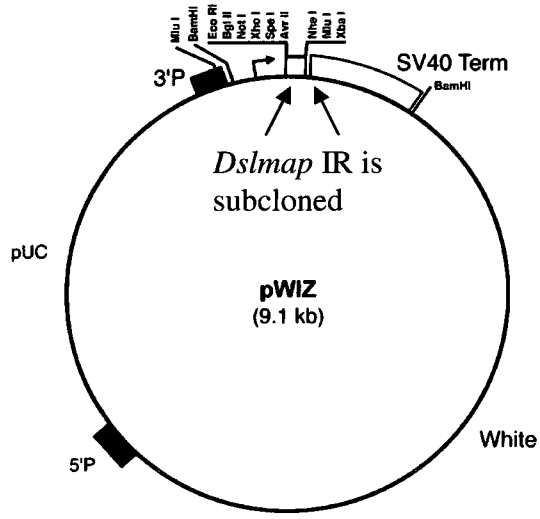


**(pWIZ) RNAi vector**

*Lee and Carthew, 2003*

**B. Structures of the RNAi construct**

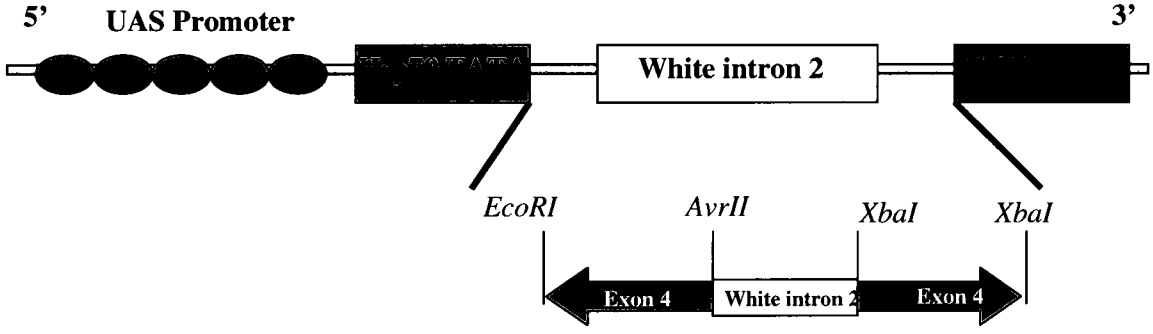

the right orientation pUAST-Dros-SLMAP was further used to clone 2X HA tag to it. The 2X HA tag was amplified from pCDNA3 using HANT-F (HA-NotI-Forward) primer and the reverse primer HANT-R. Both primers have NotI sites. The amplified 2X HA fragment was then cloned to the C-terminus of pUAST-Dros-SLMAP construct to generate pUAST-Dros-SLMAP-2X HA construct. This construct was sent for injection (Drosophila Transgenic Services, Sudbury, MA, USA) (Fig. 9) (this construct was made by Maysoon Salih and M'omena Dawood).Ten transformant lines were generated and mapped by (M'omena Dawood)

## 2.4 GAL4/UAS binary system

*DSLMAP* role during *Drosophila* heart development was analyzed by using two approaches: one for down-regulation of DSLMAP by generating the upstream activating sequence (UAS) *DSLMAP* RNAi line, the second for over-expression of *DSLMAP* by generating UAS-*DSLMAP* lines. These lines alone can't produce any expression in *Drosophila* embryonic heart, since the UAS promoter sequence is not found in fruit flies. Accordingly, the GAL4/UAS system was used, in which GAL4 a yeast transcription factor that is inactive alone in Drosophila (Duffy, 2002). The GAL4/UAS bipartite system is used to express different genes, in which the GAL4 binds to the UAS; this binding will activate the expression of the gene carried downstream the UAS promoter where ever the GAL4 is expressed in cell and tissue specific manner. The GAL4/UAS is considered as one of the most important genetic tool which is being used in *Drosophila melanogaster*, since it helped scientists to explore the function of genes in different medically and economically important processes (Duffy, 2002; Brian, 2003). Thus this system is used for the over-expression of transgenes from a UAS promoter because

## Figure 9. Generation of *D*SLMAP HA tagged over-expression construct

Panel A, pUAST vector (Brand and Perrimon, 1993) which was used to subclone the full length *DSLMAP* downstream of the UAS promoter element. Panel B *D*SLMAP over-expression construct, 2 X-HA fragments was subcloned at the C-terminus of full length *D*SLMAP.

# A. pUAST transformation vector

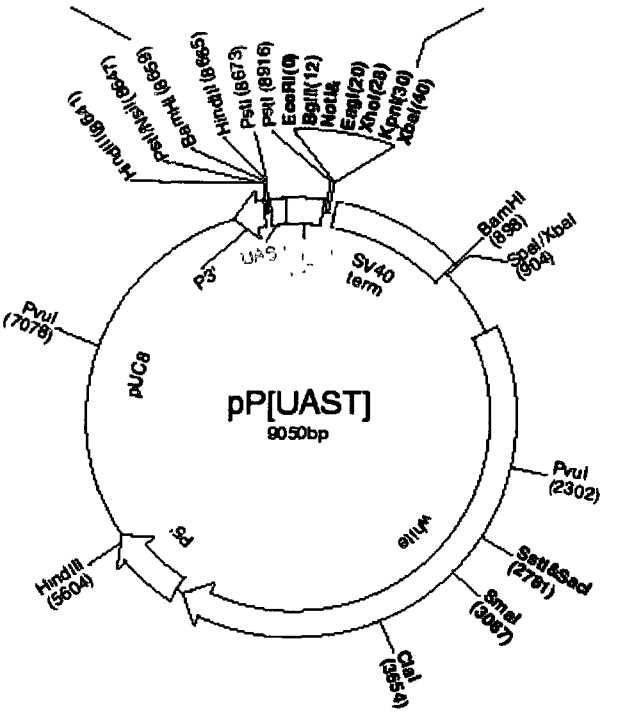


# B. UAS-DSLMAP constructs

## Figure 10. Mechanism of the GAL4/UAS binary system

Gal4 is a yeast transcription factor required to activate the expression of any coding sequence downstream of a (UAS) Upstream Activating Sequence. Two mutant flies are required: one to carry the Gal4 transgene fused to a promoter that has a specific expression pattern, and the other fly carries a coding sequence for the target gene, cloned downstream of the activating sequence. The first generation of a cross between Gal4 strain and UAS strain carry both transgenes and will express the UAS downstream gene in all cells that express GAL4.

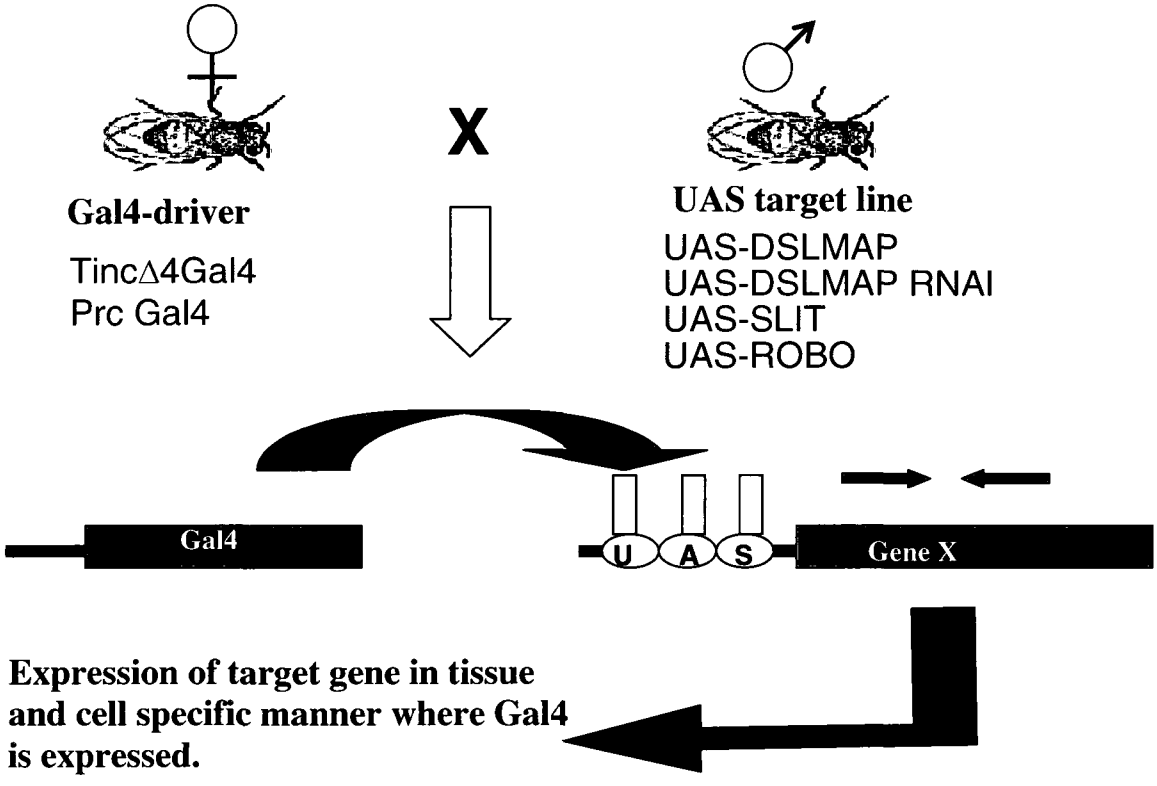
X
Gal4-driver
TincΔ4Gal4
Prc Gal4
UAS target line
UAS-DSLMAP
UAS-DSLMAP RNAI
UAS-SLIT
UAS-ROBO
Gal4
U
A
S
Gene X
Expression of target gene in tissue and cell specific manner where Gal4 is expressed.

GAL4 will drive the expression of the transgene without affecting the cells (Duffy, 2002; Brian, 2003). This is done by crossing a GAL4 driver line with a UAS line, there by the gene will be fused to UAS and expressed in a temporally and spatially specific location where ever the driver gene is normally expressed (Fig. 10) (Perrimon,1993; Brian,2003).

## 2.5 Genetic crosses generated to analyze *DSLMAP's* role during *Drosophila* heart development

In order to study the expression of DSLMAP in *Drosophila* heart the following genetic crosses were made using GAL4/UAS binary system:

1-UAS *DSLMAP* / +; WT/+

2- Tin GAL4/+; UAS *DSLMAP*/+

3- Prc GAL4/+; UAS *DSMLAP*/+

4-UAS *DSLMAP* RNAi /+; WT/+

5- Tin GAL4 /+; UAS *DSLMAP* RNAi/+

6- Prc GAL4/+; UAS *DSLMAP* RNAi/+.

7- Paired GAL4/+; UAS *DSLMAP*

8- Tin GAL4/+; WT/+

9- Prc Gal4/+; WT/+

To study genetic interaction of *DSLMAP* with the Slit/Robo pathway the following crosses were made:

1- Tin GAL4/+; UAS *Slit* / +

2- Tin GAL4/+; UAS Robo/+

3-Prc GAL4/+; UAS Robo/+

4- Prc Gal4/+; UAS DSLMAP RNAi /+; UAS ROBO RNAi

5- Tin GAL4/+; UAS DSLMAP /+; Robo $^{189}$

6-Prc GAL4/+; UAS DSLMAP RNAi /+; Robo $^{189}$

7- Tin GAL4/+; UAS DSLMAP /+; $Slit_2$

8- Prc GAL4/+; UAS DSLMAP RNAi/+; $Slit_2$

9- WT/+; $Slit^2$/+

10-WT/+; Robo $^{189}$/+

11- Tin GAL4/+; $Slit^2$/+

12- Tin GAL4/+; $Robo^{189}$/+

13- Prc GAL4/+; $Slit^2$/+

14- Prc GAL4/+; $Robo^{189}$/+

15 UAS DSLMAP/+; $Slit^2$/+

16-UAS DSLMAP RNAI/+; $Slit^2$/+

17- UAS DSLMAP/+; Robo $^{189}$/+

18- UAS DSLMAP RNAI/+; Robo $^{189}$/+

## 2.6 *In situ* hybridization

### 2.6.1Embryo collection and fixation for *in situ* hybridization

Embryos were collected on grape juice agar plates and transferred to vials which have a sieve cover. Embryos were washed with double distilled water and dechorionts in 25%commercial bleach (chlorix) in water for about 2-3 minutes. Cleared embryos then were transferred to a glass scintillation vial containing 1 ml fixation solution (4% formaldehyde in 1XPBS pH7.4) and 6ml heptane, which were shaken for 20 minutes. Using a glass pipette, the lower layer was removed, and 8 ml of methanol was added. The vials were shaken strongly for 15 seconds to burst the vitelline membrane, in order to

allow the devitelinized embryos to fall to the bottom, and be transferred to 5 ml vials and washed twice with methanol. Finally, embryos were stored in the freezer at -20C.

### 2.6.2 *In situ* hybridisation of digoxigenin (DIG)-labelled probes

*In situ* hybridization is a type of hybridization that is used to detect and localize RNA or DNA sequence in a part of small tissue such as, Drosophila embryos. It involves the hybridization of DIG labelled complementary RNA or DNA strand (probe).

Whole-mount *Drosophila* RNA *in situ* hybridization was performed as described by Nusslein-Volhard lab. Dig-labelled RNA sense and α-sense probes were generated using a Dig RNA labeling kit (Roche), with probes of 300–550 base pairs in length (Momena Dawood thesis,2006). All solutions were made in Diethyl Pyrocarbonate (DEPC) treated water. The fixed embryos stored at -20 were left at room temperature (RT) washed twice for 10 minutes in PBT (998.5ml 1XPBS;500ul DEPC;0.1% (v/v) tween20) embryos were post-fixed in 1ml PBT (4% formaldehyde) for 15 minutes, then washed 5X for 5 minutes in PBT and incubated in 0.05% Proteinase K in PBT for 5 minutes. Proteinase K digestion was terminated by incubating embryos for 2 minutes in 2 mg/ml glycine in PBT, and embryos were washed 2X for 5 minutes in PBT. Embryos were again fixed in 1ml PBT, 4% formaldehyde for 20 minutes and were washed after 5X for 5 minutes in PBT. The embryos were washed with hybridization B solution [hyb B: 50% (V/V) formaldehyde; 25% (v/v) 20X SSC; 25% (v/v) DEPC in $H_2O$] for 5 minutes and prehybridized in hybridization A solution [50% v/v) formamide; 25% (v/v) 20X SSC; 10 mg/ml sonicated salmon sperm DNA; 20 mg/ml tRNA; 100 mg/ml heparin, ph 5.0] for 1 hour in a water bath at 70°C . The liquid containing the embryos was removed, only 2 mm of solution left above the surface of settled embryos, and 2μl of the probe was added

to 60µl of the hybridization A solution containing the embryos. Hybridization was carried out in a 70°C water bath overnight. Two 15 minutes washes with hybridization B solution were performed followed by serial washes in hybridization solution in PBT for 10 minutes at RT, which were followed by several washes in PBT 3X for 10 minutes. In order to remove any nonspecific binding materials the anti-DIG antibody conjugate (1:2000) was made freshly and preabsored the 1st day of this experiment against fixed embryos. Embryos were incubated for 2 hours in 1.2 ml of the diluted, preabsorbed anti-DIG antibody complex. The embryos were washed 3X for 20 minutes in PBT, and washed 2X for 20 minutes in staining buffer [1M MgC12; 5M NaCl; 1M Levamisol; 20% Tween 20; 0.1M Tris-HCl, pH 9.5]. The signal was developed using 15 ml staining buffer containing [2.56% (v/v) NBT/BCIP] .1ml of the staining solution was added to embryos. The tubes containing the embryos were covered with aluminum foil; in order to allow the color to develop in the dark. This reaction was left to proceed until the desired staining effect was viewed under the dissecting microscope, and PBT was used to stop the reaction. The embryos were washed 2X for 10 minutes in PBT, and 2X for 10 minutes in water on the rotator. The embryos were dehydrated with an ethanol gradient beginning at 70% ethanol. The tubes were inverted several times; embryos were allowed to settle down, in order to remove the ethanol. The embryos were treated with a mix of 70% ethanol and 100% ethanol followed by inversion of the tube several times. The final step in the dehydration process involves adding 100% ethanol alone 2X for 5 minutes. The ethanol was removed and the embryos were stored in 80% glycerol at RT.

## 2.7 Non-fluorescent protein/RNA double-labeling using Dmef2 antibody and DIG-labeled *DSLMAP* riboprobes.

### 2.7.1 Embryos fixation

Embryos from different developmental stages were collected for a week at RT on grape juice agar filled Petri plates containing a small smear of live yeast paste (Fleischmann's dry). Embryos incubated for two hours at 29°C for heat shock to activate the yeast transcription factor GAL4, and then allowed to recover on for 1 hour at RT, to ensure the embryos were well differentiated. The plates containing the embryos were dechorionated for 7 minutes with 50% bleach, and were collected on a nitex sieve, and washed with distilled water. After drying the bottle using a kimwipe, the nitex sieve holding the dechorionated embryos was immersed in a scintillation vial containing a 1:1 mixture of heptane:fixation solution (fixation solution composed of 5% formaldehyde, 0.05M EGTA in 1X PBS. pH 7.0) for 30 minutes. Next the embryos were placed in an equal mixture of methanol: heptane on a shaker for 20 minutes, in order to ensure permeabilization of embryos to allow entry of the fixative and subsequent antibodies. The bottom aqueous layer was removed, replenished with fresh methanol and the vial containing the embryos was shaken vigorously for approximately twenty seconds in order to remove the vitelline membrane surrounding the embryos. The embryos then were transferred to 0.5 ml eppendorf tube using a Pasteur pipette. Traces of heptane were removed by three methanol washes.

### 2.7.2 *D*mef2 antibody staining

*D*mef2 antibody is specific for CBs and somatic muscles and it is used to stain these

embryos. The fixed embryos were washed for 15 minutes in 3% hydrogen peroxide in methanol, and then washed three times with methanol. They were then washed with PBTH for 3 X for 30 minutes (PBTH was prepared using filtered 1 X PBS, 0.1% Tween-20, 50 µg/ml heparin, and 250 µg/ml tRNA). The embryos were blocked by 100µl PBTH and 10µl NGS (Normal Goat Serum) for 30 minutes. Embryos were then incubated with Dmef2 antibody (1:1500) overnight at 4C.. Embryos were washed at RT with PBTH for 6X for 20 minute, and blocked with100µl PBTH and 10µl NGS for 30 minutes. Embryos were then incubated with biotinylated secondary antibody for 2 hours at room temperature, and washed with several changes of PBTH for 60 minutes. For detection of the biotinylated secondary antibody, Vector Lab ABC amplification system was used. The reagents were mixed according to manufacturer's instructions 30 min. prior to use. Embryos were incubated with the pre-incubated ABC mixture for 30 minutes at RT, and washed for 15-30 min. with 3-4 changes of PBTH. The signal was developed with 20 µg/ml Diaminobenzidine, 0.03% hydrogen peroxide in PBTH. A brown signal will be produced. The reaction was stopped with several rinses of PBTH.

### 2.7.3 *In situ* hybridization using DIG labelled *DSLMAP* riboprobes:

Embryos were again fixed for 20 minutes with 5% formaldehyde in PBTH at RT, and washed 3 X for 5 minutes with PBTH. The embryos were then incubated with 50 µg/ml of Proteinase K in PBT for 2-3 minutes. The Proteinase K reaction was stopped with two washes for 3 minutes of 2 mg/ml glycine in PBT, and the embryos were rinsed twice with PBT. Embryos were fixed again for 20 minutes with 5% formaldehyde in PBT at room temperature, and washed 5X with PBT for 20 minutes each wash. Then the embryos were rinsed with PBT: Hybridization buffer (1:1), and then with hybridization buffer alone.

Hybridization buffer consisted of 50%( v/v) formamide; 25% (v/v) 20X SSC; 10 mg/ml sonicated salmon sperm DNA; 20 mg/ml tRNA; 100 mg/ml heparin, ph 5.0] Embryos were Pre-hybridized in hybridization buffer for one hour at 70°C, and Digoxygenin-labelled *DSLMAP* riboprobes were added to the hybridization buffer and incubated overnight (12 to 16 hours) at the appropriate temperature. Post-hybridization washes were done for 20 minutes at the same temperature, the embryos were washed with hybridization buffer alone then PBT: hybridization buffer (1:1) and finally, with PBT alone for 5 washes. Embryos were incubated with anti-Digoxygenin antibody (Boerhinger Mannheim) conjugated to alkaline phosphatase (diluted 1:2000 in PBT) for 2 hours at room temperature. Embryos were washed with PBT 4 times for 20 minutes each wash, and rinsed with alkaline phosphatase staining buffer (100mM NaCl, 50 mM MgCl2, 100 mM Tris pH 9.5, 1 mM Levamisol, and 0.1% Tween 20). Finally the signal was developed using NBT and BCIP in the alkaline phosphatase staining buffer as described by the manufacturer (Boehringer Mannheim). The reaction was stopped with several washes of PBT. The embryos were dehydrated with an ethanol series, and rinsed several times with PBT. The embryos were mounted in 70% glycerol and 30% 0.1 M Tris pH 8.0. This experiment was done according to (Manoukian, A. and Krause, H.M protocol.1992).

## 2.8 immunohistochemistry

## 2.8.1 Embryo fixation

A large number of embryos from different developmental stages were collected overnight at RT on grape juice agar filled Petri plates containing a small spread of live yeast paste (Fleischmann's dry). Embryos were left in the incubator for two hours at 29°C for heat

shock to activate the yeast transcription factor GAL4 and then allowed to recover on lab bench for 1 hour, to ensure that the embryos are well differentiated. The plates containing the embryos were dechorionated for 7 minutes with 50% bleach, and they were collected onto a nitex sieve and washed with distilled water. After drying the bottle using a kimwipe, the nitex sieve holding the dechorionated embryos was immersed in a scintillation vial containing a fixation solution of 500µl of 37% formaldehyde, 4.5ml 1X PBS (Phosphate Buffer Saline) and 5ml heptane. Embryos were left on a shaker for 30 minutes; heptane is used to ensure permeabilization of embryos to allow entry of the fixative and the following antibodies. The aqueous layer at the bottom was removed, fresh methanol was added and the vial containing the embryos was shaken vigorously for approximately twenty seconds in order to remove the vitelline layer surrounding the embryos. The bottom layer was transferred to a plastic tube using a Pasteur pipette, and embryos were washed three timed with methanol to remove any traces of heptane, and stored in -20°C. Embryo fixation was according to standard protocol (patel, 1994). Embryo staging was according to Campos-Ortega and Hartenstein (1985).

## 2.8.2 Antibody staining

In order to carry on with antibody staining, embryos stored in methanol at -20°C were used and washed with PBT (50 ml 10X PBS containing 0.1% triton X-100 and 450ml distilled water). Embryos were washed for 2X20 minutes in PBT on a rotator, and incubated in 100µl of PBT containing 10 µl of normal goat serum (NGS) for 30 minutes to block nonspecific antibody binding. A primary antibody with specific dilution was added to embryos in blocking solution and was incubated at 4°C overnight. Remaining antibody was washed away with PBT 3X for 1 hour. The washed embryos were blocked

again in 100μl of PBT containing 10 μl of NGS for 30 minutes. The secondary antibody was added to the blocking solution and embryos were incubated for two hours at RT. The secondary antibody was then washed out with PBT for 45-60 minutes on a rotator. Vector shield was added to conserve the embryo. (Antibody staining was according to standard protocol (Patel, 1994).

## 2.8.3 Antibodies

Primary antibodies *D*mef2 (obtained from Rolf Bodmer lab university of Michigan) which is specific for myocardial and somatic muscles cells (1:1500), and ZFH1 antibody (obtained from Jim Skeath, department of genetics, Washington University) specific for pericardial cells (1:500) were used. The following primary antibodies were obtained from hybridoma bank: α-spectrin antibody to stain the cell membrane (1:10), Robo (1:10) and Slit a (1:10) were used. Anti Digoxigenin-AP primary antibody was used for in situ hybridization (Roche applied science). The secondary antibodies used are anti-rabbit IgG,anti-Digoxigenin-AP ( Roche applied science), anti-mouse IgG,anti-Digoxigenin-AP( Roche applied science), and anti-guinea pig IgG, anti-Digoxigenin-AP(Jakson).

## 2.9 Microscopy

Embryos were viewed under fluorescent, light, and confocal microscope. All the confocal images were taken at 40X.All figures were processed using Adobe Photoshop software.

## 2.10 Statistical analyses

The expressivity for the phenotypes which is the number of defects per embryo was calculated with results from three independent trials. Four phenotypes were observed which include: delayed migration, clustering/aggregation of cells, twisted heart tube, and

gaps between the heart cells. The expressivity were calculated for each phenotype alone, for instance, the expressivity for the delayed migration defect was calculated for each cross by counting the number of defective embryos carrying this phenotype, and by counting how many delays were found in each embryo, then the mean and Standard deviation were calculated using Microsoft Excel. The Penetrance for each genetic cross was calculated by dividing the number of defective embryos (with specific phenotype) by the total number of embryos counted per cross.

The p-value for the second crosses was calculated using the T-test which was performed using (http://www.graphpad.com/quickcalcs/ttest1.cfm).

# Results

## 4.1 *Drosophila* heart is composed of two cell types

*Drosophila* heart or the dorsal vessel has two types of cells: the cardioblasts (CBs) and the pericardial cells (PCs). There are 52 cells of CBs surrounded by 22 PCs on each row. CBs fuse together to form a linear heart tube by stage 17. *D*mef2, which is specifically expressed in the CBs and somatic muscles, was used to stain CBs shown in red color (Fig. 11, A arrow). Zfh1, a specific marker for PCs, was used to stain these cells which are shown in green color (Fig.11, A' arrow). Both types of cells converged at the dorsal midline to form a linear heart tube at stage 17 of embryonic development, as shown in (Fig.11, A").

## 4.2 *D*SLMAP mRNA expression during embryonic development

The expression pattern of DSLMAP was examined using *in situ* hybridization which was performed with DIG labelled, sense-*D*SLMAP and antisense-DSLMAP riboprobes. Ubiquitous expression of DSLMAP mRNA was observed throughout the embryo and at various stages of embryonic heart development, as illustrated by whole mount *in situ* hybridization (Fig. 12). This expression was detected early at stage 2 of embryonic development (Fig.12, A) which lasts for 40 min, and is characterized by rapid cell cycles that successively divide the fertilized egg. Blastoderm cell formation occurs at stage 5 of embryonic development (Fig.12, B), and cellularization takes place by means of the introgression of membrane grooves to separate single blastoderm nuclei. At stage 9 of embryonic development, dorsal mesoderm is formed which marks the beginning of dorsal vessel formation (Fig.12, C arrow).

## Figure 11. *Drosophila* heart consist of two types of cells

The heart tube in fruit flies has two cell types: the cardioblasts, and the PCs. (A-A") dorsal view of wild-type stage 16 embryos, anterior is to the left. (A) At stage 16, heart cells are aligned in two rows (arrows) forming the heart tube. The CBs, which have a cubodial shape, are identified with Dmef2 antibody (red color); somatic muscles are also seen (arrowheads). (A') PCs have a round shape (arrowhead) and are identified with Zfh1 antibody(green color). Lymph glands are also indicated due to Zfh-1 expression (arrowheads). (A'') The embryo is double-labelled with Dmef2 and Zfh1 antibodies. Scale bar =10 μm

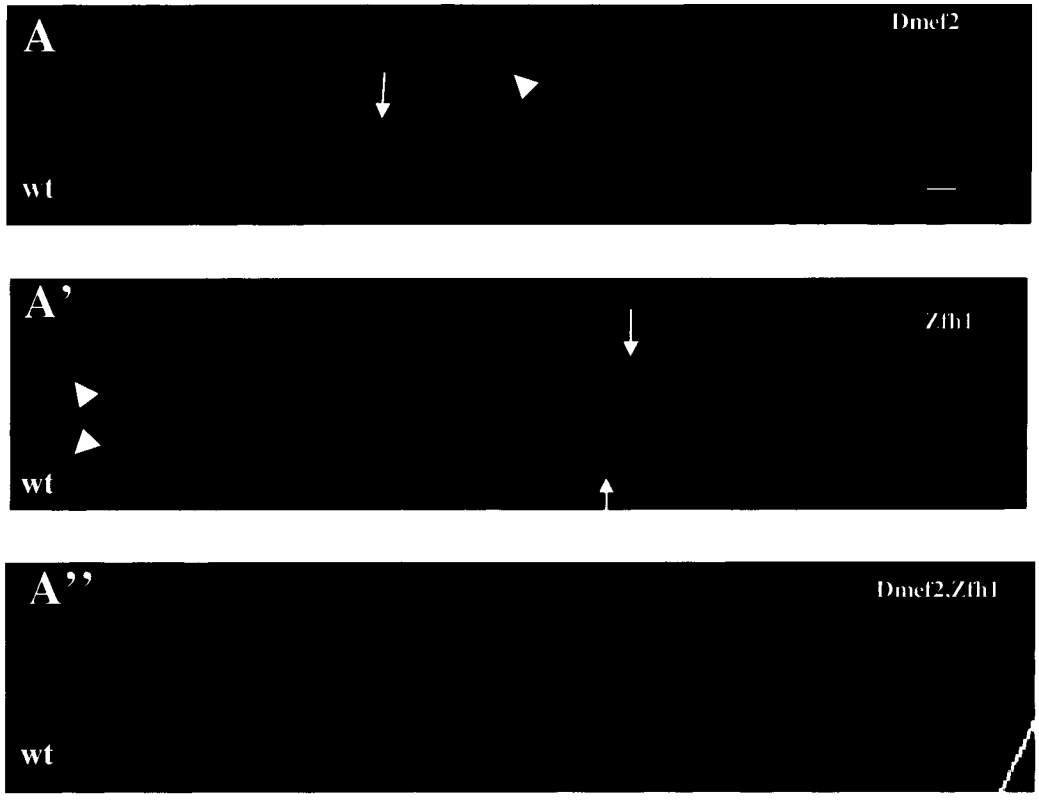
A
Dmef2
wt
A'
Zfh1
wt
A''
Dmef2,Zfh1
wt

At stage 14, heart cells are assembled in two rows, and DSLMAP transcript is noted in these cells due to hybridization with anti-sense DSLMAP riboprobe compared to the sense DSLMAP riboprobes at the same stage (Fig.12, D arrow). *DSLMAP* transcript is still noticeable at stage 15 where the dorsal mesoderm has finished fusion at anterior and posterior parts but not at the middle (Fig. 12, E, arrow head). Sense-*D*SLMAP RNA riboprobe was used as a control where no hybridization signal is observed during various stages of embryonic heart morphogenesis (Fig.12, right panel A, B, C, D, and E).

## 4.3 *D*mef2 protein and *DSLMAP* mRNA localization

Non-fluorescent protein/RNA double-labeling was used to determine the expression of *DSLMAP* in the heart since the whole mount *in situ* hybridization showed that *DSLMAP* is ubiquitously expressed during embryonic development. *D*mef2 antibody stains the CBs and somatic muscles, while the DIG-labeled *DSLMAP* riboprobes were used to examine the *DSLMAP* mRNA expression.

This double labeling illustrates that *D*SLMAP is expressed in the heart at early stages of embryonic development. No clear differences between *D*mef2 staining and *DSLMAP* mRNA localization were evident in heart cells or somatic muscles. However, darker signal was observed in these areas, which is indicative of *D*SLMAP expression in CBs at various stages of heart development. CBs and somatic muscles are observed at stage 14 with purple color, which is double labeled with *D*mef2 and antisense *DSLMAP* riboprobe (Fig.13, A). Double labeling with *D*mef2 and sense *D*SLMAP riboprobes were used as a control where no signal was obtained (Fig. 13, B).

These results indicate that *D*SLMAP expression in the embryonic heart detected from the beginning of heart tube formation, and that *D*SLMAP is a component of CBs.

## Figure 12. Embryonic expression of *DSLMAP* mRNA in *Drosophila*

(A-E) Whole mount *in situ* hybridization was performed using DIG-labelled riboprobes at various stages of embryonic development; left panel: embryos were labelled with anti-sense *D*SLMAP riboprobe; right panel: embryos were labelled with sense riboprobes used as a control. All the embryos were anterior to the left

(A) Ubiquitous expression of *DSLMAP* at stage 2 of embryonic development. (B) *DSLMAP* mRNA expression did not change at stage 5 of embryonic development, and cellularization process occurred at this stage (arrow). (C) Saggital view of stage 9 embryo where DSLMAP transcripts is highly concentrated in the dorsal mesoderm (arrowhead) and the midgut (arrow). (D) Saggital view of stage 14 embryo showing heart cells aligned in a row (arrow) and the somatic muscles are also seen (arrowhead). (E) Dorsal view of stage 15 embryo showing the expression of DSLMAP transcript in the heart position (arrow). Scale bar = 20 μm

A

B

C

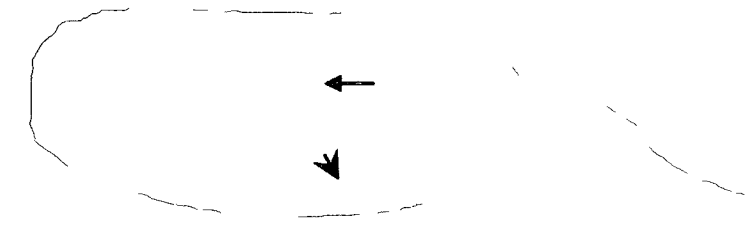

D

E

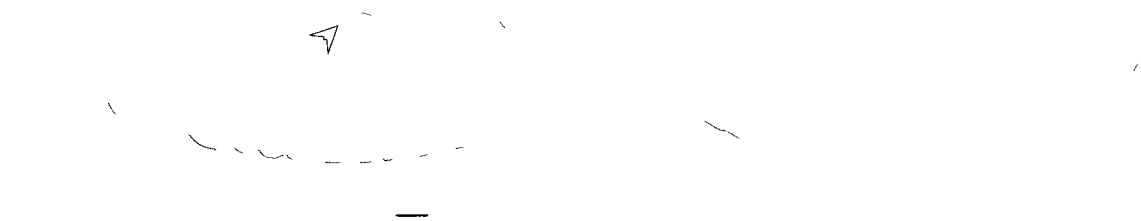

## Figure 13. Double-labeling using Dmef2 antibody and digoxigenin-labeled *DSLMAP* riboprobes

Panel A: dorsal view of wild-type stage 14 embryo anterior to the left: this embryo was double labelled with *D*mef2 - which is specific for cardioblasts and somatic muscles - and *DSLMAP* anti-sense riboprobe. Two rows of cardioblasts are clearly seen (arrows), in addition the somatic muscles are also detected (arrow head). Panel B: dorsal view of wild-type stage 14 embryo anterior to the left, this control embryo was double labelled with Dmef2 and *DSLMAP* sense riboprobe; two rows of the cardioblasts with no hybridization signal are seen (arrows), also the somatic muscles showing no signal (arrowhead). Scale bar = 20 μm

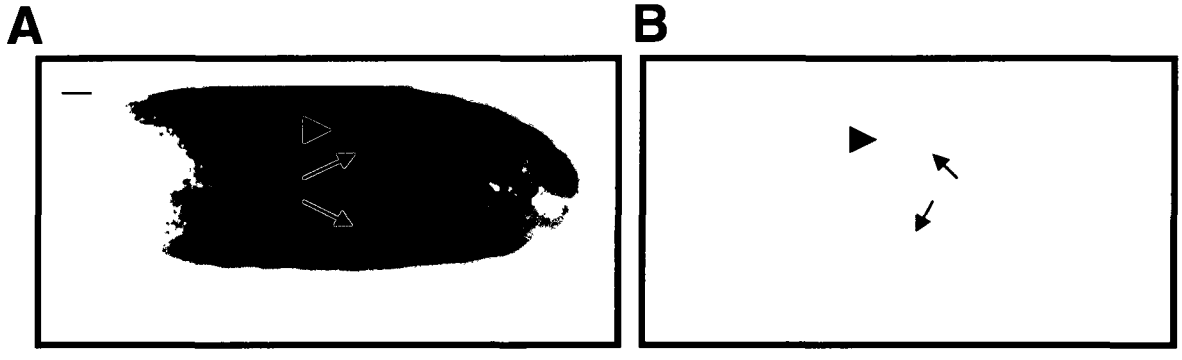
A
B

## 4.4 *DSLMAP* is expressed at all stages of *Drosophila* heart development

Dmef2/DSLMAP mRNA double labeling indicate that *DSLMAP* is expressed through all stages of *Drosophila* embryonic heart development. This expression did not appear to change from early stage 13 to stage 16. Double labeling with *D*mef2 antibody and *DSLMAP* mRNA riboprobes was detected from the beginning of embryonic heart formation at stage 13, suggesting that both are expressed in the CBs (Fig. 14 A, arrow). The double labeling was also noted in the somatic muscles as illustrated in (Fig. 14 A, arrow). *D*mef2 antibody was used to stain the CBs alone on another collection of wild type embryos at different stages of development. Immunostaining of CBs was obvious at stage 13 (Fig.14 A', arrow). The somatic muscles are also indicated as shown in (Fig.14 A', arrowheads).

Double labelling with *DSLMAP* mRNA and Dmef2 antibody is localized at the CBs, where two rows of cells are formed by stage 14 (Fig.14 B, arrows), and the somatic muscles are also indicated (Fig.14 B, arrowheads). At the same stage, *D*mef2 antibody staining similarly shows two rows of CBs, and the somatic muscles (Fig.14 B' arrows, arrowheads). CBs migrated dorsally as observed in the double labelling with Dmef2 antibody and DSLMAP riboprobe at stage 15 of embryonic development (Fig.14 C, arrow), and the somatic muscles are also double labelled as shown in (Fig.14 C, arrowheads). Similarly at the same stage, the anti-Dmef2 staining of the CBs showed that they migrate dorsally, and the somatic muscles are also indicated (Fig. 14 C' arrow, arrowheads). At stage 16, the double labelling showed that the CBs are aligned to form the heart tube as shown in (Fig. 14 D arrow), and the somatic muscles are shown in (Fig.

14 D arrowheads). Dmef2 antibody staining also illustrates that the CBs are forming the heart tube (Fig.14 D' arrow); the somatic muscles were also detected as shown in (Fig.14 D' arrowheads). This data illustrates that DSLMAP is expressed through the different stages of embryonic heart development in the CBs.

## 4.5 Down-regulation of DSLMAP mRNA using RNA interference in *Drosophila* heart

Flies carrying specific GAL4 heart driver TincΔ4GAL4, which is specific for CBs, were crossed to flies carrying UAS *DSLMAP* RNAi transgene in order to down-regulate mRNA expression of *DSLMAP* which was examined by *In situ* hybridization (Fig.15, A-B). Down-regulation of *DSLMAP* mRNA expression was observed through various stages of embryonic heart development. This expression was detected at stage 13, which is the beginning of heart tube development, in which a reduced intensity of anti-sense DSLMAP riboprobe was seen in the heart (Fig, 15 B, arrow), while increased intensity was seen in the CNS and hind gut as shown in (Fig, 15 B, arrowheads), compared to the wild type embryo which had a ubiquitous expression of *DSLMAP* transcript, as illustrated in (Fig. 15 A, arrow).

DSLMAP down-regulation using TincΔ4GAL4 heart driver showed 61.8% reduced intensity of anti sense *DSLMAP* riboprobe among 30 embryos, compared to wild type embryos which had only 13% reduced intensity of anti sense *DSLMAP* riboprobe (Fig.15 C).

Accordingly, DSLMAP mRNA expression using the specific heart driver showed that DSLMAP transcript intensity was reduced in *Drosophila* heart.

**Figure 14. *DSLMAP* mRNA expression doesn't change through *Drosophila* embryonic heart developments.**

Left panel: wild-type embryos double labelled with Dmef2 protein/*DSLMAP* riboprobe. Right panel: wild-type embryos immunolabelled with Dmef2 antibody alone. Arrows indicate the CBs, and arrowheads, somatic muscles. (A, A') Stage 13, sagittal view, (B, B') Stage 14, dorsal view, (C, C') Stage 15, sagittal view, (D, D') Stage 16, dorsal view. *DSLMAP* mRNA expression did not change during *Drosophila* heart development. At stage 13, CBs are seen with purple color, which indicates that both *D*mef2 and *DSLMAP* mRNA transcripts are hybridized where the CBs form a row of cells (A, arrow). The CBs stained with anti-*D*mef2 are also forming a row of cells, as shown in (A', arrow). At stage 14, the CBs are aligned in two rows of cells, as indicated with the double labelling in (B, arrows). Two rows of the CBs are_immunolabelled with *D*mef2 antibody (B' arrows). The CBs migrated dorsally at stage 15 as shown in (C, C' arrows), and the heart tube begin its formation at stage 16, where the CBs continued their alignment and migration towards their destination (D, D'). Scale bar =20 μm

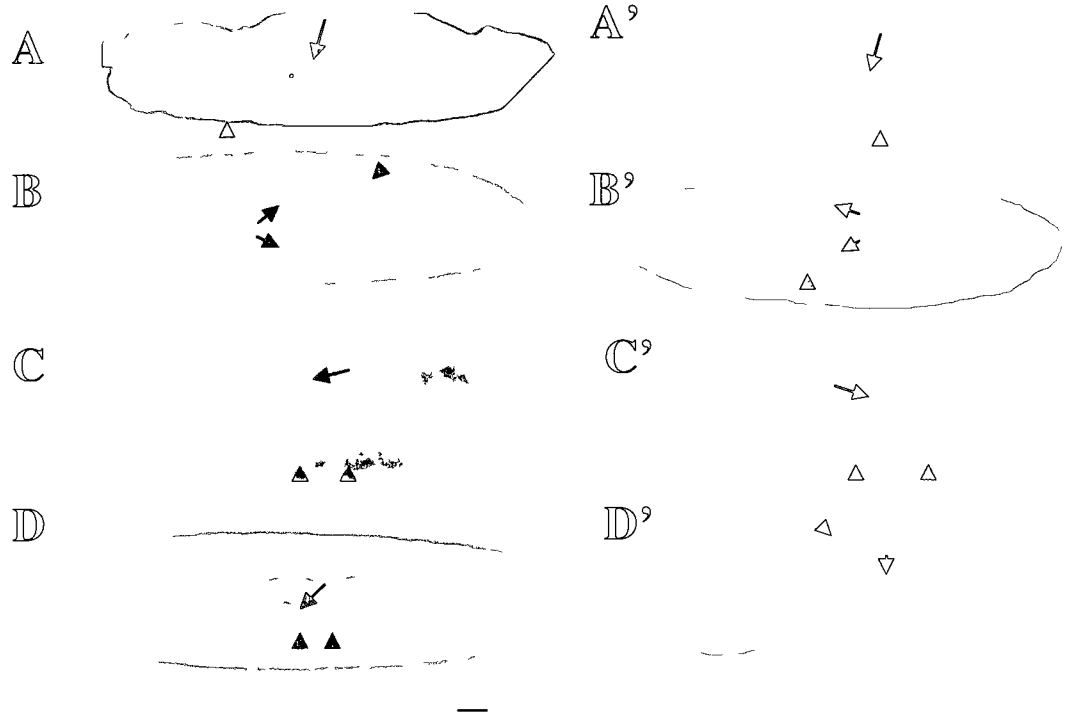
A
A'
B
B'
C
C'
D
D'

**Figure 15. Down-regulation of *DSLMAP* mRNA expression in *Drosophila* heart**

(A-B) Whole mount *in situ* hybridization performed on embryos at stage 13 using anti-sense *DSLMAP* riboprobe. All the embryos have a dorsal view, anterior is to the left. (A) Wild type embryo at stage 13, the intensity of the color did not change through the whole embryo and DSLMAP transcript is intense in the heart (arrow). (B) Obvious reduction in *DSLMAP* mRNA intensity in TincΔ4 Gal4/+;UAS *DSLMAP* RNAi/+ embryo is seen in the heart (arrow), compared to the darker staining which is seen in the nervous system, and the hind gut (arrow heads). (C) Quantitative analysis of *D*SLMAP down-regulated embryos compared to the wild type. Among 30 embryos, 61% of them had a reduction in DSLMAP mRNA intensity in DSLMAP down-regulated embryos driven by TincΔ4Gal4, compared to 13% in the wt embryos. Scale bar =20 μm

**A.**

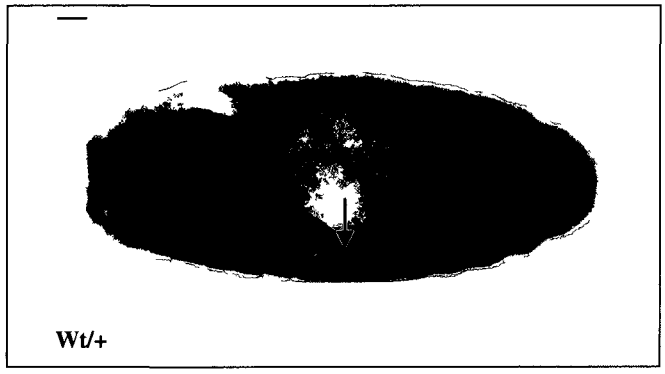
Wt/+

**B.**

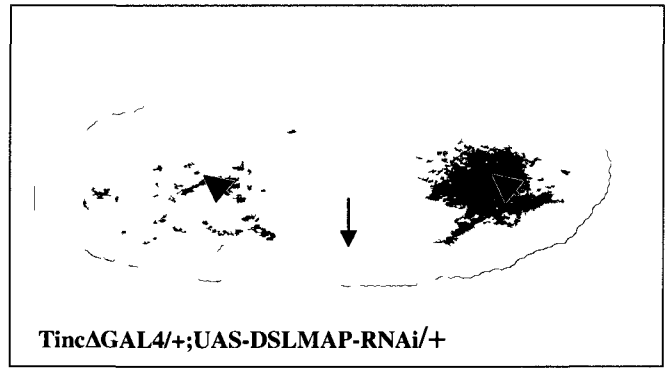
TincΔGAL4/+;UAS-DSLMAP-RNAi/+

**C.**

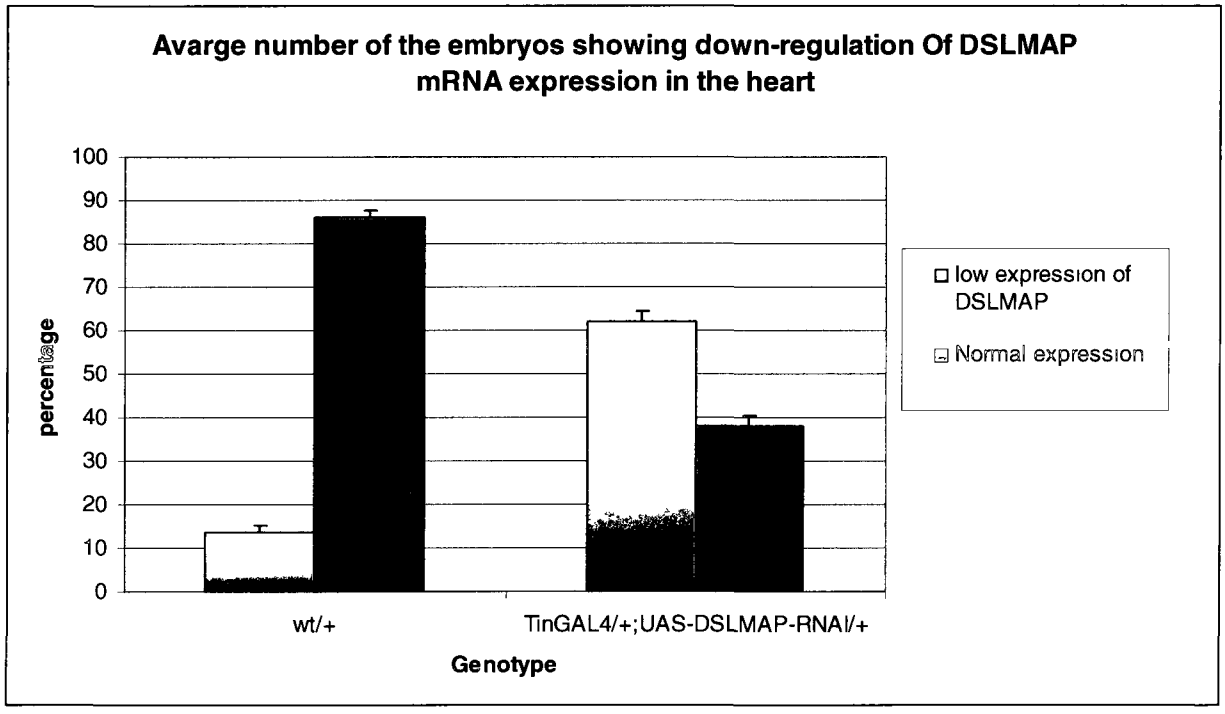
Avarge number of the embryos showing down-regulation Of DSLMAP mRNA expression in the heart
100
90
80
70
60
50
40
30
20
10
0
percentage
wt/+
TinGAL4/+;UAS-DSLMAP-RNAI/+
Genotype
low expression of DSLMAP
Normal expression

## 4.6 Confirmation of *DSLMAP* over-expression.

UAS-*DSLMAP* construct was tagged with HA (hemagglutinin) in order to detect *D*SLMAP protein. The UAS DSLMAP lines were generated in the lab, and tested for over-expression of DSLMAP in these lines, by crossing female flies carrying the pairedGAL4 driver to male flies carrying the UAS-DSLMAP transgene. The embryos were collected, fixed, and stained with HA antibody to detect the expressed DSLMAP protein (Fig. 16 A-B"). Anti-HA staining indicates that *DSLMAP* is expressed early during dorsal vessel morphogenesis where dorsal mesoderm is formed by stage 9. At this stage, HA antibody staining shows 7 stripes in *DSLMAP* over-expressed embryo (Fig.16 B, numbers). The detection of the stripes confirms the over-expression of *DSLMAP*, since control embryo at the same stage shows no stripes at all (Fig. 16, A).

## 4.7 Cardiac specific deregulation of *DSLMAP* caused defective heart tube formation

### 4.7.1 Cardiac specific *DSLMAP* down-regulation causes delayed migration and misalignment in both the CBs and the PCs

While a linear heart tube is noted in control embryos, a significant change in the morphology of the heart tube was seen in embryos carrying the UAS-*DSLMAP*-RNAi transgene as shown in (Fig. 17, 18). These changes were characterized by severe alignment and migration defects in heart cells. These defects included: delayed migration, clustering of cells (which include clumps of 2-3 cells, double rows), gaps, and twisted heart tube. Dmef2 antibody was used to stain CBs (red color) while Zfh1 antibody was used to stain PCs (green color).

## Figure 16. Confirmation of *D*SLMAP over-expression

(A-B) Saggital view of stage 9 embryos, anterior is to the left. (A) Control embryo of paired-GAL4 and $w^{118}$ stained with HA antibody, no stripes were observed. (B) *DSLMAP* over-expressed embryo driven by pairedGAL4 was tagged with HA tag, stripes that confirm the over-expression were detected using HA antibody, 7 stripes are shown at stage 9 (numbers). Scale bar =10 μm

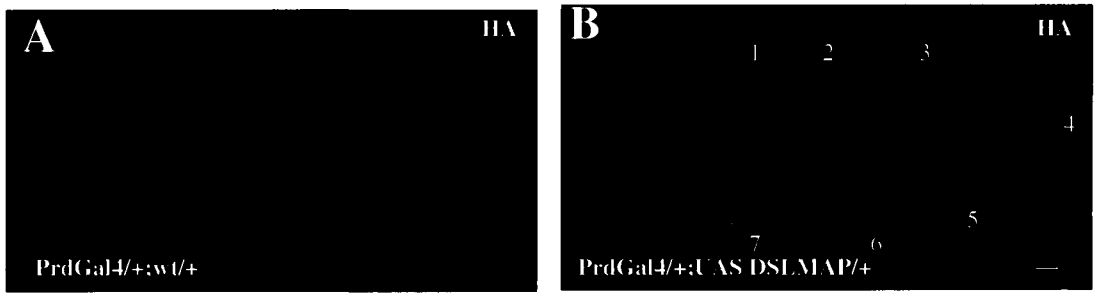
A
HA
PrdGal4/+;wt/+
B
HA
1
2
3
4
5
6
7
PrdGal4/+;UAS DSLMAP/+

When *DSLMAP* was down-regulated, heart cells were unable to go to their destination and migrate dorsally to form the heart tube; instead, they were either migrated inward or outward causing delays in heart tube assembly.

The two heart drivers used to derive the UAS-*DSLMAP*-RNAi transgene showed that there was a delayed migration in both the CBs and PCs. At stage 15, these cells seemed to fail to migrate in the right direction (Fig. 17, B, B' arrows), compared to the control embryo at the same stage (Fig. 17, A, A'). To quantify this defect penetrance (number of defective embryos divided by total number of counted embryos was calculated; among 65 embryos) TinGAL4; UAS-*DSLMAP*-RNAi demonstrated that 49.16% of the embryos were carrying this defect (Table.1, A). The expressivity, which is the number of the defects per embryo, was also calculated and reached up to 66.5% for the delayed migration in this cross as displayed in (Table.1, B).

PrcGAL4; UAS-*DSLMAP*-RNAi also showed delayed defects in PCs (Fig.18, B arrow) compared to control embryos at the same stage (Fig.18, A) and the penetrance for the delayed migration defects reached up to 47.4% among 65 embryos (Table.2, A). The expressivity of this defect in PCs reached up to 69.9%, as shown in (Table. 2, B). The CBs in this cross had also clustering/aggregation of 2-3 cells in one row of the CBs as shown in (Fig. 18, B), compared to the control embryo which had normal alignment (Fig. 18, A).

*DSLMAP* down-regulation using the two heart drivers showed alignment and migration defects in both cell types, which suggest a role of *DSLMAP* in organizing these cells during *Drosophila* heart development.

**Figure 17. *DSLMAP* down-regulation in the CBs results in delays in heart cells migration.**

(A-B") Stage 15 embryos, dorsal view, anterior to the left. (A) Control embryo stained with *D*mef2 specific for CBs and somatic muscles, showing normal CBs alignment (arrow). (B) Down-regulation of *DSLMAP* expression driven by TinGAL4 heart driver led to delayed migration in CBs (arrow). (A') Control embryo stained with Zfh1 antibody which is specific for PCs, where these cells have normal alignment (arrow). (B') Delayed migration defect is seen in the PCs (arrow). (A"-B") Double labelled with Dmef2 and Zfh1 antibodies. Scale bar = 10 μm

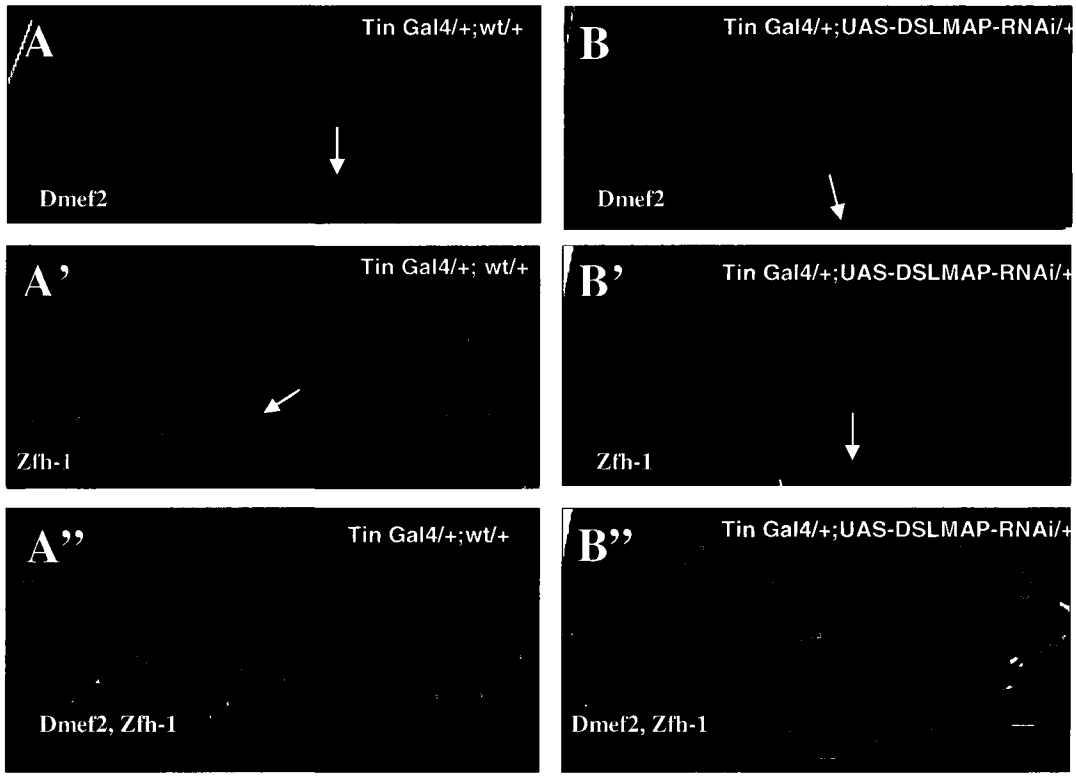
A
Tin Gal4/+;wt/+
Dmef2
B
Tin Gal4/+;UAS-DSLMAP-RNAi/+
Dmef2
A'
Tin Gal4/+; wt/+
Zfh-1
B'
Tin Gal4/+;UAS-DSLMAP-RNAi/+
Zfh-1
A''
Tin Gal4/+;wt/+
Dmef2, Zfh-1
B''
Tin Gal4/+;UAS-DSLMAP-RNAi/+
Dmef2, Zfh-1

**Figure 18. *DSLMAP* down-regulation in PCs results in defective heart tube**

(A-B") All the embryos are at stage 17, dorsal view, anterior to the left, Dmef2 antibody (red), Zfh1 antibody (green). (A-A") Control embryo of UAS DSLMAP RNAi and $w^{118}$embryos showing organized heart tube. (A) Control embryo showing an organized heart tube (arrow). (B) Down regulation of *DSLMAP* expression driven by Prc GAL4 heart driver resulted in clustering/aggregation of the CBs (arrow). (A') Control embryo which have organized PCs (arrow). (B') pericardial expression of UAS *DSLMAP* RNAi led to delayed migration in the PCs. (A"-B") Embryos double labelled with both antibodies. Scale bar =10 μm

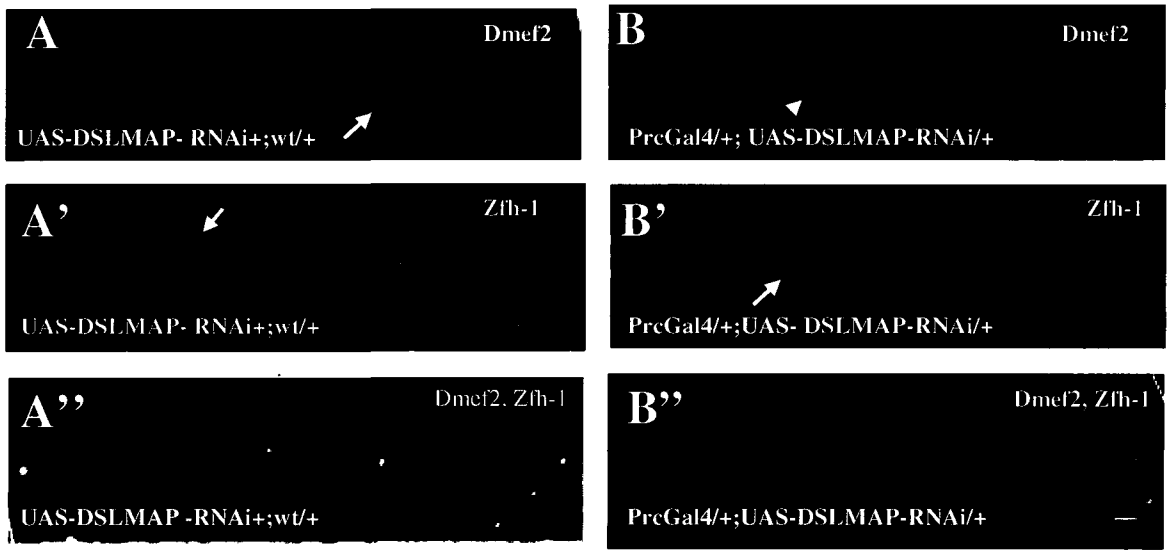
A
Dmef2
UAS-DSLMAP- RNAi+;wt/+
B
Dmef2
PrcGal4/+; UAS-DSLMAP-RNAi/+
A'
Zfh-1
UAS-DSLMAP- RNAi+;wt/+
B'
Zfh-1
PrcGal4/+;UAS- DSLMAP-RNAi/+
A''
Dmef2, Zfh-1
UAS-DSLMAP -RNAi+;wt/+
B''
Dmef2, Zfh-1
PrcGal4/+;UAS-DSLMAP-RNAi/+

### 4.7.2 Cardiac specific over-expression of *DSLMAP* causes defective heart tube development: potential effects on cardiac cell migration and fusion

In order to further address any defects which results from de-regulation of *DSLMAP* levels; over expression of *DSLMAP* in CBs was achieved by crossing TinGAl4 to the UAS lines (UAS line-4 and UAS line-10), and embryos were examined closely to quantify any effects on heart tube development (Fig. 19, 20 and 21) (Table. 1, 2).

At stage 14 of embryonic development, forced expression of UAS-*DSLMAP* in CBs (TinGAL4/+;UAS-*DSLMAP*-4/+) revealed that the CBs which were stained with Dmef2 antibody, had lost their columnar shape and many cells appeared to be aggregated or fused to the adjacent cell in each row, with a failure of dorsal closure (Fig. 19, B). This phenotype was detected in 32.2% of the embryos (n=65) as displayed in (Table.1, A), and the expressivity of this phenotype was ~ 35.29% (Table.1, B). On the other hand, the control embryos TinGAL4/+;wt/+ at the same developmental stage showed no defects in heart tube development (Fig. 19, A). Over-expression of *DSLMAP* in the CBs also had a secondary effect on the PCs which were stained with Zfh-1 antibody, where gaps between PCs were seen at the same stage (Fig. 19, B'), and the penetrance of this phenotype reached ~19.98% (n=65) as shown in (Table.2, A), while the expressivity reached up to 27.3% (Table.2, B).

Forced expression of *DSLMAP* in PCs using PrcGAL4 crossed with UAS-SLMAP line 4 also resulted in failure of dorsal closure, compared to the organized heart tube of the control embryo at the same stage (Fig. 20, A-B). PrcGAL4/+;UAS-DSLMAP/+ embryos showed delayed migration in the PCs which were labelled with Zfh-1 antibody compared

to the control embryos at the same stage (Fig. 20, A', B'). Pericardial expression of UAS-*DSLMAP* also exhibited secondary effects on the CBs which exhibited clustering/aggregation of the cells as shown in (Fig. 20, B). The penetrance for both phenotypes reached up to 47.85 and 13.76% respectively (Graph.1, A) and the expressivity was 56.75% and 47%, respectively (Table.1, B). Myocardial CB over-expression of *DSLMAP* (line 10), was also studied using TinGAL4, which revealed that the main defect was delayed migration in both cell types (Fig. 20, A-B") with a penetrance of up to 47.6% (Table.1, A), and the expressivity reached up to 63.4% as displayed in (Table1, B), in contrast to the control embryo at the same stage which shows a well developed heart tube as illustrated in (Fig, 21, A). Furthermore, the number of the CBs that reached the dorsal midline were counted and the average number of the CBs in *DSLMAP* over-expression was 97±1.8 (n=18), compared to wild type embryos, which had an average of 103±1.1 as shown in (Table.3). Accordingly, *DSLMAP* over-expression in CBs or PCs led to defects in heart cells alignment and migration, similar to those seen during *DSLMAP* down-regulation. These results indicate that a regulated amount of *DSLMAP* may be critical to ensure proper heart tube formation.

## 4.8 *DSLMAP* may serve a role in CBs adhesion and positioning

Spectrin is a cytoskeletal protein that resides at the intracellular side of the plasma membrane of different cell types. In *Drosophila,* α-Spectrin is localized to the basal-lateral surface of the myocardial epithelium and plays an important role in the determination of cell shape (Lee *et al.*, 1993). The CBs labelled with Dmef2 antibody have a columnar shape in wild type embryos.

## Figure 19. *DSLMAP* over-expression in CBs leads to fusion defects

*DSLMAP* over-expression results in different defects and one of the most interesting is fused CBs. (A-B") Embryos are at dorsal view stage 14, anterior to the left. (A) Control embryo heterozygous for Tin-GAL4 and $w^{118}$ stained with Dmef2. (B) Fused CBs are observed in UAS *DSLMAP* (line 4) driven by TinGAL4 (arrowhead). (A') Control embryo stained with Zfh1, which is specific for PCs. (B') Gaps between PCs are observed in the *DSLMAP* over-expressed embryo (arrowhead). (A"-B") Embryos are double-labelled with Dmef2 and Zfh1 antibodies. Scale bar = 10 μm

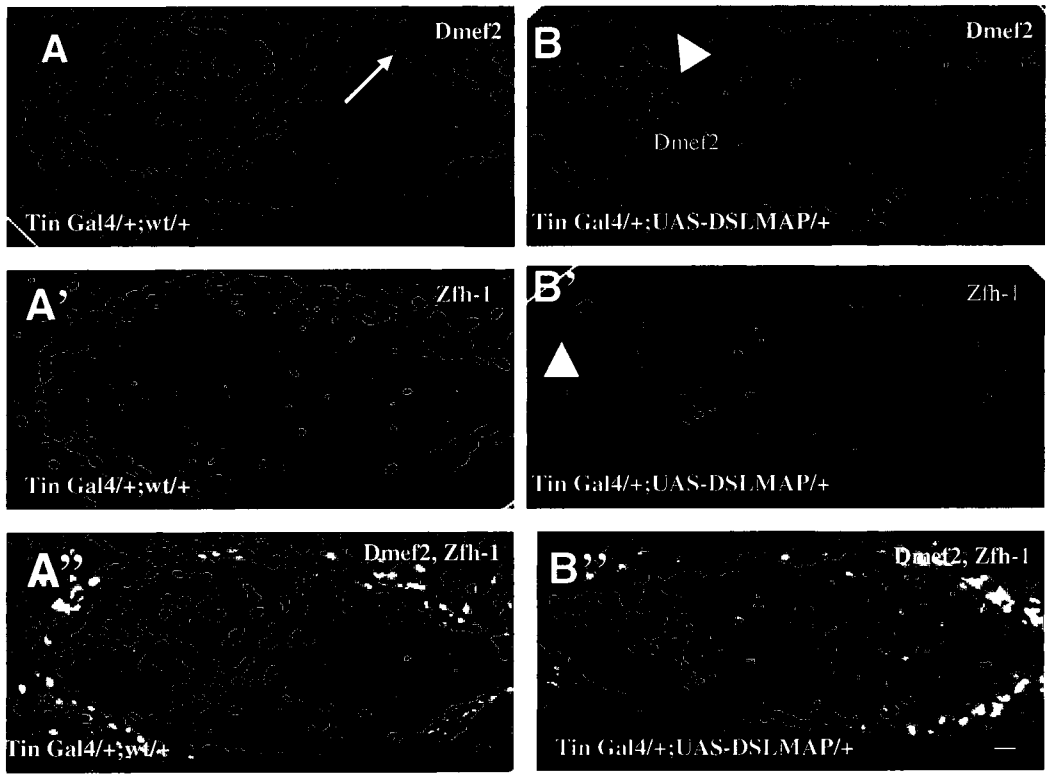
A
Dmef2
Tin Gal4/+;wt/+
B
Dmef2
Dmef2
Tin Gal4/+;UAS-DSLMAP/+
A'
Zfh-1
Tin Gal4/+;wt/+
B'
Zfh-1
Tin Gal4/+;UAS-DSLMAP/+
A''
Dmef2, Zfh-1
Tin Gal4/+;wt/+
B''
Dmef2, Zfh-1
Tin Gal4/+;UAS-DSLMAP/+

**Figure 20. *DSLMAP* over-expression in the PCs leads to delayed migration.**

(A-B") All of the embryos are at dorsal view, stage 14, anterior to the left. (A) Control embryo heterozygous for Prc-GAL4 and $w^{118}$ stained with Dmef2. (B) Clustered/clumps of 2-3 cells of the CBs are observed in UAS *DSLMAP* driven by Prc-GAL4 (white arrow). (A') Control embryo stained with Zfh1, which is specific for PCs. (B') Delays in PCs are observed in the same embryo (white arrow). (A"-B") Embryos are double-labelled with Dmef2 and Zfh1 antibodies. Scale bar = 10 μm

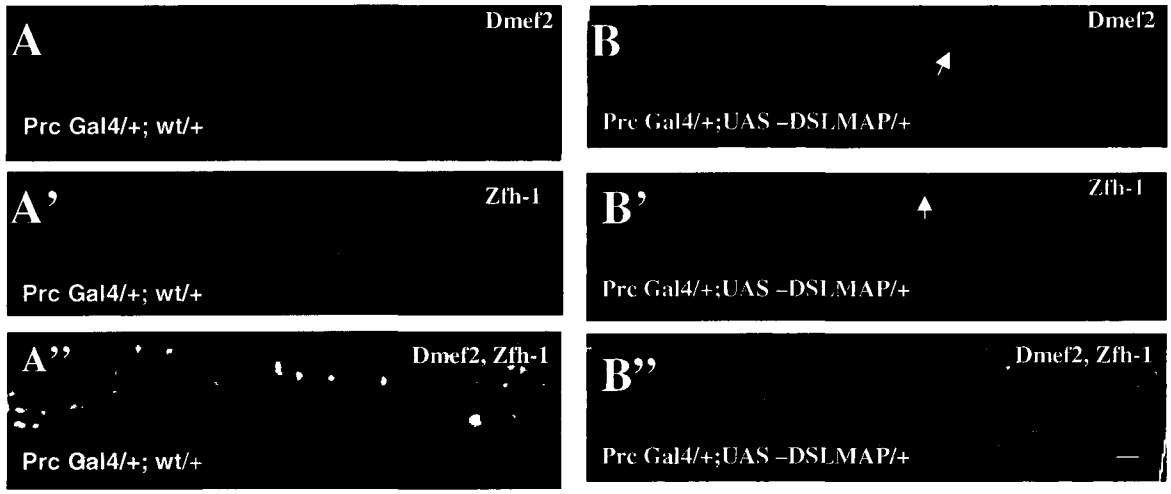
A
Dmef2
Prc Gal4/+; wt/+
B
Dmef2
Prc Gal4/+;UAS -DSLMAP/+
A'
Zfh-1
Prc Gal4/+; wt/+
B'
Zfh-1
Prc Gal4/+;UAS -DSLMAP/+
A''
Dmef2, Zfh-1
Prc Gal4/+; wt/+
B''
Dmef2, Zfh-1
Prc Gal4/+;UAS -DSLMAP/+

**Figure 21. *DSLMAP* over-expression leads to delayed migration in heart cells.**

*(*A-B") All of the embryos are at dorsal view stage 17, anterior to the left. (A) Control embryo heterozygous for Tin-GAL4 and $w^{118}$ stained with Dmef2. (B) Delayed migration defect in the CBs is observed in UAS *DSLMAP* (line10) driven by TinGAL4 (arrow). (A') Control embryo stained with Zfh1, which is specific for PCs. (B') Similar to CBs, delayed migration defect is also observed in PCs within the same embryo (arrow), in addition some gaps is seen between PCs (arrow head). (A"-B") Embryos are double labelled with Dmef2 and Zfh1 antibodies. Scale bar = 10 μm

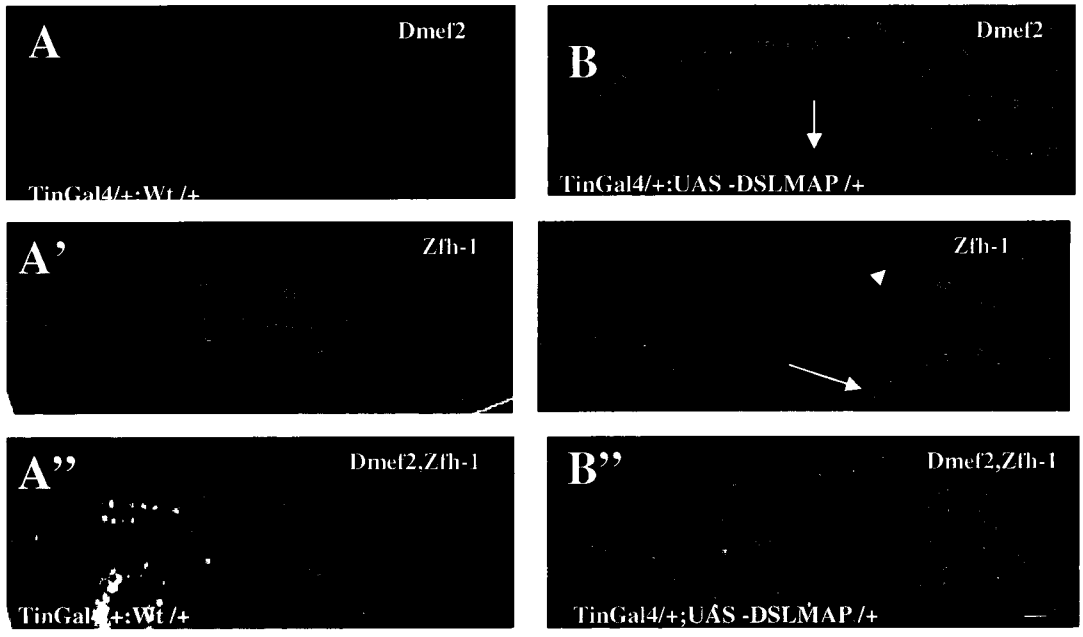
A
Dmef2
TinGal4/+:Wt /+
B
Dmef2
TinGal4/+:UAS -DSLMAP /+
A'
Zfh-1
Zfh-1
A''
Dmef2,Zfh-1
TinGal4/+:Wt /+
B''
Dmef2,Zfh-1
TinGal4/+;UAS -DSLMAP /+

## Table 1. Quantitative analysis of the defects observed in CBs for *DSLMAP* over-expression and down-regulation

Two heart drivers were used to examine the defects in both *DSLMAP* over-expression and down-regulation, which are: TincΔ4GAL4, and PrcGAL4. Embryos screened were from stage 14-17, and the sample size of the embryos was 65 for each cross. Two different lines of *DSLMAP* over-expression were used to examine the severity of the defects: line-4 and 10. (A) Penetrance for the phenotypes observed in CBs. Dmef2 antibody was used to stain the CBs. (B) Expressivity of the phenotypes observed in CBs. The expressivity of the delays for the two UAS-DSLMAP lines was similar: 62.8% and 63.9% respectively, but clustering of cells were higher for line-4 which reached up to 35%, but for line-10 it was 29.4%. RNAi line showed higher expressivity for the delayed migration defects in the CBs than the over expression lines, and reached up to 69.9%.

**A.** The penetrance of the phenotypes observed in the CBs

| Phenotypes / Genotype | Penetrance % (n=65) | | | | |
|---|---|---|---|---|---|
| | Delayed migration | Clustering of cells | Gaps | Twist | Non defective embryos |
| PrcGal4/+;wt/+ | 4.5 | 4.5 | 0 | 0 | 93.3 |
| TinGal4/+;wt/+ | 9 | 0 | 4.5 | 0 | 95 |
| UAS-DSLMAP-4/+;wt/+ | 0 | 4.5 | 9 | 4.5 | 93.3 |
| UAS-DSLMAP-10/+;wt/+ | 9 | 4.5 | 0 | 0 | 96.6 |
| UAS-DSLMAP-RNAi/+;wt/+ | 9 | 4.5 | 0 | 4.5 | 95 |
| PrcGal4/+;UAS-DSLMAP-RNAi/+ | 47.7 | 15.36 | 16.95 | 9. 16 | 21.49 |
| TinGal4/+;UAS-DSLMAP-RNAi/+ | 49.16 | 23.01 | 15.36 | 16.94 | 24.6 |
| TinGal4/+;UASDSLMAP-4/+ | 48.46 | 32.2 | 15.4 | 12.34 | 18.45 |
| TinGal4/+;UASDSLMAP-10/+ | 51.46 | 13.6 | 13.79 | 9.5 | 19.98 |
| PrcGal4/+;UAS-DSLMAP-4/+ | 47.8 | 21.5 | 13.7 | 12.2 | 19.91 |

**B.** The expressivity of the phenotypes observed in the CBs

| Phenotypes / Genotypes | Expressivity% | | | |
|---|---|---|---|---|
| | Delayed migration | Clustering of cells | Gaps | Twist |
| PrcGal4/+;UAS-DSLMAP-RNAi/+ | 66.5 | 25.4 | 25 | 13.3 |
| TinGal4/+;UAS-DSLMAP-RNAi/+ | 69.9 | 52 | 37.5 | 15.82 |
| TinGal4/+;UASDSLMAP-4/+ | 62.89 | 29.4 | 22.2 | 15.5 |
| TinGal4/+;UASDSLMAP-10/+ | 63.4 | 35.29 | 27.7 | 13.49 |
| PrcGal4/+;UAS-DSLMAP-4/+ | 56.75 | 47 | 25 | 15.5 |

## Table 2. Quantitative analysis of the defects observed in pericardial cells for *DSLMAP* over-expression and down-regulation

Both TincΔ4GAL4 and PrcGAL4Two heart drivers were used to examine the defects in both *DSLMAP* over-expression and down-regulation. Embryos screened were from stage 14-17, and the sample sizes of the embryos were 65 for each cross. In addition two different lines of DSLMAP over-expression were used to examine the severity of the defects which are line-4 and line-10. (A) Penetrance of the phenotypes observed in pericardial cells. Zfh-1 antibody was used to stain these cells. The penetrance for the delayed migration was the highest among all the phenotypes.

(B) The expressivity of the phenotypes observed in pericardial cells. The expressivity of the delayed migration reached up to 57.1% in PrcGAL4/+;UAS-DSLMAP-4/+, and 55.7% in TinGAL4/+;UAS-DSLMAP-4/+, and it was higher in TinGAL4/+;UAS-DSLMAP-10/+ where it reached up to 61.5%, while in TinGAL4/+;UAS-DSLMAP-RNAi/+ it was 56.3%, and in PrcGAL4/+;UAS-DSLMAP-RNAi/+ it reached up to 57.1%. Lower expressivity was seen in the other phenotypes. The error bars represent slandered error of the mean.

**A.**

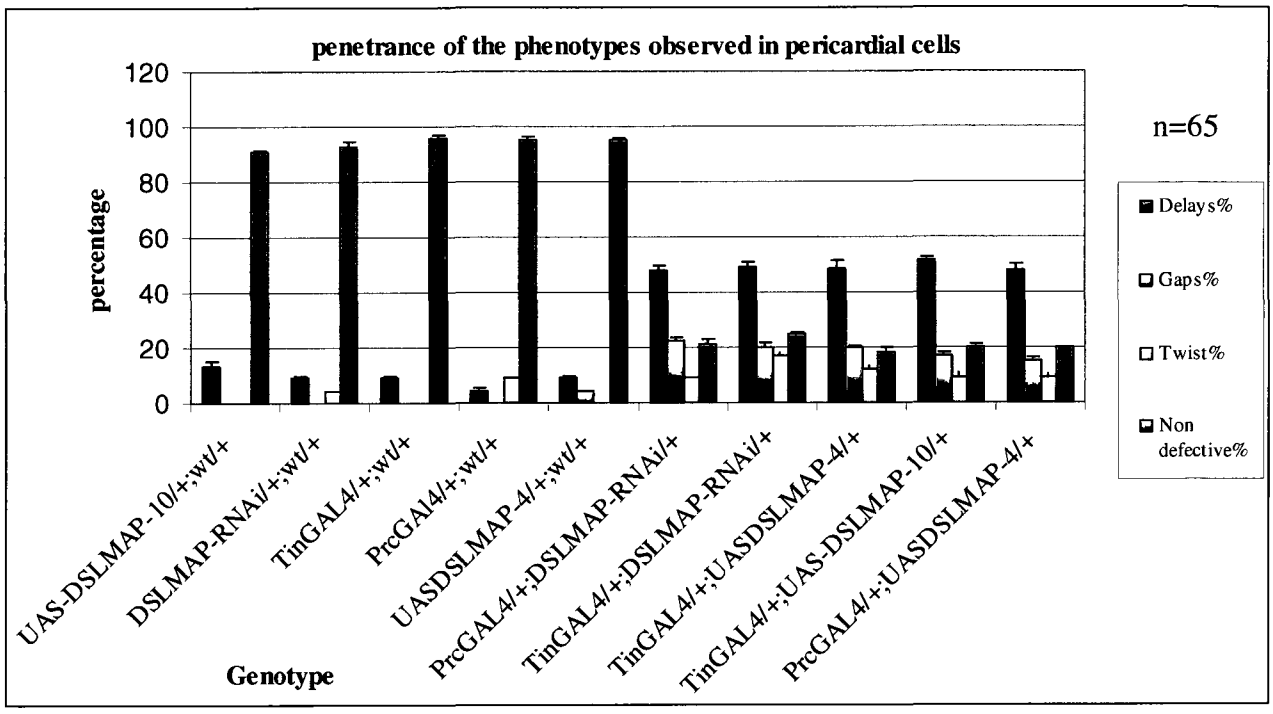
penetrance of the phenotypes observed in pericardial cells
120
100
80
60
40
20
0
percentage
n=65
Delays%
Gaps%
Twist%
Non defective%
UAS-DSLMAP-10/+;wt/+
DSLMAP-RNAi/+;wt/+
TinGAL4/+;wt/+
PrcGAl4/+;wt/+
UASDSLMAP-4/+;wt/+
PrcGAL4/+;DSLMAP-RNAi/+
TinGAL4/+;DSLMAP-RNAi/+
TinGAL4/+;UASDSLMAP-4/+
TinGAL4/+;UAS-DSLMAP-10/+
PrcGAL4/+;UASDSLMAP-4/+
Genotype

**B.**

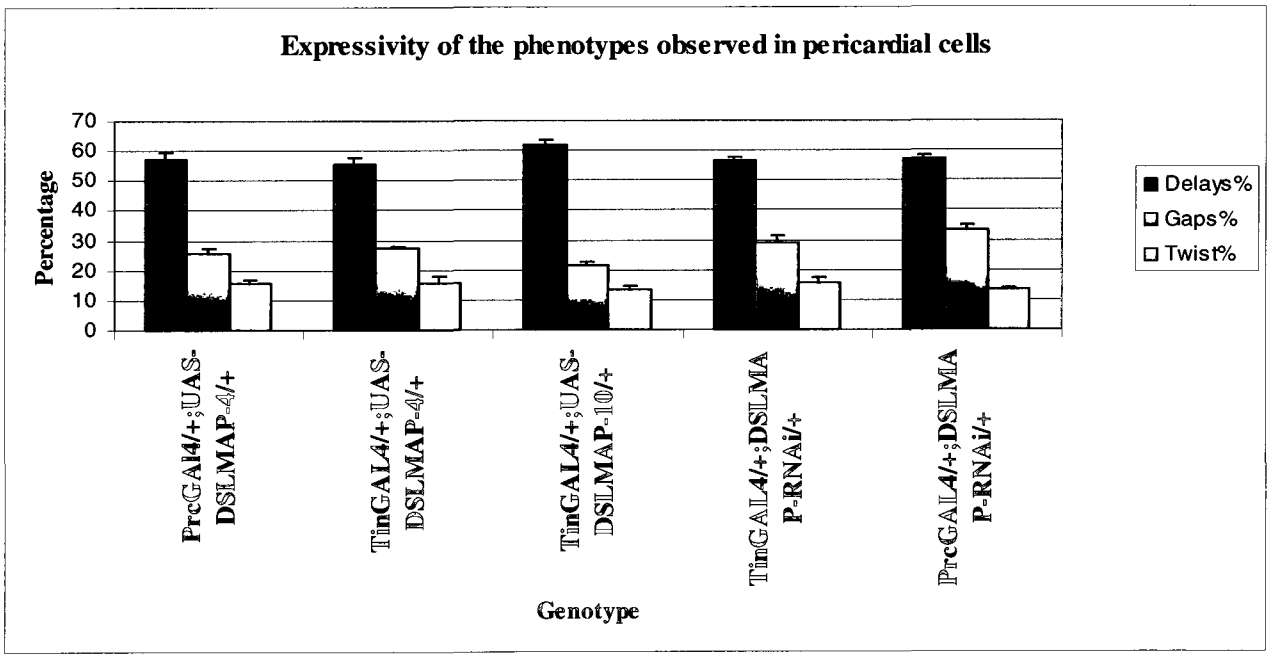
Expressivity of the phenotypes observed in pericardial cells
70
60
50
40
30
20
10
0
Percentage
Delays%
Gaps%
Twist%
PrcGAl4/+;UAS-DSLMAP-4/+
TinGAL4/+;UAS-DSLMAP-4/+
TinGAL4/+;UAS-DSLMAP-10/+
TinGAL4/+;DSLMA P-RNAi/+
PrcGAL4/+;DSLMA P-RNAi/+
Genotype

## Table 3. CB numbers observed in *DSLMAP* over-expression and down regulation

Changed expression of *DSLMAP* affected the number of CBs that reached the dorsal midline, at stage 17 of embryonic development. This Table shows that both *DSLMAP* over-expression and down-regulation had a reduced number of the CBs, reaching up to 97 ± 1.8, and 97± 1.5, respectively. The number of the CBs for wild type embryos at the same stage reached up to 103±1.1. The P-value was calculated using the unpaired t-test, where it was 0.001 for *DSLMAP* over-expression, and 0.0022 for *DSLMAP* down-regulation, both of which are considered as significant P-values. The error bars represent slandered error of the mean.

**A**

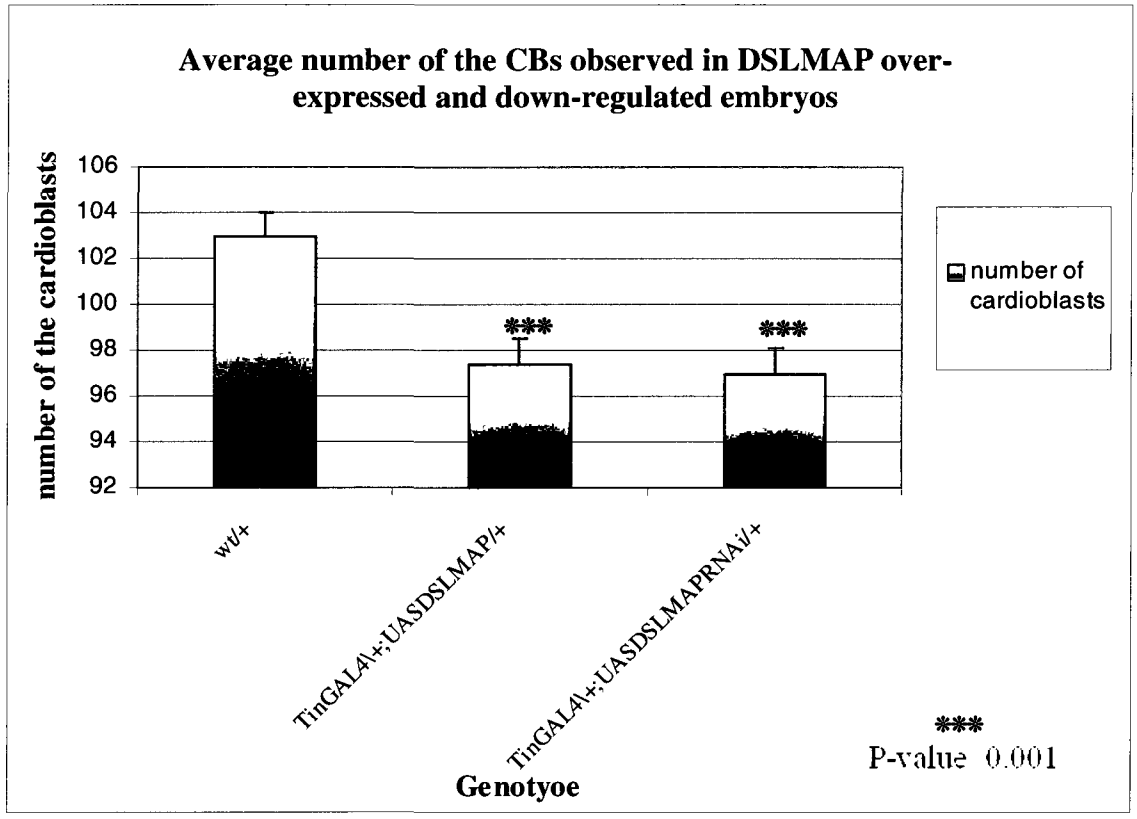
Average number of the CBs observed in DSLMAP over-expressed and down-regulated embryos
number of the cardioblasts
106
104
102
100
98
96
94
92
***
***
number of cardioblasts
wt/+
TinGAL4/+;UASDSLMAP/+
TinGAL4/+;UASDSLMAPRNAi/+
Genotyoe
***
P-value 0.001

α-Spectrin antibody which labels the cell membrane was used to detect changes in the shape of the CBs when *DSLMAP* is over-expressed or down-regulated (Fig. 22, 23). Targeted over-expression of *DSLMAP* resulted in remarkable alteration in CBs shape, positioning, and adhesion. The CBs were aggregated to each other compared to those seen in the control embryo at the same stage (Fig. 22 A, A' arrow). α-Spectrin antibody staining showed that some of the CBs had lost their columnar shape, and some were not surrounded by the cell membrane compared to the control embryo at the same stage (Fig.22, A", B" arrow). Similarly down-regulation of DSLMAP caused an obvious change in the cell shape and positioning. The CBs were clustered to each other, and the alignment was perturbed compared to the control embryo at the same stage (Fig.23 A, and A' arrow). Labelling with α-spectrin showed that some of the CBs are sharing the same cell membrane because of the aggregation of these cells, also the shape of these cells seemed to be changed, as it was no longer columnar (Fig 23 A", and B" arrow). This data suggests that the morphology of the heart tube changes as a result of changes in properties such as shape and aggregation of CBs ( examined by α-spectrin staining) when DSLMAP is de-regulated.

## 4.9 *Down*-regulation of *DSLMAP* or *Robo* results in similar cardiac defects

It has already been shown that *DSLMAP* genetically interacts with the Slit/Robo pathway in the CNS in *Drosophila* (Dawood *et al.*, 2007). In order to study the relationship between *D*SLMAP and the Slit/Robo pathway in *Drosophila* heart; I first compared the phenotypes that resulted from crossing PrcGAL4 to UAS-D*SLMAP*-RNAi, with the phenotypes that resulted from crossing PrcGAL4 to UAS-*Robo*-RNAi transgene.

**Figure 22. Over-expression of *DSLMAP* changes the cell membrane of the CBs.**

The cell membrane in embryos having over-expression of *DSLMAP* is different from the control embryo at the same stage. (A-B'") embryos are at stage 14, dorsal view anterior to the left. (A) Control embryo stained with Dmef2. (B) Over-expression in *DSLMAP* leads to fused CBs (arrow), compared to the control embryo at the same stage. (A') Control embryo stained with α-spectrin, which is specific for cell membrane. (B') Cell membrane stained with α-spectrin in over-expressed *DSLMAP* embryo, changes in the cell membrane are observed (arrow). (A") Control embryo double-labelled with Dmef2 and α-spectrin in wild type embryo. (B") Over-expressed *DSLMAP* embryo double labelled with Dmef2 and α-spectrin, some of the cells are sharing the same cell membrane because of fusion (arrow). (A''' and B''') magnification of A" and B", with higher magnification you can clearly see the space between the cells in *DSLMAP* over-expressed embryos compared to the control embryos (arrow). Scale bar =10 μm

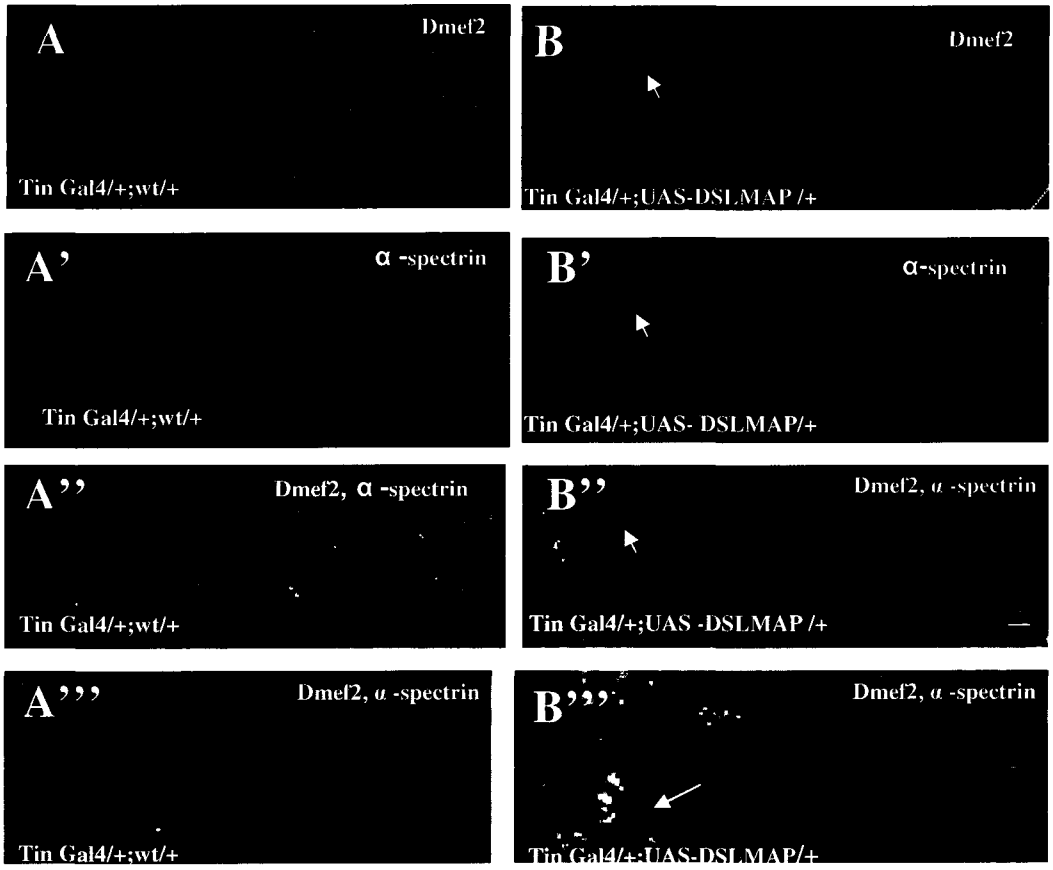
A
Dmef2
Tin Gal4/+;wt/+
B
Dmef2
Tin Gal4/+;UAS-DSLMAP /+
A'
α -spectrin
Tin Gal4/+;wt/+
B'
α-spectrin
Tin Gal4/+;UAS- DSLMAP/+
A''
Dmef2, α -spectrin
Tin Gal4/+;wt/+
B''
Dmef2, α -spectrin
Tin Gal4/+;UAS -DSLMAP /+
A'''
Dmef2, α -spectrin
Tin Gal4/+;wt/+
B'''
Dmef2, α -spectrin
Tin Gal4/+;UAS-DSLMAP/+

## Figure 23. Down-regulation of *DSLMAP* alters the cell membrane of the CBs

Defective cell membrane is seen when DSLMAP is down-regulated compared to the wild type. (A-B"') Embryos are at stage 15, dorsal view, anterior to the left. (A) Control embryo stained with Dmef2. (B) Changes in the shape of the CBs compared to the wild type at the same stage are seen (arrow). (A') Control embryo stained with α-spectrin which is specific for cell membrane. (B') Cell membrane stained with α-spectrin in down-regulated *DSLMAP* embryo, changes in the cell membrane are seen (arrow). (A") Control embryo double-labelled with Dmef2 and α-spectrin. (B") Down-regulated *DSLMAP* embryo is double-labelled with Dmef2, and α-spectrin. (A"'-B"') Magnification of the control embryo and *DSLMAP* down-regulated embryos double-labelled with *D*mef2, and α-spectrin in *DSLMAP* down-regulated embryos; there are some cells sharing the same cell membrane (arrow), compared to the control embryo, which has organized alignment of CBs surrounded by the cell membrane (arrow). Scale bar =10 μm

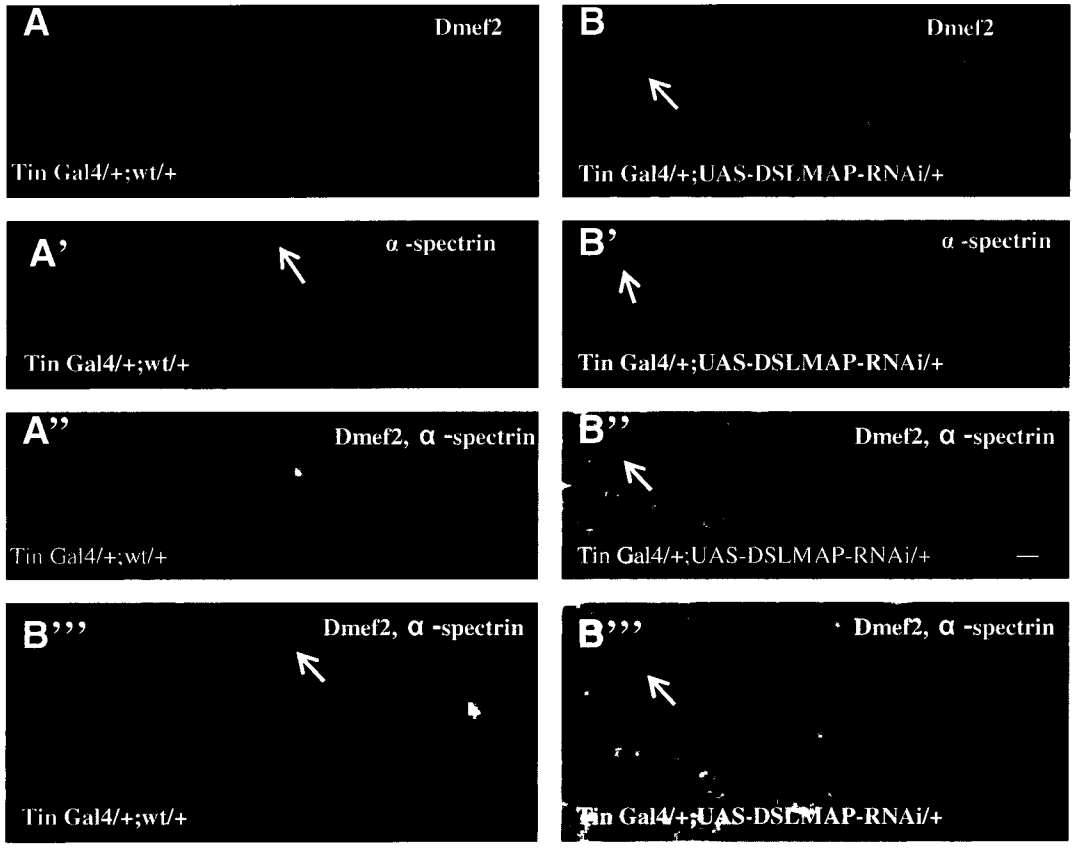
A
Dmef2
Tin Gal4/+;wt/+
B
Dmef2
Tin Gal4/+;UAS-DSLMAP-RNAi/+
A'
α -spectrin
Tin Gal4/+;wt/+
B'
α -spectrin
Tin Gal4/+;UAS-DSLMAP-RNAi/+
A''
Dmef2, α -spectrin
Tin Gal4/+;wt/+
B''
Dmef2, α -spectrin
Tin Gal4/+;UAS-DSLMAP-RNAi/+
B'''
Dmef2, α -spectrin
Tin Gal4/+;wt/+
B'''
Dmef2, α -spectrin
Tin Gal4/+;UAS-DSLMAP-RNAi/+

PrcGAL4/+;UAS-RoboRNAi/+ showed delayed migration in the PCs compared to the control embryo at the same stage as displayed in (Fig. 24 A', and B' arrow). Similarly when *DSLAMP was* down-regulated, delayed migration in the PCs was observed at the same stage as shown in (Fig. 24 C' arrow). The penetrance of the delays in Robo down-regulated embryos reached ~33.8 %( n=65) (Table. 4 A) and the expressivity was ~ 55.3% as illustrated in (Table. 4, B). The CBs also appeared to be affected by the pericardial down regulation of Robo expression where these cells had a failure of dorsal closure compared to the control embryo at the same stage, as shown in (Fig. 24 A, and B). Similar findings were seen in *DSLMAP* down-regulated embryos, where the CBs had failure of dorsal closure compared to the control embryos, as shown in (Fig. 24 A, and C). TinGAL4 heart drivers were also used to compare the phenotypes obtained from *DSLMAP* or *Robo* down-regulation, where TinGAL4 driver were crossed to UAS-DSLMAP-RNAi transgene, and to UAS-*Robo*-RNAi transgene. Both of these crosses had similar phenotypes as illustrated in (Fig. 24 E-G"). The CBs had delayed migration defects, and aggregation of the CBs in both Robo down-regulation, or *DSLMAP* down regulation compared to the organised CBs rows in the control embryo as shown in (Fig. 24 E, F, and G arrows). Down-regulation of *DSLMAP* or *Robo* had a secondary effect on the PCs which also had delayed migration defects compared to the control embryo at the same stage as displayed in (Fig. 24 E', F', and G' arrows). The penetrance of the delayed migration in *Robo* down-regulation reached ~ 33.8% , and the expressivity of this defect in the CBs reached ~54.54%, while in the PCs it reached 55.3% as shown in (Table 4,5 A and B). These results indicate that similar defects in heart tube development are noted, with the targeted down regulation of *DSLMAP* or *Robo* in heart cells.

**Figure 24. Phenotypes observed in *DSLMAP* down-regulation or *Robo* down-regulation.**

The phenotypes in *DSLMAP* down-regulation and Robo down-regulation were thoroughly examined using PrcGAl4, and TinGAL4 heart drivers as illustrated in (A-G"). Embryos are at stage 17, anterior to the left, dorsal view. Anti-*D*mef2 was used to label the CBs (red), and Zfh-1 was used to mark the PCs (green). (A) PrcGAL4 crossed to the wild type was used as a control. (B) *Robo* Down-regulation caused failure of dorsal closure in the CBs rows (arrow). (C) *DSLMAP* down-regulation also resulted in failure of dorsal closure in the CBs (arrow). (A') control embryo stained with Zfh1, which is specific for PCs. (B') *Robo* down-regulation in the PCs, led to delayed migration in these cells (star). (C') Similar defects are observed in PCs in *DSLMAP* down-regulated embryo (arrow). (A"), (B"), and (C") Embryos are double-labelled with *D*mef2 and Zfh1 antibodies. (E) TinGAL4 crossed to the wild type was used as a control. (F) *Robo* down regulation in the CBs led to aggregation of these cells and to delayed migration in the CBs rows (arrow). (G) *DSLMAP* down-regulation also had clustering/aggregation of the CBs and failure of dorsal closure (arrow). (E') Control embryo stained with Zfh-1 antibody. (F') Robo down regulation using Tin Gal4 also had a secondary effect in the PCs, where these cells had delayed migration defects (arrow). (G') *DSLMAP* down-regulation using TinGAL4 also had a secondary effect on the PCs, and resulted in delayed migration defects in these cells (arrow). (E"), (F"), and (G") embryos are labelled with *D*mef2 and Zfh-1 antibodies.

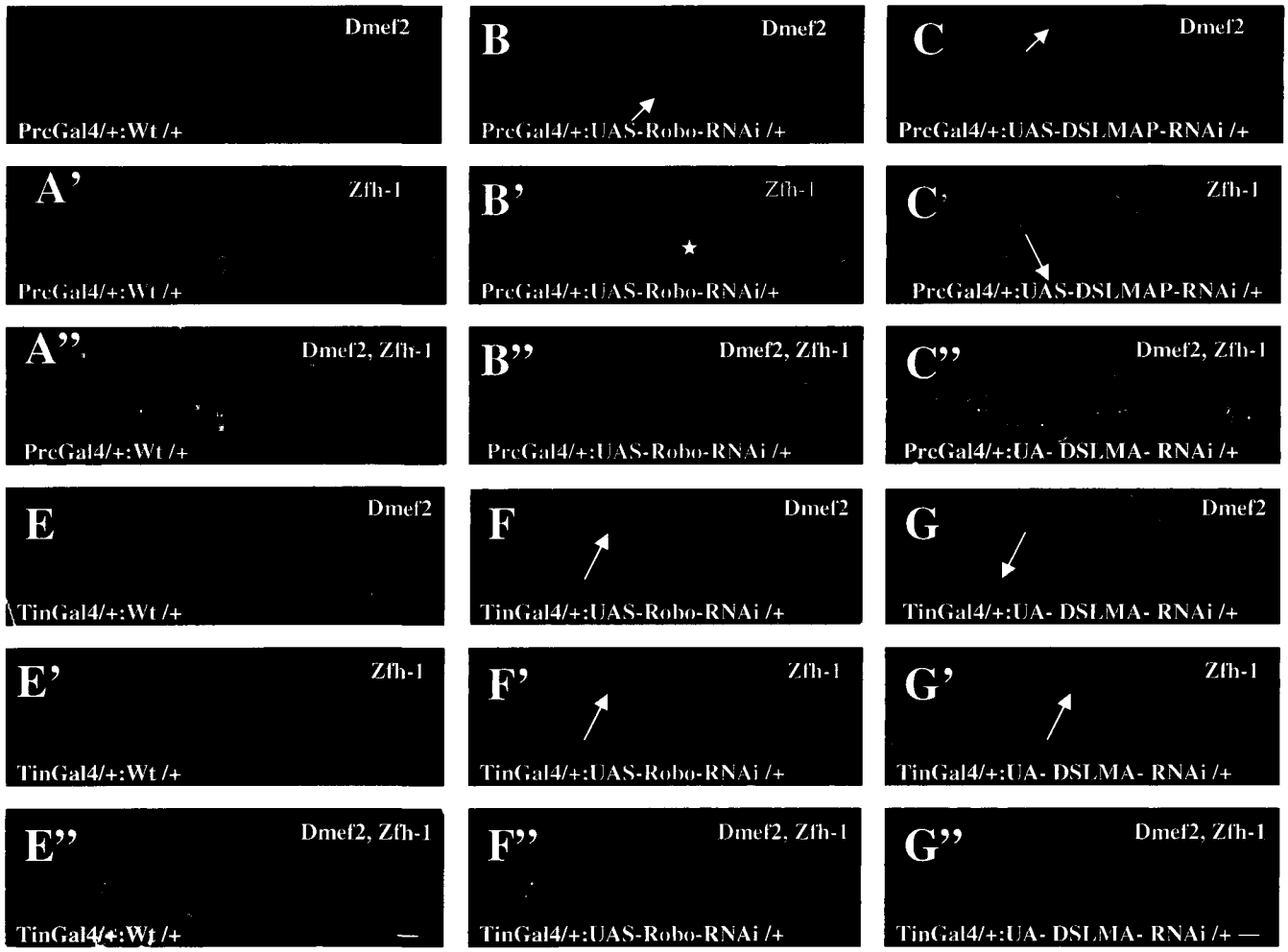
Dmef2
PrcGal4/+:Wt /+
B
Dmef2
PrcGal4/+:UAS-Robo-RNAi /+
C
Dmef2
PrcGal4/+:UAS-DSLMAP-RNAi /+
A'
Zfh-1
PrcGal4/+:Wt /+
B'
Zfh-1
PrcGal4/+:UAS-Robo-RNAi/+
C'
Zfh-1
PrcGal4/+:UAS-DSLMAP-RNAi /+
A''
Dmef2, Zfh-1
PrcGal4/+:Wt /+
B''
Dmef2, Zfh-1
PrcGal4/+:UAS-Robo-RNAi /+
C''
Dmef2, Zfh-1
PrcGal4/+:UA- DSLMA- RNAi /+
E
Dmef2
TinGal4/+:Wt /+
F
Dmef2
TinGal4/+:UAS-Robo-RNAi /+
G
Dmef2
TinGal4/+:UA- DSLMA- RNAi /+
E'
Zfh-1
TinGal4/+:Wt /+
F'
Zfh-1
TinGal4/+:UAS-Robo-RNAi /+
G'
Zfh-1
TinGal4/+:UA- DSLMA- RNAi /+
E''
Dmef2, Zfh-1
TinGal4/+:Wt /+
F''
Dmef2, Zfh-1
TinGal4/+:UAS-Robo-RNAi /+
G''
Dmef2, Zfh-1
TinGal4/+:UA- DSLMA- RNAi /+

## 4.10 Robo is mislocalized in *DSLMAP* down-regulated embryos

To investigate whether *DSLMAP* down-regulation in CBs or PCs affects Robo localization, embryos generated from crossing TinGAl4 with UAS-*DSLMAP*-RNAi, and PrcGAL4 with UAS-*DSLMAP*-RNAi were examined for Robo protein. Dmef2 antibody was used to stain the CBs, while Zfh-1 antibody was used to mark the PCs, and Robo antibody was used to examine Robo localization as shown in (Fig. 25 A-D"). In wild type embryos Robo is localized on the apical surface of CBs as shown in (Fig. A"). In embryos derived from the TinGAL4/+;UAS-DSLMAP-RNAi lines, Robo is not localized in the lumen compared to the control embryo at the same stage (Fig. 25 A, and B). The CBs in this cross had delayed migration compared to the control embryo at the same stage (Fig. 25 B, and B'). Similar data was observed in PrcGAL4/+;UAS-*DSLMAP*-RNAi/+, where Robo localization was altered in these embryos compared to the control embryo at the same stage (Fig. 25 C'', and D"). The PCs in this cross had a delayed migration compared to the control embryo at the same stage as demonstrated in (Fig. 25 C', and D').

Accordingly, DSLMAP down-regulation alters the localization of Robo, and this may impact the migration and alignment defects that occurred to the cardiac cells, and result in defective heart tube formation.

## 4.11 Targeted over-expression of *DSLMAP* has similar cardiac defects as Slit over-expression

To address any potential relationship between *D*SLMAP and Slit during heart development, the phenotypes generated from targeted over-expression of *DSLMAP* were compared to the phenotypes that resulted from Slit over-expression.

## Figure 25. Robo localization during DSLMAP down-regulation

DSLMAP down-regulation was found to affect Robo localization at stage 17 of heart development. (A-D") Embryos are at stage 17, anterior to the left, dorsal view. (A) Control embryo of TinGAL4/+;wt/+ stained with Robo shows the localization of Robo concentrated in the lumen of the heart (arrow). (B) *DSLMAP* down-regulated embryo stained with Robo. The localization of Robo is altered, as it's no longer localized in the lumen, but is instead moved outside the lumen as shown by (arrow). (A') Control embryo stained with Dmef2 shows organized CBs (arrow). (B') *DSLMAP* down-regulated embryo stained with Dmef2 shows delayed migration of the CBs (arrow). (A") Control embryo double labelled with robo and ZFh1. Robo is localized in the lumen between the CBs. (B") Down-regulated *DSLMAP* embryo double-labelled with Robo and Dmef2. Robo localization is changed compared to control embryo (arrow). (C) Control embryo of Prc, Robo is localized in the lumen of the heart (arrow). (D) *DSLMAP* down-regulated embryo shows alteration in Robo localization compared to control embryo at the same stage. (C') Control embryo stained with Zfh-1 shows non defective PCs. (D') *DSLMAP* down-regulated embryo has a delayed migration in PCs. (C") Robo is localized in the center of the lumen in control embryo. (D") Robo localization is altered in DSLMAP down regulated embryo using PrcGal4 heart driver.

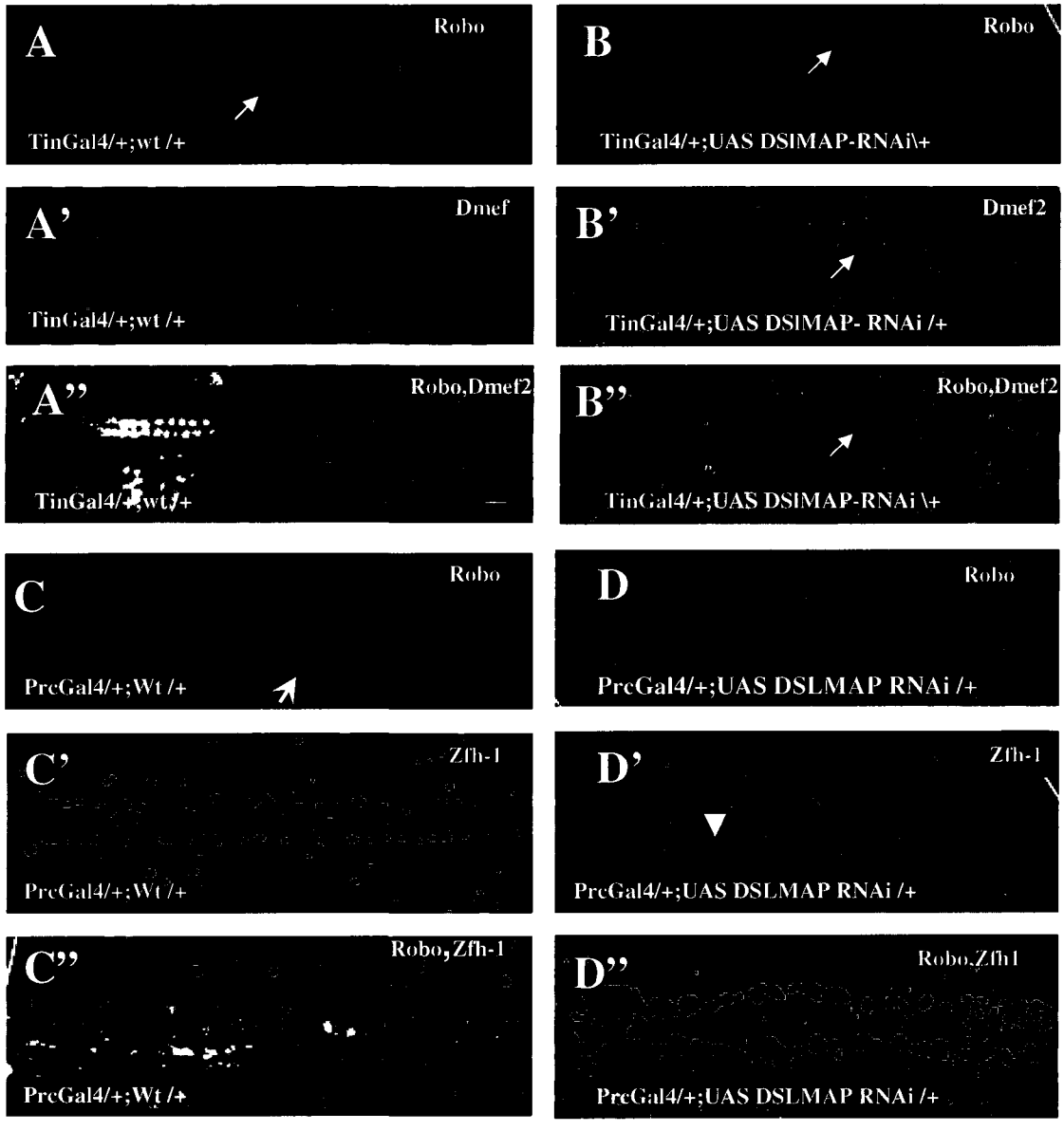
A
Robo
TinGal4/+;wt /+
B
Robo
TinGal4/+;UAS DSIMAP-RNAi\+
A'
Dmef
TinGal4/+;wt /+
B'
Dmef2
TinGal4/+;UAS DSIMAP- RNAi /+
A''
Robo,Dmef2
TinGal4/+;wt /+
B''
Robo,Dmef2
TinGal4/+;UAS DSIMAP-RNAi \+
C
Robo
PrcGal4/+;Wt /+
D
Robo
PrcGal4/+;UAS DSLMAP RNAi /+
C'
Zfh-1
PrcGal4/+;Wt /+
D'
Zfh-1
PrcGal4/+;UAS DSLMAP RNAi /+
C''
Robo,Zfh-1
PrcGal4/+;Wt /+
D''
Robo,Zfh1
PrcGal4/+;UAS DSLMAP RNAi /+

TinGal4 were crossed to UAS-*DSLMAP*, and to the UAS-Slit to generate lines with targeted expression in CBs. Dmef2 antibody was used to identify the CBs, while Zfh-1 antibody was used to mark the PCs (Fig. 26 A-C"). The resulted phenotypes include: delayed migration, missing cells, and clustering of cells in these lines. TinGAL4/+;UAS-*Slit*/+ led to failure of dorsal closure, in which the cells were not migrating dorsally to form a regular heart tube, both the CBs and the PCs showed this phenotype as illustrated in (Fig. 26 B and B' arrows).

The penetrance of the delayed migration observed in heart cells due to Slit over-expression reached ~38.45% in both cell types as displayed in (Table 4 and 5 A). Similarly, *DSLMAP* over-expression also showed failure of dorsal closure when *DSLMAP* was over-expressed in both cell types as shown in (Fig.26 C and C' arrows). In comparison, the control embryo had an organized heart tube at the same stage (Fig.26 A-A' arrows).

To further study the relationship between *D*SLMAP and Slit; PrcGAl4 driver was crossed to UAS-*DSLMAP*, and to UAS-*Slit*. These two crosses also had similar defects, as illustrated in (Fig. 26 E-G"). Over-expression of *Slit* or *DSLMAP* in the PCs, caused delayed migration defects in these cells compared to the control embryo at the same stage as shown in (Fig. 26 E', F', G' arrows). *Slit* over-expression, and *DSLMAP* over-expression also affected the CBs and caused failure of dorsal closure compared to the organized CBs in the control embryo as displayed in (Fig. 26 E, F, and G). The penetrance of this phenotype in Slit over-expression reached ~26.3%, while the expressivity of this phenotype in the CBs reached ~40%, and in the PCs reached ~ 45% as illustrated in (Table 4, 5 A and B).

**Figure 26. Phenotypes observed in *Slit* over-expression or *DSLMAP* over-expression**

Two heart drivers were used to examine the phenotypes in UAS-*DSLMAP* and UAS-*Slit*. (A-G") Embryos are at stage 17, anterior to the left, dorsal view. The embryos were stained with *D*mef2 which is specific for the CBs and the somatic muscles, and Zfh-1 which is specific for the PCs. (A) TinGAL4 crossed to the wt is used as a control which has normal CBs alignment. (B) *Slit* over-expression in the CBs resulted in failure of dorsal closure in the CBs (star). (C) *DSLMAP* over-expression also shows failure of dorsal closure (star). (A') Control embryo stained with Zfh1 which is specific for PCs. (B') *Slit* over-expression also showed delayed migration in the PCs (star). (C') Similar delayed migration defect is observed in PCs in *DSLMAP* over-expression (star). (A") Control embryo double labelled with Dmef2 and Zfh1. (B") *Slit* over-expressed embryo double labelled with Dmef2 and Zfh1. (C") DSLMAP over-expressed embryo double-labelled with *D*mef2 and Zfh1. (E) PrcGAl4 crossed to the wt is used as a control. (F) *Slit* over-expression in the PCs, where the CBs are affected and had delayed migration defects (arrow). (G) *DSLMAP* over-expression in the PCs, the CBs also have delayed migration defects (arrow). (E') control embryo stained with Zfh-1. (F') *Slit* over-expression in the PCs, where the PCs have delayed migration defects (arrow). (G') *DSLMAP* over-expression in the PCs resulted in delayed migration defects in theses cells similar to *Slit* over-expression (arrow). (E"), (F"), and (G") all the embryos are double-labelled with *D*mef2 and Zfh-1 antibodies.

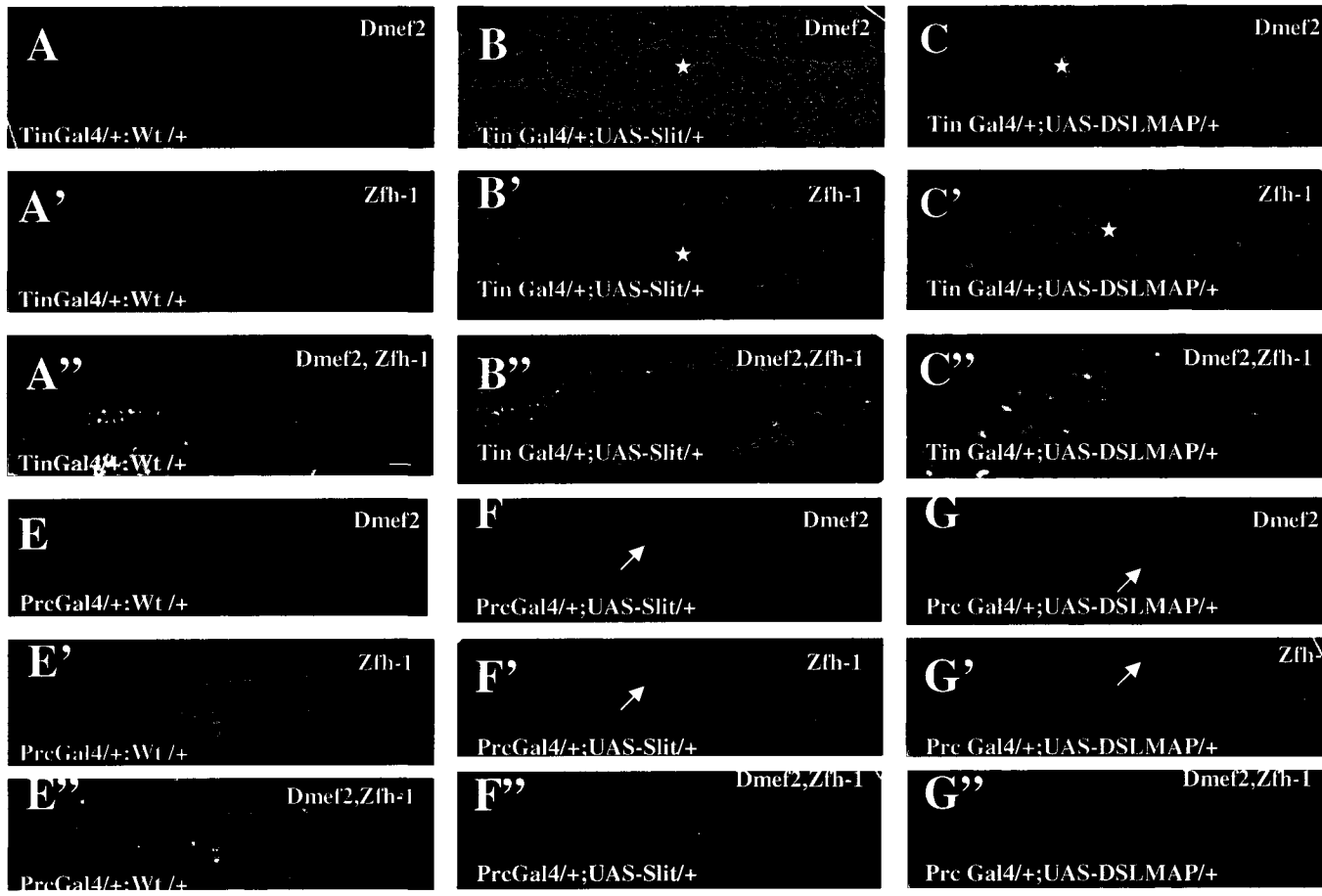
A
Dmef2
TinGal4/+:Wt /+
B
Dmef2
Tin Gal4/+;UAS-Slit/+
C
Dmef2
Tin Gal4/+;UAS-DSLMAP/+
A'
Zfh-1
TinGal4/+:Wt /+
B'
Zfh-1
Tin Gal4/+;UAS-Slit/+
C'
Zfh-1
Tin Gal4/+;UAS-DSLMAP/+
A''
Dmef2, Zfh-1
TinGal4/+:Wt /+
B''
Dmef2,Zfh-1
Tin Gal4/+;UAS-Slit/+
C''
Dmef2,Zfh-1
Tin Gal4/+;UAS-DSLMAP/+
E
Dmef2
PrcGal4/+:Wt /+
F
Dmef2
PrcGal4/+;UAS-Slit/+
G
Dmef2
Prc Gal4/+;UAS-DSLMAP/+
E'
Zfh-1
PrcGal4/+:Wt /+
F'
Zfh-1
PrcGal4/+;UAS-Slit/+
G'
Zfh-1
Prc Gal4/+;UAS-DSLMAP/+
E''
Dmef2,Zfh-1
PrcGal4/+:Wt /+
F''
Dmef2,Zfh-1
PrcGal4/+;UAS-Slit/+
G''
Dmef2,Zfh-1
Prc Gal4/+;UAS-DSLMAP/+

Both *DSLMAP* and *Slit* over-expression exhibited similar phenotypes characterized by delayed migration, and this may suggest a role for DSLMAP in guiding theses cells towards their destination, as has been proposed for the Slit protein.

## 4.12 Slit localization in the heart tube lumen is altered during *DSLMAP* over-expression

In order to detect if Slit localization is affected by DSLMAP over-expression, TinGAl4 heart driver lines were crossed to UAS-DSLMAP and examined with Dmef2 antibody which is identifies CBs and the somatic muscles, and the Slit antibody, which labels Slit protein (Fig. 27 A-B"). Slit is normally localized in the midline between CBs (Fig. 27 A"). An alteration in Slit localization was observed when *DSLMAP* was over-expressed, at stage 17 of embryonic development. The CBs were not able to form a normal lumen due to delayed migration, and exhibited a failure of dorsal closer compared to control embryo at the same stage, as shown in (Fig. 27 A' and B' arrows). Slit is mislocalized and is not found in the lumen in *DSLMAP* over-expressed embryos compared to the control at the same stage (Fig. 27 A", B" arrows).

These results indicate that *DSLMAP* over-expression has heart tube defects similar to those seen during cardiac specific slit-over-expression; but DSLMAP levels also affect slit localization, which may imply a relationship between these two proteins.

## 4.13 *D*SLAMP genetically interacts with the *Slit/Robo* pathway

To investigate any genetic interaction between *D*SLMAP and the Slit/Robo pathway, many genetic crosses were performed, where TinGAL4, and PrcGAl4 heart drivers were crossed to UAS-*DSLMAP*, and UAS-*DSLMAP*-RNAi, and the virgin female flies were crossed to UAS-*Slit* and UAS-*Robo*-RNAi.

## Figure 27. Slit localization is altered in *DSLMAP* over-expressed embryos

Slit localization is found to be altered, when there is a defect in *DSLMAP* over-expressed embryos. (A-C"') Embryos are at stage 17, anterior to the left, dorsal view. (A) Control embryo stained with Slit, which shows the localization of Slit in the lumen. (B) *DSLMAP* over-expressed embryo, where the localization of Slit is changed - it's not localized in the lumen anymore, compared to control embryo at the same stage (arrow). (A') Control embryo stained with Dmef2 specific for CBs, which has an organized alignment (arrow). (B') Failure of dorsal closure in heart cells is seen in over-expressed *DSLMAP* embryo (arrow). ( A") Control embryo double-labelled with slit and Dmef2, Slit is localized in the lumen between CBs (arrow). (B") *DSLMAP* over-expressed embryo double-labelled with slit and Dmef2, the localization of Slit is changed compared to the control embryo (arrow). (A'"-B'") magnification of A", B" that shows the alteration in Slit localization in DSLMAP over-expressed embryo compared to the control embryo at the same stage.

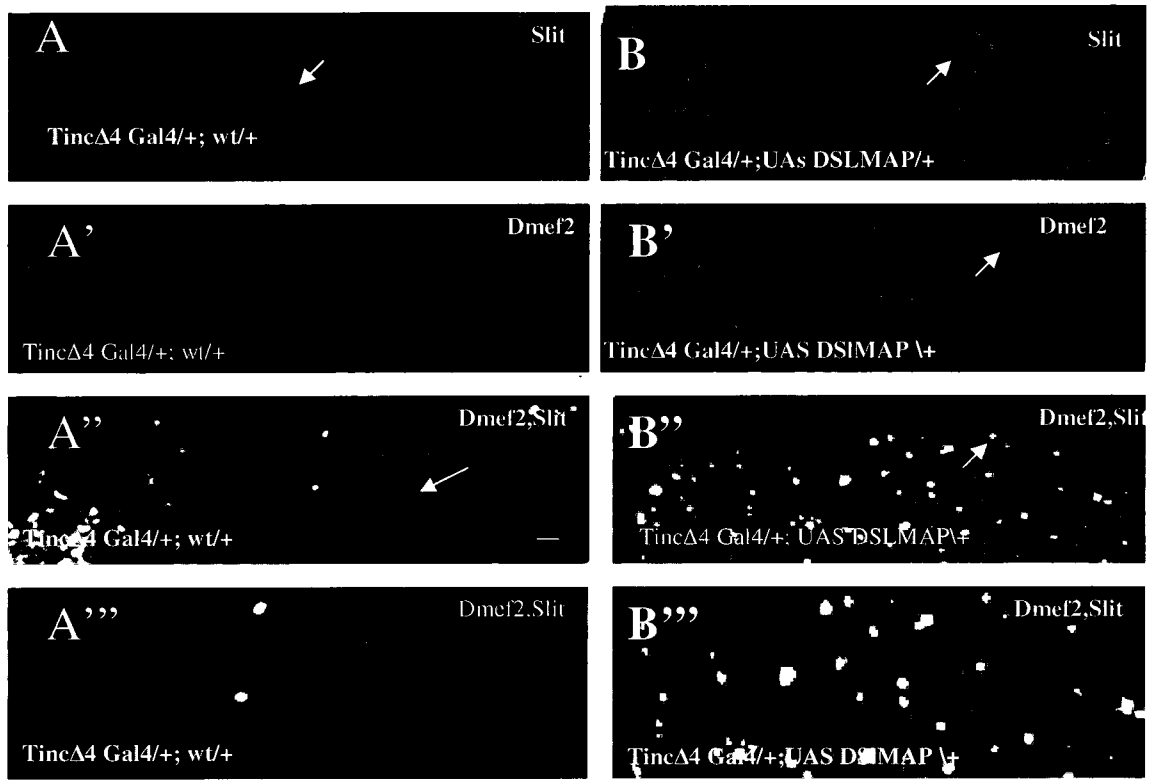
A
Slit
TincΔ4 Gal4/+; wt/+
B
Slit
TincΔ4 Gal4/+;UAs DSLMAP/+
A'
Dmef2
TincΔ4 Gal4/+; wt/+
B'
Dmef2
TincΔ4 Gal4/+;UAS DSlMAP \+
A''
Dmef2,Slit
TincΔ4 Gal4/+; wt/+
B''
Dmef2,Slit
TincΔ4 Gal4/+; UAS DSLMAP\+
A'''
Dmef2,Slit
TincΔ4 Gal4/+; wt/+
B'''
Dmef2,Slit
TincΔ4 Gal4/+;UAS DSLMAP \+

## Table4. Quantitative analysis of the defects observed in the CBs for *slit* over-expression, and Robo down-regulation

Both TincΔ4GAL4 and PrcGAL4 heart drivers were used to examine the defects in Slit over-expression, and Robo down-regulation. Embryos screened were from stage 14-17 and the sample size was 65 embryos for each cross. (A) Penetrance of the phenotypes observed in CBs stained with Dmef2 antibody. Delayed migration had the highest penetrance among all the crosses. (B) Expressivity of the phenotypes observed in CBs. The expressivity of the delays reached up to 55.3% for PrcGal4/+;UAS- *Robo*-RNAi/+, and up to 54% for TinGAL4/+;UAS-*Robo*-RNAi, and up to 46.46% in TinGal4/+;UAS-*Slit*/+, and up to 36.38% for PrcGAL4/+;UAS-*Slit*/+.

**A.** The penetrance of the phenotypes observed in the CBs

| Phenotypes / Genotype | Penetrance % | | | | |
|---|---|---|---|---|---|
| | Delayed migration | Clustering of cells | Gaps | Twist | Non defective embryos |
| PrcGal4/+;wt/+ | 4.5 | 4.5 | 0 | 0 | 93.3 |
| TinGal4/+;wt/+ | 9 | 0 | 4.5 | 0 | 95 |
| UAS-Robo-RNAi/+;wt/+ | 4.5 | 9 | 0 | 0 | 96.6 |
| UAS-Slit/+;wt/+ | 4.5 | 0 | 4.5 | 0 | 95 |
| PrcGal4/+;UAS-Robo-RNAi/+ | 33.83 | 19.98 | 11.61 | 18.46 | 12.3 |
| TinGal4/+;UAS-Robo-RNAi/+ | 40.9 | 24.59 | 18.39 | 16.95 | 16.95 |
| TinGal4/+;UAS-Slit/+ | 38.45 | 32.22 | 16.95 | 12.93 | 15.36 |
| PrcGal4/+;UAS-Slit/+ | 26.03 | 24.43 | 10.71 | 10.71 | 26.16 |

**B.** The expressivity of the phenotypes observed in the CBs

| Genotypes | Expressivity% | | | |
|---|---|---|---|---|
| | Delayed migration | Clustering of cells | Gaps | Twist |
| PrcGal4/+;UAS-Robo-RNAi/+ | 55.3 | 43.9 | 28.7 | 28.6 |
| TinGal4/+;UAS-Robo-RNAi/+ | 54.1 | 34.6 | 25 | 28 |
| TinGal4/+;UAS-Slit/+ | 46.46 | 36.6 | 33.3 | 18.1 |
| PrcGal4/+;UAS-Slit/+ | 36.7 | 26.5 | 19.16 | 12.4 |

## Table 5. Quantitative analysis of the defects observed in the PCs for *slit* over-expression, and Robo down-regulation

Both TincΔ4GAL4 and PrcGAL4 heart drivers were used to examine the defects in Slit over-expression, and Robo down-regulation. Embryos screened were from stage 14-17, and the sample size was 65 embryos for each cross. (A) Penetrance of the phenotypes observed in PCs labelled with Zfh-1 antibody. Delayed migration had the highest penetrance among all the crosses. (B) Expressivity of the phenotypes observed in the PCs. The expressivity for the delayed migration in PrcGal4/+;UAS-*Robo*-RNAi/+ reached up to 42.4%, and for TinGAL4/+;UAS-*Robo*-RNAi 47.9%, and up to 46.9% in TinGal4/+;UAS-*Slit*/+, and up to 45.4 % for PrcGAL4/+;UAS-*Slit*/+. Lower expressivity was seen in the other phenotypes. The error bars represent slandered error of the mean.

**A.**

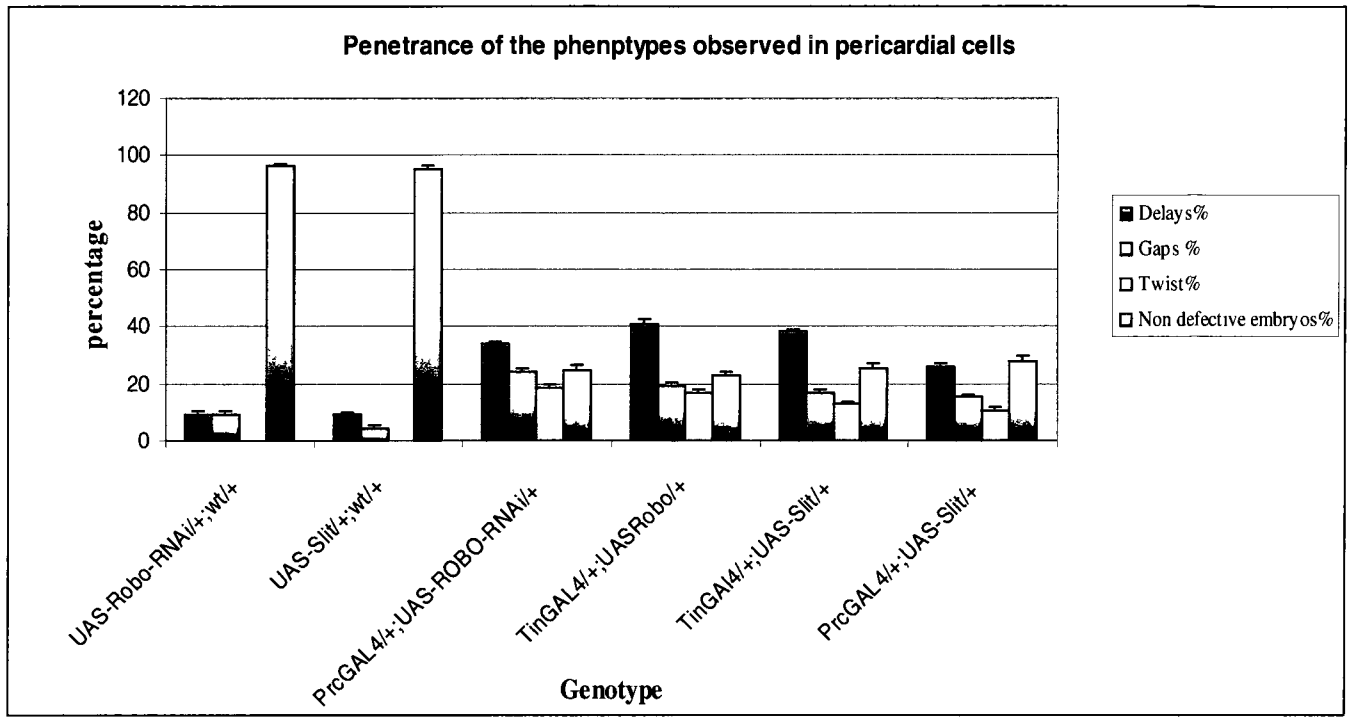
Penetrance of the phenptypes observed in pericardial cells
120
100
80
60
40
20
0
percentage
Delays%
Gaps %
Twist%
Non defective embryos%
UAS-Robo-RNAi/+;wt/+
UAS-Slit/+;wt/+
PrcGAL4/+;UAS-ROBO-RNAi/+
TinGAL4/+;UASRobo/+
TinGAl4/+;UAS-Slit/+
PrcGAL4/+;UAS-Slit/+
Genotype

**B.**

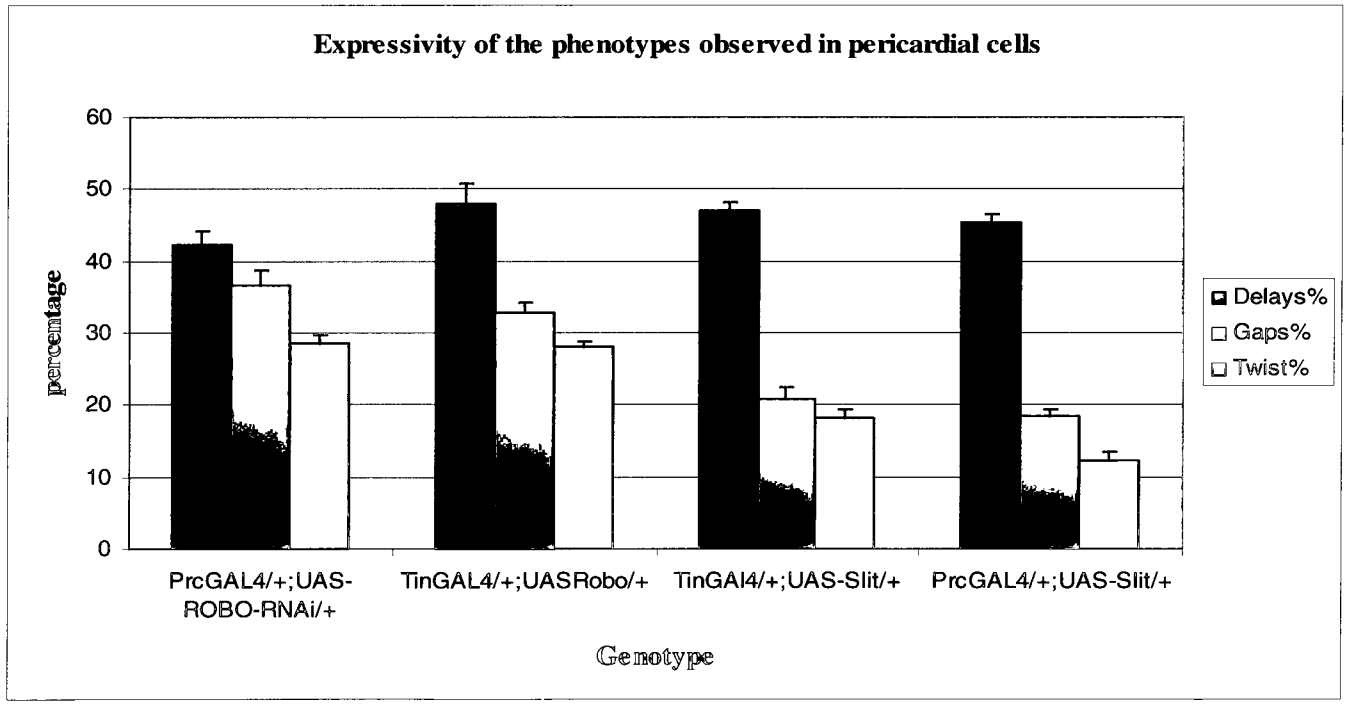
Expressivity of the phenotypes observed in pericardial cells
60
50
40
30
20
10
0
percentage
Delays%
Gaps%
Twist%
PrcGAL4/+;UAS-ROBO-RNAi/+
TinGAL4/+;UASRobo/+
TinGAl4/+;UAS-Slit/+
PrcGAL4/+;UAS-Slit/+
Genotype

Furthermore, to study the relation between DSLMAP and slit/Robo pathway, targeted over-expression of *DSLMAP* in the CBs of $slit^2$ and $robo^{189}$ mutant heterozygous background, and targeted down-regulation of *DSLMAP* in the PCs of $slit^2$ and $robo^{189}$ mutant heterozygous background were done.

### 4.13.1 *DSLMAP* over expression or down-regulation in the PCs of UAS-*Robo*-RNAi transgene led to less defective embryos

The genetic interaction between DSLMAP and Robo in PCs or CBs was studied by crossing PrcGal4-UAS-*DSLMA*P-RNAi to UAS-*Robo*-RNAi, and PrcUAS-*DSLMAP* was crossed to UAS-*Robo*-RNAi. The embryos generated were stained with *D*mef2 antibody to mark the CBs and somatic muscles, while Zfh-1 antibody was used to stain the PCs. In PrcGal4-UAS-*DSLMAP*-RNAi/+;UAS-*Robo*-RNAi/+, the CBs and the PCs had showed recovery from the defects seen in *DSLMAP* over-expression alone (Fig.28 A-B"). In this genetic cross, the CBs had a more organized heart tube with no delays in migration, which is similar to the control embryo at the same stage (Fig. 28 A and B arrows). Similar phenotypes were observed in PCs, and no migration defects were seen (Fig. 28 A' and B' arrows). A significant increase in the penetrance of none defective embryos reached up to 47.5% in both types of cells (Table. 6 A and B) and (Table 7, A and B). PrcGal4-UAS-*DSLMAP*/+;UAS-*Robo*-RNAi/+ also showed a significant recovery of the defective heart tube, with an increased number of non defective embryos but with a lower penetrance ~ 55% as displayed in (Table.6, A) and (Table 7, A). However, some of the embryos still have delayed migration as shown in (Fig. 29 A-B"). Both the CBs and PCs showed delayed migration defects compared to the control embryo

**Figure 28. Pericardial expression of *DSLMAP* down-regulation reduced migration defects in *Robo* down-regulated embryo**

A partial recovery had been observed in embryos having both UAS-*DSLMAP*-RNAi, and UAS Robo RNAi transgenes. (A-B") Embryos are at stage 17, anterior to the left, dorsal view. (A) Control embryo stained with *D*mef2 (B) *DSLMAP* down-regulation in the PCs of *Robo* down-regulated embryos led to normal CBs alignment (arrow). (A') PCs stained with Zfh1 in control embryo (B') PCs also shows normal PCs alignment (arrow). (A"), (B") Embryos are double-labelled with anti-*D*mef2 and anti-Zfh1.

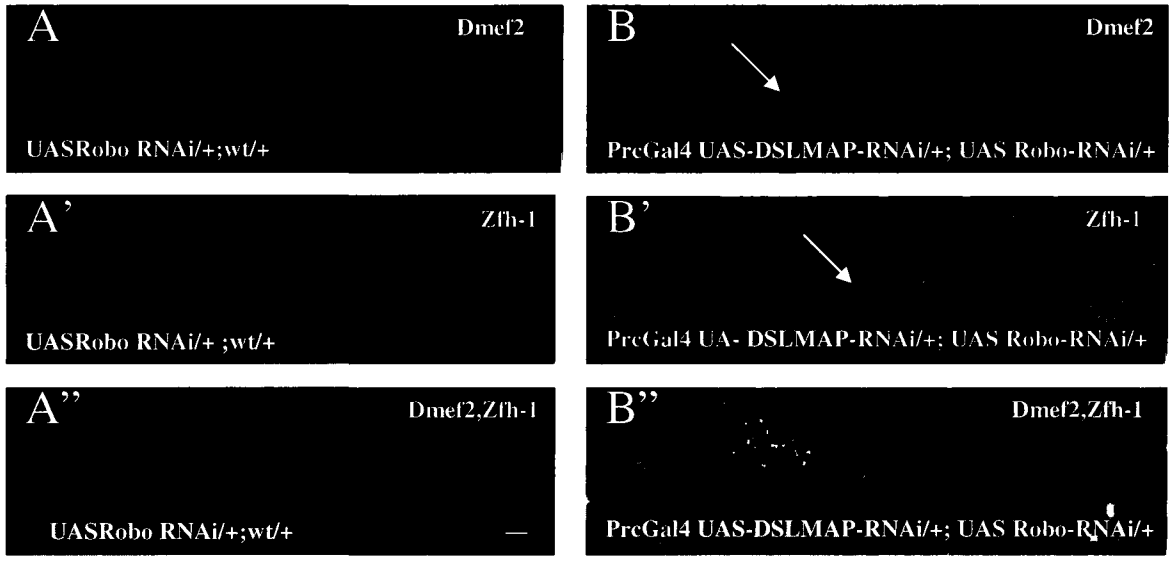
A
Dmef2
UASRobo RNAi/+;wt/+
B
Dmef2
PrcGal4 UAS-DSLMAP-RNAi/+; UAS Robo-RNAi/+
A'
Zfh-1
UASRobo RNAi/+ ;wt/+
B'
Zfh-1
PrcGal4 UA- DSLMAP-RNAi/+; UAS Robo-RNAi/+
A''
Dmef2,Zfh-1
UASRobo RNAi/+;wt/+
B''
Dmef2,Zfh-1
PrcGal4 UAS-DSLMAP-RNAi/+; UAS Robo-RNAi/+

**Figure 29. Pericardial expression of UAS-*DSLMAP* transgene led to minor delays in *Robo* down-regulated embryos**

Robo down-regulation reduces the cardiac defects produced by *DSLMAP* over-expression, but some of the embryo still has delayed migration. (A-B") Embryos are at stage 17, anterior to the left, dorsal view. (A) Control embryo stained with Dmef2. (B) *DSLMAP* over-expression in the PCs of *Robo* down-regulated embryo shows minor delays in CBs migration (star). (A') PCs stained with Zfh1 in control embryo. (B') *DSLMAP* over-expression in the PCs of *Robo* down-regulated embryo, the PCs also show minor delays in PCs migration (A"), (B") Embryos are double-labelled with *D*mef2 and Zfh1 antibodies.

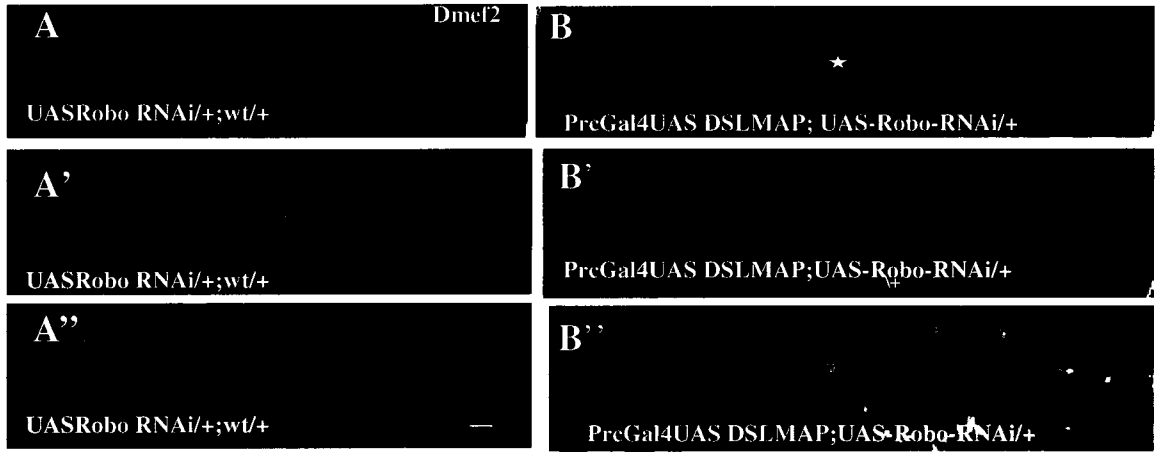
A
Dmef2
UASRobo RNAi/+;wt/+
B
PrcGal4UAS DSLMAP; UAS-Robo-RNAi/+
A'
UASRobo RNAi/+;wt/+
B'
PrcGal4UAS DSLMAP;UAS-Robo-RNAi/+
A''
UASRobo RNAi/+;wt/+
B''
PrcGal4UAS DSLMAP;UAS-Robo-RNAi/+

at the same stage, which had none of these defects (Fig.29 A and B, A' and B' arrows), and a significant reduction in the penetrance of the delayed migration was noted in both the CBs and the PCs reached up to 17% as illustrated in (Table.6, A and B) and (Table 7, A and B). These data suggest that there might be genetic interactions between DSLMAP and Robo, since the heart cells had less migration and alignment defects compared to *DSLMAP* over-expression alone or *Robo* down-regulation alone.

### 4.13.2 Down-regulation of *DSLMAP* reduced the cardiac defects observed in *Slit* over-expression.

To further investigate the relationship between DSLMAP and Slit, another genetic cross was performed using PrcGal4-UAS-*DSLMAP*-RNAi, and UAS-*Slit*. The progeny was examined by staining with *D*mef2 antibody and Zfh-1 antibody. This genetic cross Prc Gal4-UAS-*DSLMAP*RNAi/+;UAS-*Slit*/+ showed that Slit over-expression was able to minimize all the defects that were observed in *DSLMAP* down-regulated embryos in both the CBs and the PCs. All the phenotypes including delayed migration, clusters/aggregation of the CBs, gaps, and twist were reduced, and the heart tube was more organized as shown in (Fig. 30 A-B"). The CBs were more aligned and organized compared to the DSLMAP down-regulated embryos at the same stage, as illustrated in (Fig. 30 A and B arrows). Similar data was seen in the PCs with minimal migration defects (Fig.30 A' and B' arrows). The penetrance for the non-defective embryos is increased significantly and reached up to ~ 42.55%, and for the delayed migration defects, a notable reduction is seen in both cell types and it was reduced up to ~18.17% as shown in (Table. 6, A and B) and (Table 7 A and B). Consequently, DSLMAP may genetically interact with Slit for the normal development of the heart tube.

**Figure 30. Down-regulation of DSLMAP in the CBs of Slit over-expressed embryos had an organized heart tube.**

Recovered heart tube formation has been detected in embryos with both UAS-*DSLMAP*-RNAi and UAS-Slit. (A-B") Embryos at stage 17, anterior are to the left, dorsal view. (A) Control embryo stained with Dmef2. (B) *DSLMAP* down-regulation and slit over-expression genetic interactions led to recovered heat tube formation (arrowhead). (A') PCs stained with Zfh1 in control embryo. (B') PCs also show a normal alignment of PCs compared to control embryo at the same stage (arrowhead). (A"), (B") embryos are double-labelled with Dmef2, and Zfh-1 antibodies.

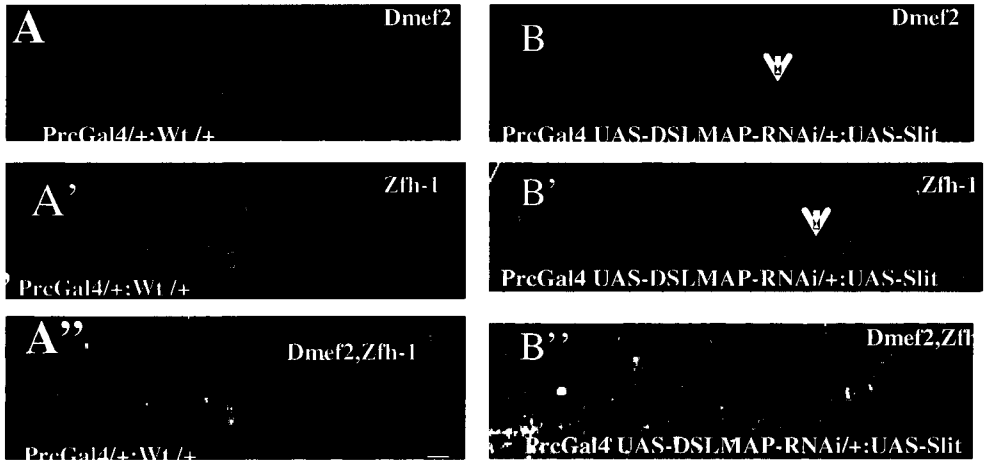
A
Dmef2
PrcGal4/+:Wt /+
B
Dmef2
PrcGal4 UAS-DSLMAP-RNAi/+:UAS-Slit
A'
Zfh-1
PrcGal4/+:Wt /+
B'
Zfh-1
PrcGal4 UAS-DSLMAP-RNAi/+:UAS-Slit
A''
Dmef2,Zfh-1
PrcGal4/+:Wt /+
B''
Dmef2,Zfh
PrcGal4 UAS-DSLMAP-RNAi/+:UAS-Slit

### 4.13.3 *DSLMAP* over-expression in the CBs reduced the delayed migration associated defects with *Robo* down-regulation or *Slit* over-expression

To further study any genetic interaction between the DSLMAP and Slit/Robo pathway, two genetic crosses were done, in which TinGAL4 UAS-*DSLMAP* was crossed with UAS-*Slit*, and also crossed to UAS-*Robo*-RNAi. The heart tube appeared normal with both the CBs and the PCs more aligned exhibiting less delayed migration as shown in (Fig. 31 A-C"). The CBs were stained with Dmef2 antibody, and anti-Zhh-1 was used to label the PCs. In TinGal4-UAS-*DSLMAP*/+;UAS-*Slit*/+, both the CBs and the PCs recovered from the delayed migration defects, and had similar alignment to the control embryo at the same stage as shown in (Fig. 31 A,B and A', B' arrows).

TinGal4-UAS-*DSLMAP*/+;UAS-*Robo*-RNAi/+ also showed similar recovery in both the CBs and the PCs compared to the control embryo at the same stage as displayed in (Fig, 31 A,C and A',B' arrows). The penetrance of the non-defective embryos has increased significantly in TinGal4-UAS-DSLMAP/+;UAS Slit/+ and reached up to ~40% in both the CBs and the PCs (Table. 6 A and B) and (Table 7 A and B). In addition, the delayed migration defects were notably reduced for this cross in both the CBs and the PCs and reached up to ~20% compared with those seen in DSLMAP over-expression. On the other hand, the penetrance of the non-defective embryos in TinGal4-UAS-DSLMAP/+;UAS-Robo-RNAi/+ has increased significantly and reached up to ~45%, and the delayed migration defects were notably reduced to ~16.9% as displayed in (Table.6 A and B) and (Table.& A and B). This result implies a potential interactionbetween the DSLMAP and Slit/Robo pathways.

**Figure 31. Myocardial over-expression of *DSLMAP* reduced cardiac defects associated with Slit over-expression or Robo down-regulation**

(A-C") Embryos at stage 17, anterior are to the left, dorsal view. Embryos are labelled with Dmef2 antibody for the CBs (Red) and Zfn-1 antibody for the PCs (green). (A) Control embryo stained with Dmef2. (B) *DSLMAP* over-expression in the CBs of slit over-expressed embryos led to recovered CBs alignment (arrow). (C) Myocardial expression of DSLMAP in UAS-Robo-RNAi transgene led to organized CBs alignment. (A') PCs stained with Zfh1 in control embryo. (B') PCs also show a normal alignment, compared to control embryo at the same stage (arrow). (C') The PCs were also more organized similar to the control embryo. (A"), (B"), and (C") Embryos are double-labelled with dmef2 and Zfh-1 antibodies.


A
Dmef2
UAS-SLit/+ ;wt/+
B
Dmef2
TinGal4 UAS-DSLMAP/+:UAS-Slit/+
C
Dmef2
TinGal4 UAS-DSLMAP/+:UAS-Robo-
A'
Zfh-1
UAS-SLit/+ ;wt/+
B'
Zfh-1
TinGal4 UAS-DSLMAP/+:UAS-Slit/+
C'
Zfh-1
Tin UAS-DSLMAP/+:UAS-Robo-RNAit/+
A''
Dmef2,Zfh-1
UAS-SLit/+ ;wt/+
B''
Dmef2,Zfh-1
TinGal4 UAS-DSLMAP/+:UAS-Slit/+
C''
Dmef2,Zfh-1
Tin UAS-DSLMAP/+:UAS-Robo-RNAit/+

**Table.6 Quantitative analysis of phenotypes observed in the CBs for *DSLMAP* genetic interactions with slit over-expression and Robo down-regulation.**

The phenotypes quantified in these crosses were examined in the CBs stained with Def2 antibody antibody. These phenotypes include: delays, gaps, twist, and clustering of cells. (A) Penetrance of the phenotypes observed in the CBs. (B) P-value for the phenotypes in the CBs. In all the crosses, the percentage of non-defective embryo was increased. PrcGal4-UAS *DSLMAP*/+; UAS-Robo-RNAi/+ scored the highest percentage for non-defective embryos which had normal heart cells alignment and this percentage reached up to 55%. While Tin Gal4-UAS-*DSLMAP*-RNAi/+;UAS-Slit/+ had the lowest percentage of non-defective embryos, which reached up to 40%. Delayed migration defect in the CBs, had the highest overall percentage defects. The P-value was calculated using the unpaired t-test.

**The penetrance of the phenotypes observed in the CBs**

**A.**

| Genotype | Penetrance % | | | | |
|---|---|---|---|---|---|
| | Delayed migration | Clustering of cells | Gaps | Twist | Non defective embryos |
| PrcGal4/+;UAS-DSLMAP-RNAi/+ | 47.7 | 15.36 | 16.95 | 9. 16 | 21.49 |
| TinGal4/+;UAS-DSLMAP-RNAi/+ | 49.16 | 23.01 | 15.36 | 16.94 | 24.6 |
| TinGal4/+;UASDSLMAP-4/+ | 48.46 | 32.2 | 15.4 | 12.34 | 18.45 |
| TinGal4/+;UASDSLMAP-10/+ | 51.46 | 13.6 | 13.79 | 9.5 | 19.98 |
| PrcGal4/+;UAS-DSLMAP-4/+ | 47.8 | 21.5 | 13.7 | 12.2 | 19.91 |
| PrcGal4/+;UAS-Robo-RNAi/+ | 33.83 | 19.98 | 11.61 | 18.46 | 12.3 |
| TinGal4/+;UAS-Robo-RNAi/+ | 40.9 | 24.59 | 18.39 | 16.95 | 16.95 |
| TinGal4/+;UAS-Slit/+ | 38.45 | 32.22 | 16.95 | 12.93 | 15.36 |
| PrcGal4/+;UAS-Slit/+ | 26.03 | 24.43 | 10.71 | 10.71 | 26.16 |
| Prc Gal4 UAS-DSLMAP-RNAi/+;UAS-Slit/+ | 18.17 | 19.6 | 16.94 | 9.1 | 42.55 |
| Prc Gal4 UAS-DSLMAP-RNAi/+;UAS-Robo-RNAi/+ | 26.15 | 28.9 | 22.98 | 18.15 | 47.5 |
| Prc Gal4 UAS-DSLMAP/+; UAS-Robo-RNAi | 25.5 | 21.29 | 0 | 7.6 | 55 |
| TinGal4 UAS-DSLMAP/+; UAS-Slit/+ | 13.7 | 14 | 16.9 | 10.7 | 40 |
| TinGal4 UAS-DSLMAP/+; UAS-Robo-RNAi/+ | 16.94 | 13.76 | 9.1 | 9.1 | 45 |

**B.**

| Phenotypes / Genotype | P value | | | | |
|---|---|---|---|---|---|
| | Delayed migration | Clustering of cells | Gaps | Twist | Non defective embryos |
| Prc Gal4 UAS-DSLMAP-RNAi/+;UAS-Slit/+ | 0.0025 | 0.0483 | 0.9968 | 0.9708 | 0.0053 |
| Prc Gal4 UAS-DSLMAP-RNAi/+;UAS-Robo-RNAi/+ | 0.0052 | 0.0173 | 0.1057 | 0.0208 | 0.0046 |
| Prc Gal4 UAS-DSLMAP/+; UAS-Robo-RNAi | 0.015 | 0.9120 | 0.0054 | 0.115 | 0.0013 |
| TinGal4 UAS-DSLMAP/+; UAS-Slit/+ | 0.0002 | 0.9745 | 0.3754 | 0.354 | 0.0240 |
| TinGal4 UAS-DSLMAP/+; UAS-Robo-RNAi/+ | 0.0003 | 0.9926 | 0.9952 | 0.9836 | 0.0041 |

**Table.7 Quantitative analysis of phenotypes observed in the PCs for *DSLMAP* genetic interactions with slit over-expression and Robo down-regulation.**

The phenotypes quantified in these crosses were examined in the PCs stained with Zfh-1 antibody. These phenotypes include: delays, gaps, and twist (A) Penetrance of the phenotypes observed in the PCs. (B) P-value for the phenotypes in the PCs.

PrcGal4-UAS*DSLMAP*/+; UAS-Robo-RNAi/+ scored the highest percentage for non-defective embryos among all the genetic crosses which had normal heart cells alignment and this percentage reached up to 55%, and in all the crosses, the percentage of non-defective embryo was increased, while TinGal4-UAS-*DSLMAP*-RNAi/+;UAS-Slit/+ had the lowest percentage of non-defective embryos, which reached up to 40%. Delayed migration in the PCs had the highest overall percentage defects. The P-value was calculated using the unpaired t-test

**A.**

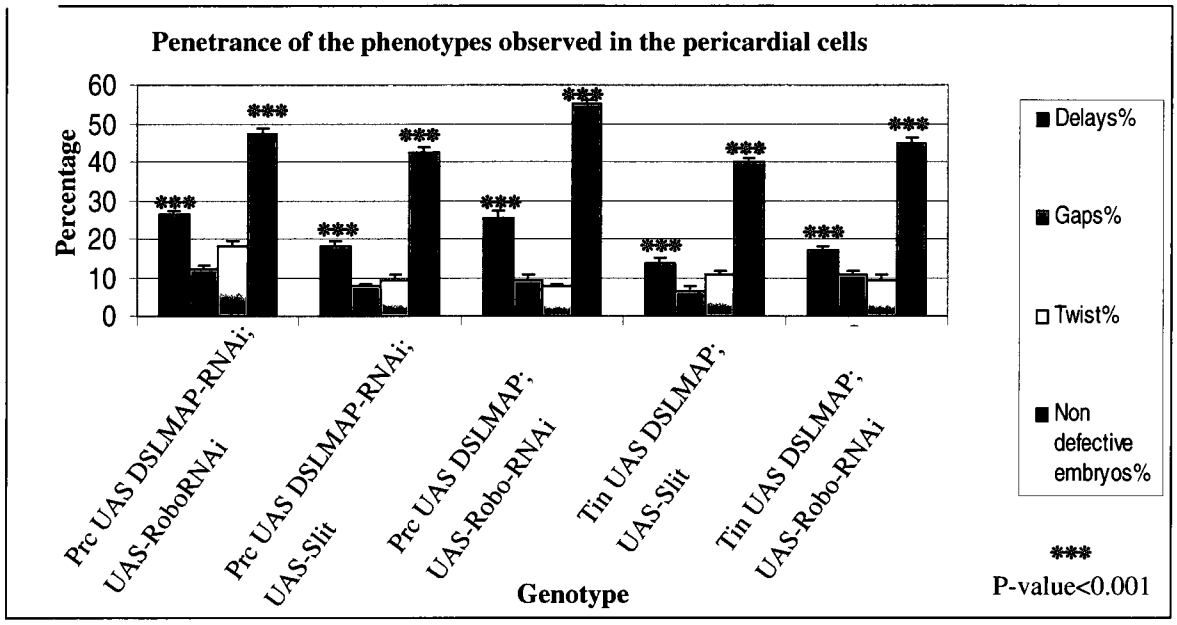


**B.**

| Phenotypes / Genotype | P value | | | |
|---|---|---|---|---|
| | Delayed migration | Gaps | Twist | Non defective embryos |
| Prc Gal4 UAS-DSLMAP-RNAi/+;UAS-Slit/+ | 0.0025 | 0.1457 | 0.9708 | 0.0053 |
| Prc Gal4 UAS-DSLMAP-RNAi/+;UAS-Robo-RNAi/+ | 0.0052 | 0.9396 | 0.0208 | 0.0046 |
| Prc Gal4 UAS-DSLMAP/+; UAS-Robo-RNAi | 0.015 | 0. 0004 | 0.115 | 0.0013 |
| TinGal4 UAS-DSLMAP/+; UAS-Slit/+ | 0.0002 | 0.9968 | 0.354 | 0.0240 |
| TinGal4 UAS-DSLMAP/+; UAS-Robo-RNAi/+ | 0.0003 | 0.0639 | 0.9836 | 0.0041 |

### 4.13.4 Phenotypes observed in Slit$^2$ and Robo$^{189}$ mutants in Drosophila heart

Slit ligand is a secreted protein from the myocardial progenitor, and binds to Robo receptor to form a complex that plays a major role in cardiac cells alignment and migration during *Drosophila* heart development. *Slit2* and *robo$^{189}$* loss of function mutants showed severe alignment, and migration defects in the heart which included: delays, large gaps , clustering of cells, double rows and others (Fig. 32 A-C").

*Slit$^2$* embryo had a big gap in both CBs and PCs compared to the control embryo at the same stage (Fig. 32 A and B stars, A' and B' star), while in *robo$^{189}$*, the heart tube had crossed lines compared to the well-organized heart cells in the control embryo, as shown in (Fig.32 A and B arrows , A' and B' arrows).

### 4.13.5 DSLMAP protein can reduce heart tube defects observed in Slit$^2$ and Robo$^{189}$ loss of function mutants.

To further understand any role for DSLMAP in heart tube development, and the Slit /Robo pathway, myocardial expression of UAS-*DSLMAP* transgene in *slit$^2$* and *robo$^{189}$* heterozygous background were examined, where two genetic crosses were generated: Tin Gal4-UAS-DSLMAP/+;*slit$^2$*/+ and TinGal4UAS-DSLMAP/+;*robo$^{189}$*/+. Over-expression of DSLMAP in *slit$^2$* and *robo$^{189}$* mutants' background had shown a significant reduction in the phenotypes observed in both *slit$^2$* and *robo$^{189}$* mutants alone as displayed in (Fig.33 A-C", and Fig.34 A-C").

When DSLMAP was over-expressed in *slit$^2$* heterozygous background, the CBs stained with anti-*D*mef2 had normal cell alignment, similar to the control embryos at the same stage of development as shown in (Fig.33 A, B, and C arrows).

**Figure 32. Gaps and lack of lumen formation are seen in *slit*$^{2}$ and *robo*$^{189}$ loss of function mutant**

(A-C") Embryos are at stage 17, anterior to the left, dorsal view. (A) Control embryo stained with Dmef2 antibody which is specific for labelling the CBs. (B) *slit*$^{2}$ loss of function mutant stained with anti-Dmef2 which is specific for the CBs, large gap in the CBs is seen (Star). (C) *robo*$^{189}$ loss of function mutant embryo stained with Dmef2 antibody shows crossed rows of the CBs (arrow). (A') Control embryo stained with Zfh1 antibody which is specific for PCs. (B') *slit*$^{2}$ loss of function mutant embryo stained with ZFH1 also a big gap is seen in PCs (star). (C') *robo*$^{189}$ loss of function mutant also shows defective PCs (arrow). (A"), (B"), (C") Embryos are double-labelled with Dmef2 and Zfh1 antibodies.

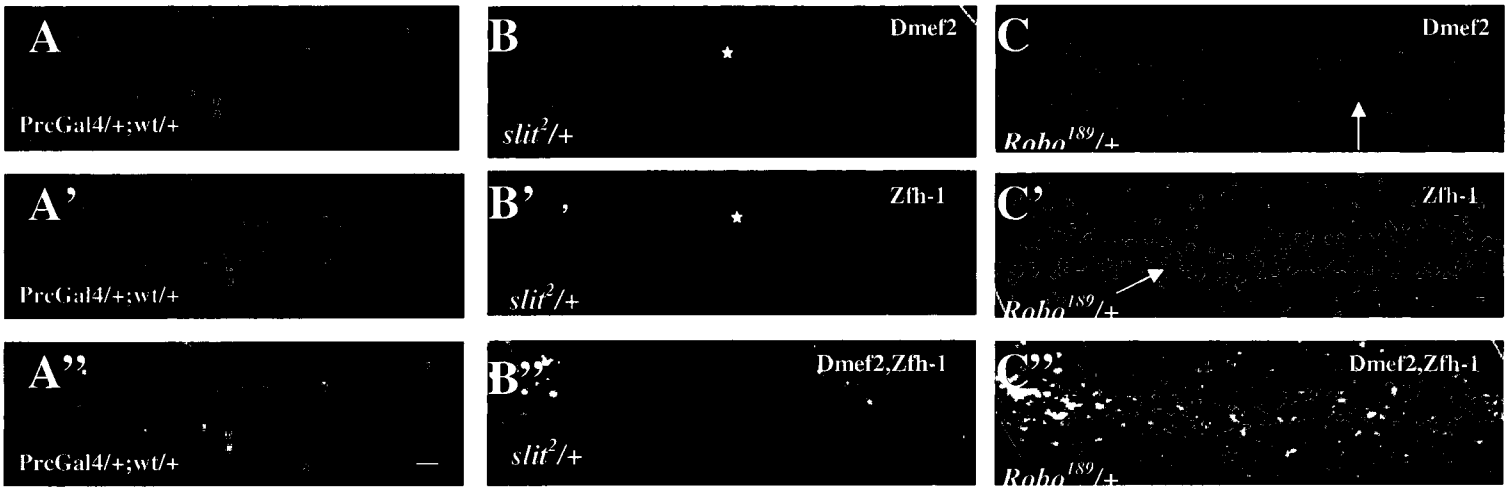
A
PrcGal4/+;wt/+
B
Dmef2
slit2/+
C
Dmef2
Robo189/+
A'
PrcGal4/+;wt/+
B'
Zfh-1
slit2/+
C'
Zfh-1
Robo189/+
A''
PrcGal4/+;wt/+
B''
Dmef2,Zfh-1
slit2/+
C''
Dmef2,Zfh-1
Robo189/+

**Figure 33. *DSLMAP* over-expression reduced the phenotypes observed in *slit*$^2$ loss of function mutant**

TinGAL4 driver was used with UAS-*DSLMAP* transgenic line-10 and crossed to *slit*$^2$ mutant. (A-C") Embryos at stage 17, dorsal view, anterior to the left, and stained with Dmef2 antibody red color Zfh1 antibody green color. (A-C") Embryos are at stage 17, anterior to the left, dorsal view. (A) Heterozygous control embryo of TinGAL4/+; *slit*$^2$/+ stained with Dmef2 antibody, shows normal CBs alignment (arrow). (B) Heterozygous control embryo of UAS-*DSLMAP*\+;*slit*$^2$/+stained with Dmef2,also have organized CBs (arrow). (C) TinGal4-UAS-*DSLMAP*\+; Slit$^2$ shows recovered CBs alignment similar to the control embryo at the same stage (arrow). (A') TinGAL4/+; *slit*$^2$/+control embryo stained with Zfh1, has organized PCs (arrow). (B') Heterozygous control embryo of UASDSLMAP\+; *slit*$^2$ /+stained with Zfh-1, shows normal PCs alignment (arrow)(C') TinGal4-UAS-*DSLMAP*\+; *slit*$^2$/+ shows recovered PCs alignment (arrow), stained with Zfh-1 antibody. (A"), (B"),(C") Embryos are all double-labelled with Dmef2 and Zfh1 antibodies.

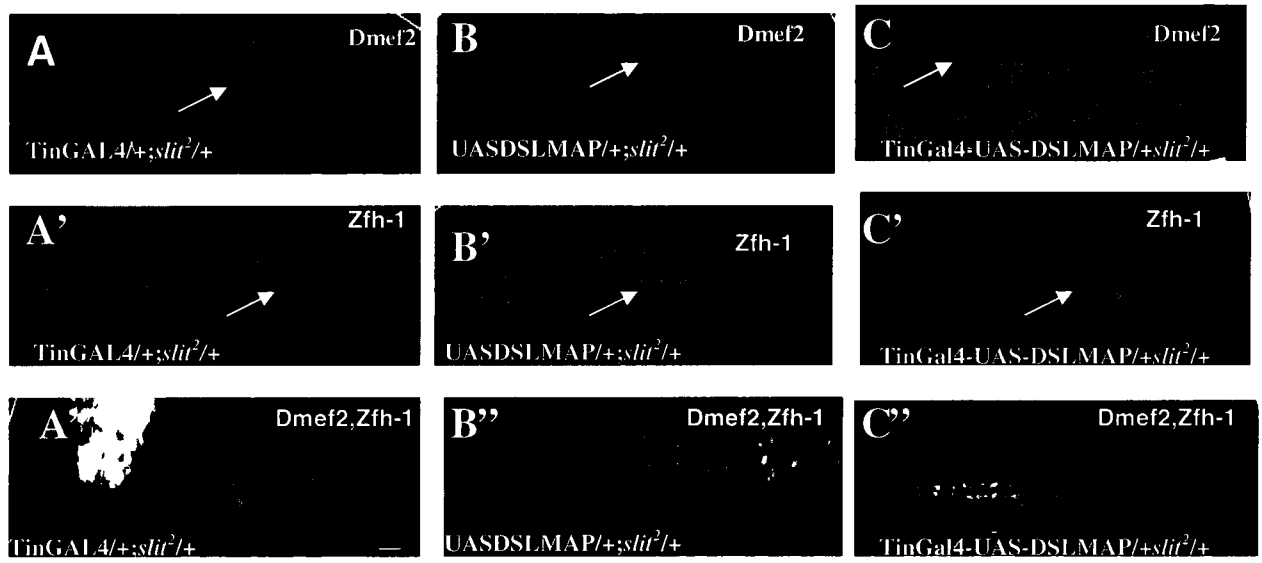
A
Dmef2
TinGAL4/+;slit²/+
B
Dmef2
UASDSLMAP/+;slit²/+
C
Dmef2
TinGal4-UAS-DSLMAP/+slit²/+
A'
Zfh-1
TinGAL4/+;slit²/+
B'
Zfh-1
UASDSLMAP/+;slit²/+
C'
Zfh-1
TinGal4-UAS-DSLMAP/+slit²/+
A''
Dmef2,Zfh-1
TinGAL4/+;slit²/+
B''
Dmef2,Zfh-1
UASDSLMAP/+;slit²/+
C''
Dmef2,Zfh-1
TinGal4-UAS-DSLMAP/+slit²/+

Also, the PCs stained with anti-Zfh-1 had normal alignment, just like the control embryo (Fig.33, A', B', and C' arrows). The penetrance for non-defective embryos reached up to 72.33% (n=65), and all the other phenotypes were significantly reduced as displayed in (Table. 7 A and B).

The myocardial targeted over-expression of *DSLMAP* in $robo^{189}$ heterozygous background demonstrated that the large gaps, the clustering of cells, and the delays were significantly reduced, and the CBs showed normal cardiac tube development, much similar to the control embryos as shown in (Fig.34 A, B, and C).

Similarly, the PCs had normal cells alignment, just as both control embryos, as shown in (Fig.34 A', B', and C'). The penetrance of non-defective embryos in both the CBs and the PCs reached up to 70.77% (n=65), as displayed in (Table.8 A and B) and (Table.9 A and B).

*In situ* hybridization showed that DSLMAP is expressed in the heart; while Robo is expressed in both the CBs and the PCs. Slit is expressed only by the CBs but not in the PCs, but the phenotypes observed in $slit^2$ mutant indicated that any defect in the CBs will have an impact on the PCs; these defects include gaps, delayed migration in the heart cells and others. In order to study the genetic interaction of DSLMAP with $Slit^2$ and $robo^{189}$ mutants in the PCs, targeted pericardial down-regulation of DSLMAP was done in both $slit^2$ and $robo^{189}$ mutants.

Two genetic crosses were obtained: PrcGal4-UAS-*DSLMAP*-RNAi/+;$slit^2$/+, and Prc Gal4-UAS-*DSLMAP*-RNAi/+;$robo^{189}$/+, a significant decrease in all the phenotypes seen in $slit^2$ and $robo^{189}$ were seen, as in (Fig.35 A-C", and Fig.36 A-C").

*DSLMAP* down-regulation using PrcGAL4 in *slit*$^{2}$ heterozygous background (Prc Gal4-UAS-*DSLMAP*-RNAi/+;*slit*$^{2}$/+) showed that the PCs labelled with anti-Zfh-1 had regular cardiac tube formation as in both control embryos (Fig.35 A', B', and C' arrows), and the CBs stained with ani-*D*mef2 had normal alignment at stage 17 of embryonic development, the same as the both control embryos as displayed in (Fig.35 A, B, and C arrows). The penetrance for non-defective embryos reached up to 72.39% (n=65), and all the other phenotypes were significantly reduced as shown in (Table.7 A and B).

The pericardial targeted down-regulation of *DSLMAP* in *robo*$^{189}$ heterozygous background (PrcGal4-UAS-*DSLMAP*-RNAi/+;*robo*$^{189}$) indicated that the defects that were seen in the *robo*$^{189}$ mutant were all decreased, and most of the embryos had normal cardiac cells alignment, similar to wild type embryo at the same stage (Fig.36 A-C"). At stage 17 of embryonic development, the PCs showed similar organized alignment of these cells that resembles the control embryos at the same stage (Fig.36 A', B', and C' arrows), and the CBs were able to form a normal lumen, and had a normal cells alignment compared to the control embryos at the same stage (Fig.36 A, B, and C arrows). The penetrance of the phenotypes observed in *robo*$^{189}$ mutant were significantly decreased in both the CBs and the PCs , and the penetrance for non-defective embryos reached up to 66.12% (n=65) as illustrated in (Table.8 A and B) and (Table.9 A and B).. Accordingly, when DSLMAP was over-expressed in the CBs of *slit*$^{2}$ mutants, there was a significant reduction in all the defects seen in the CBs of *slit*$^{2}$ mutants alone. In addition, the PCs also had a reduction in all of the phenotypes observed in *slit*$^{2}$ mutants. Further, when *DSLMAP* was over-expressed in the CBs of *robo*$^{189}$ loss-of-function mutants, the number of non-defective CBs had increased, and similar effects were seen in the PCs.

**Figure 34. *DSLMAP* over-expression reduced the phenotypes seen in *robo*$^{189}$ loss of function mutant**

TinGAL4 driver was used with UAS-DSLMAP transgenic line-10 and crossed to *robo*$^{189}$ mutant. (A-C") Embryos at stage 15, dorsal view, anterior to the left, and stained with Dmef2 antibody (red color) Zfh1 antibody (green color) and β-gal (green color). (A) Heterozygous control embryos of UAS-*DSLMAP* /+; *robo*$^{189}$/+, stained with Dmef2 antibody, shows organized CBs (arrow). (B) Heterozygous control embryos of TinGAL4/+; Robo$^{189}$/+ stained with Dmef2 antibody, has normal alignment (arrow). (C) Heterozygous embryo of TinGal4-UAS-*DSLMAP*-RNAi/+; *robo*$^{189}$/+, has recovered CBs alignment similar to the control embryos at the same stage. (A') Heterozygous control embryos of UAS-*DSLMAP* /+; *robo*$^{189}$/+ stained with Zh1 and β-gal antibody, shows organized PCs alignment (arrow). (B') Heterozygous control embryo of TinGAL4/+; *robo*$^{189}$/+ stained with Zfh1, and β -gal antibodies, shows aligned PCs (arrow). (C') Heterozygous embryo of Tin; UAS-*DSLMAP*-RNAi/+; *robo*$^{189}$/+, has recovered PCs (arrow). (A"), (B'), (C") Embryos are all double-labelled with Dmef2 and Zfh1 and β-gal antibodies.

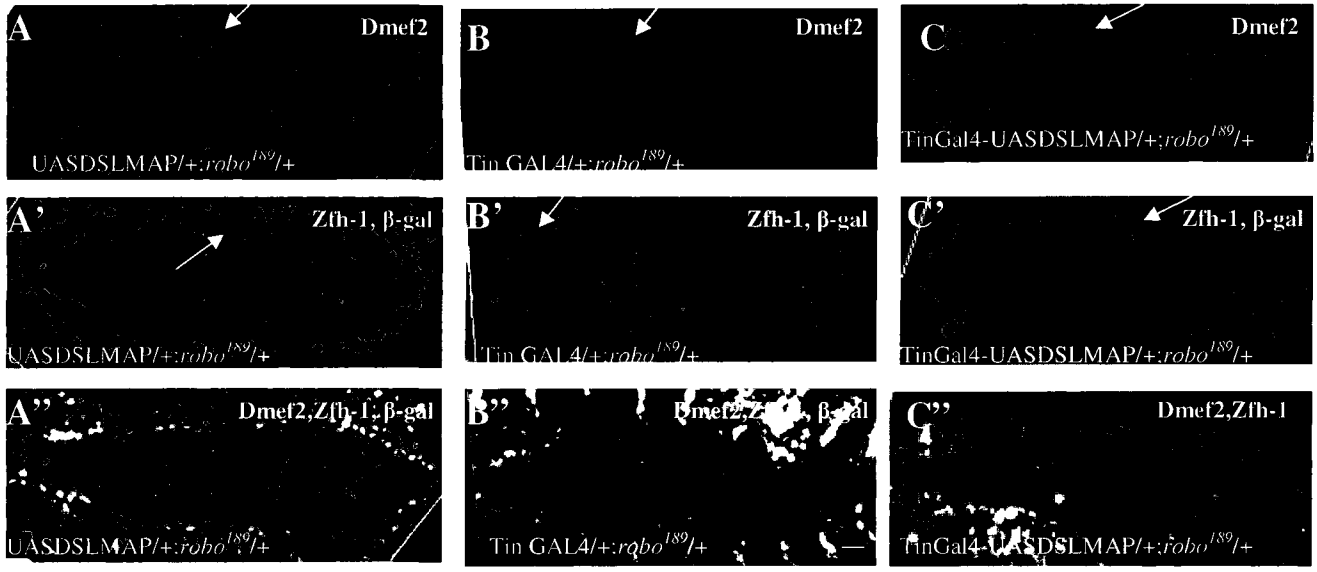
A
Dmef2
UASDSLMAP/+;robo189/+
B
Dmef2
Tin GAL4/+;robo189/+
C
Dmef2
TinGal4-UASDSLMAP/+;robo189/+
A'
Zfh-1, β-gal
UASDSLMAP/+;robo189/+
B'
Zfh-1, β-gal
Tin GAL4/+;robo189/+
C'
Zfh-1, β-gal
TinGal4-UASDSLMAP/+;robo189/+
A''
Dmef2,Zfh-1, β-gal
UASDSLMAP/+;robo189/+
B''
Tin GAL4/+;robo189/+
C''
Dmef2,Zfh-1
TinGal4-UASDSLMAP/+;robo189/+

**Figure 35. *DSLMAP* down-regulation reduced the defects observed in *slit*$^2$ loss-of-function mutant.**

Prc GAL4 driver was used with the UAS-*DSLMA*- RNAi transgenic line and crossed to *slit*$^2$ null mutant. (A-C") Embryos at stage 17, dorsal view, anterior to the left, and stained with *D*mef2 antibody (red color) Zfh1 antibody (green color). (A) Heterozygous control embryo of UAS-*DSLMAP*-RNAi/+; *slit*$^2$/+ stained with Dmef2 antibody shows normal CBs alignment (arrow). (B) Heterozygous embryo of PrcGal4-UAS-*DSLMAP*-RNAi/+; *slit*$^2$/+ shows normal CBs alignment similar to the control embryo (arrow). (C) Heterozygous control embryo of PrcGAL4/+; *slit*$^2$/+ stained with Dmef2 antibody shows aligned CBs (arrow). (A') Heterozygous control embryo of UAS-*DSLMAP*-RNAi/+; *slit*$^2$/+ stained with Zfh1, has organized PCs alignment (arrow). (B') Heterozygous embryo of Prc;UAS-*DSLMAP*-RNAi/+; *slit*$^2$/+ shows recovered PCs, stained with Zfh-1 (arrow). (C') Heterozygous control embryo of PrcGAL4/+; *slit*$^2$/+ stained with Zfh1, shows organized PCs (arrow). (A"), (B'),(C") Embryos are all double-labelled with *D*mef2 and Zfh1 antibodioes.

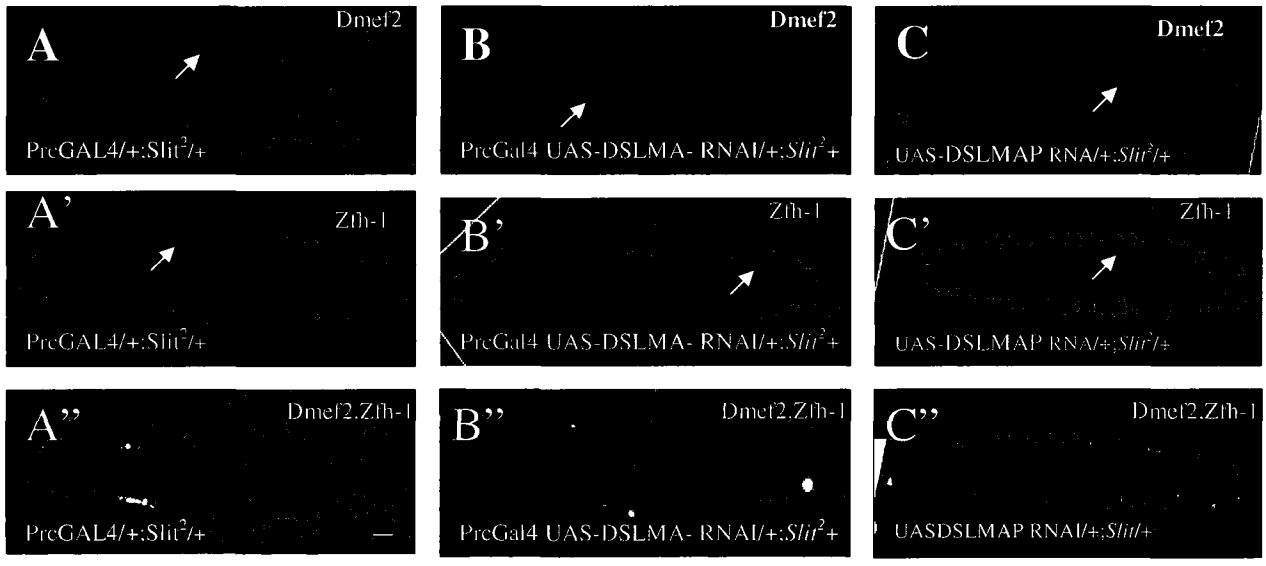
A
Dmef2
PrcGAL4/+;Slit²/+
B
Dmef2
PrcGal4 UAS-DSLMA- RNAI/+;Slit²+
C
Dmef2
UAS-DSLMAP RNA/+;Slit²/+
A'
Zfh-1
PrcGAL4/+;Slit²/+
B'
Zfh-1
PrcGal4 UAS-DSLMA- RNAI/+;Slit²+
C'
Zfh-1
UAS-DSLMAP RNA/+;Slit²/+
A''
Dmef2,Zfh-1
PrcGAL4/+;Slit²/+
B''
Dmef2,Zfh-1
PrcGal4 UAS-DSLMA- RNAI/+;Slit²+
C''
Dmef2,Zfh-1
UASDSLMAP RNAI/+;Slit/+

**Figure 36. *DSLMAP* down-regulation reduced the defects seen in *robo*$^{189}$ loss-of-function mutant**

Prc GAL4 driver was used with DSLMAP RNAi transgenic line and crossed to *robo* $^{189}$ loss-of-function mutant. (A-C") Embryos at stage 17, dorsal view, anterior to the left, and stained with Dmef2 antibody (red color), Zfh1 antibody (green color) and β-gal (green color). (A) Heterozygous control embryos of UAS-*DSLMAP*-RNAi/+; *robo* $^{189}$ /+ stained with *D*mef2 antibody, has aligned CBs (arrow). (B) Heterozygous embryo of Prc-Gal4-UAS-*DSLMAP*-RNAi/+; *robo* $^{189}$/+ shows normal CBs alignment similar to the control embryo (arrow). (C) Heterozygous control embryo of PrcGAL4/+; *robo* $^{189}$ /+ stained with *D*mef2 antibody, shows organized CBs (arrow). (A') Heterozygous control embryos of UAS-*DSLMAP*-RNAi/+; *robo* $^{189}$ /+ stained with Zfh1 and β -gal antibodies, has organized PCs (arrow). (B') Heterozygous embryo of Prc;UAS-*DSLMAP*-RNAi/+;*robo* $^{189}$/+ shows normal PCs alignment, similar to control embryo (arrow). (C') Heterozygous control embryo of PrcGAL4/+;*robo* $^{189}$/+ stained with Zfh-1 has organized PCs (arrow). (A"), (B'), (C") Embryos are all double-labelled with Dmef2 and Zfh1 and β –gal antibodies.

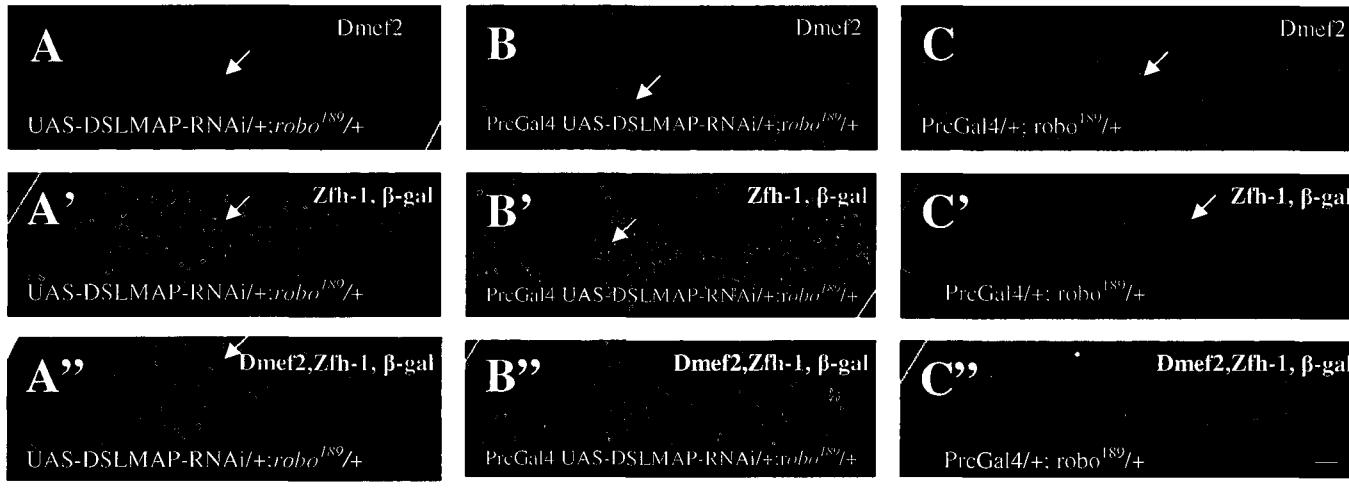
A
Dmef2
UAS-DSLMAP-RNAi/+;robo189/+
B
Dmef2
PrcGal4 UAS-DSLMAP-RNAi/+;robo189/+
C
Dmef2
PrcGal4/+; robo189/+
A'
Zfh-1, β-gal
UAS-DSLMAP-RNAi/+;robo189/+
B'
Zfh-1, β-gal
PrcGal4 UAS-DSLMAP-RNAi/+;robo189/+
C'
Zfh-1, β-gal
PrcGal4/+; robo189/+
A''
Dmef2,Zfh-1, β-gal
UAS-DSLMAP-RNAi/+;robo189/+
B''
Dmef2,Zfh-1, β-gal
PrcGal4 UAS-DSLMAP-RNAi/+;robo189/+
C''
Dmef2,Zfh-1, β-gal
PrcGal4/+; robo189/+

**Table 8. Quantitative analysis of the phenotypes observed in the CBs of DSLMAP genetic interaction with *slit*$^{2}$ and *robo* $^{189}$ loss of function mutants**

*DSLMAP* over-expression and *DSLMAP* down-regulated transgenic lines were crossed to *slit*$^{2}$ and *robo* $^{189}$ loss-of-function mutants, using two different heart drivers: Tinc4Gal4 for myocardial expression, and PrcGAL4 specific for pericardial expression. (A) The penetrance for the phenotypes observed in CBs. (B) P-value for the phenotypes observed in the CBs. The penetrance for the non-defective embryos was increased in the CBs of all the genetic crosses where in TinGal4-UAS-DSLMAP/+;*slit*$^{2}$/+ it reached up to 72.33%, in TinGal4-UAS-DSLMAP/+;*robo* $^{189}$ /+ it reached to 70.99%, PrcGal4-UAS-DSLMAP-RNAi/+; *slit*$^{2}$/+ 73.8%, and in PrcGal4-UAS-DSLMAP-RNAi/+; *robo* $^{189}$ /+ it reached up to 66.12%. The P-value was calculated using the unpaired t-test, and it was highly significant in both the delayed migration defects, and for the penetrance in non-defective embryos. The P-value was calculated using the unpaired t-testd.

.

**A.**

| Phenotype / Genotype | Penetrance % | | | | |
|---|---|---|---|---|---|
| | Delayed migration | Clustering of cells | Gaps | Twist | |
| UAS-*DSLMAP*/+;*slit*$^{2}$/+ | 9 | 4.5 | 0 | 0 | 93.3 |
| UAS-*DSLMAP*/+;*robo*$^{189}$/+ | 4.4 | 0 | 0 | 0 | 96.6 |
| UAS-*DSLMAP*-RNAi/+; slit$^{2}$/+ | 9 | 0 | 0 | 0 | 95 |
| UAS-*DSLMAP*-RNAi/+; *robo*$^{189}$/+ | 4.5 | 0 | 0 | 0 | 96.6 |
| PrcGal4/+; *robo*$^{189}$/+ | 0 | 0 | 0 | 0 | 100 |
| PrcGal4/+; *slit*$^{2}$/+ | 0 | 0 | 0 | 0 | 100 |
| TinGal4/+; *robo*$^{189}$/+ | 0 | 0 | 0 | 0 | 100 |
| TinGal4/+; *slit*$^{2}$/+ | 0 | 0 | 0 | 0 | 100 |
| *slit*$^{2}$/+; *slit*$^{2}$/+ | 64.91 | 35.4 | 33.9 | 10 | 0 |
| *robo*$^{189}$/+; *robo*$^{189}$/+ | 27.6 | 49.9 | 40.2 | 15.4 | 0 |
| Prc Gal4 UAS-DSLMAP-RNAi/+; *robo*$^{189}$/+ | 16.94 | 10.7 | 0 | 0 | 66.12 |
| Prc Gal4 UAS-DSLMAP-RNAi/+; *slit*$^{2}$/+ | 23 | 12.26 | 0 | 0 | 72.39 |
| TinGal4 UAS-DSLMAP/+; *robo*$^{189}$/+ | 13.6 | 15.3 | 0 | 0 | 70.73 |
| TinGal4 UAS-DSLMAP/+; *slit*$^{2}$/+ | 16.95 | 13.7 | 0 | 0 | 72.33 |

**B.**

| Phenotype / Genotype | P value | | | | |
|---|---|---|---|---|---|
| | Delayed migration | Clustering of cells | Gaps | Twist | |
| Prc Gal4 UAS-DSLMAP-RNAi/+; *robo*$^{189}$/+ | 0.0176 | 0.0002 | 0.0001 | 0.0001 | <0.0001 |
| Prc Gal4 UAS-DSLMAP-RNAi/+; *slit*$^{2}$/+ | 0.0004 | 0.0008 | <0.0001 | 0.0001 | <0.0001 |
| TinGal4 UAS-DSLMAP/+; *robo*$^{189}$/+ | 0.0164 | 0.0003 | <0.0001 | < 0.0001 | <0.0001 |
| TinGal4 UAS-DSLMAP/+; *slit*$^{2}$/+ | 0 .0001 | 0.0023 | 0.0005 | < 0.0001 | <0.0001 |

## Table 9. Quantitative analysis of the phenotypes observed in the PCs in DSLMAP genetic interaction with *slit*$^{2}$ and *robo* $^{189}$ loss of function mutants

In order to quantify the phenotypes observed in the PCs of *DSLMAP* over-expression and *DSLMAP* down-regulated transgenic lines which were crossed to *slit*$^{2}$ and *robo* $^{189}$ loss-of-function mutants, using two different heart drivers: Tinc4Gal4 for myocardial expression, and PrcGAL4 specific for pericardial expression the penetrance for all these crosses was calculated as displayed in (A) The penetrance of the phenotypes observed in PCs. (B) P-value for the phenotypes observed in the PCs. The penetrance for the non-defective embryos was increased in the CBs of all the genetic crosses where in Tin Gal4 UAS-DSLMAP/+;*slit*$^{2}$/+ it reached up to 72.33%, in Tin Gal4-UAS-DSLMAP/+;*robo* $^{189}$ /+ it reached to 70.99%, PrcGal4-UAS-DSLMAP-RNAi/+; *slit*$^{2}$/+ 73.8%, and in Prc Gal4-UAS-DSLMAP-RNAi/+; *robo* $^{189}$ /+ it reached up to 66.12%. The P-value was calculated using the unpaired t-test, and it was highly significant in both the delayed migration defects, and for the penetrance in non-defective embryos.

**A.**

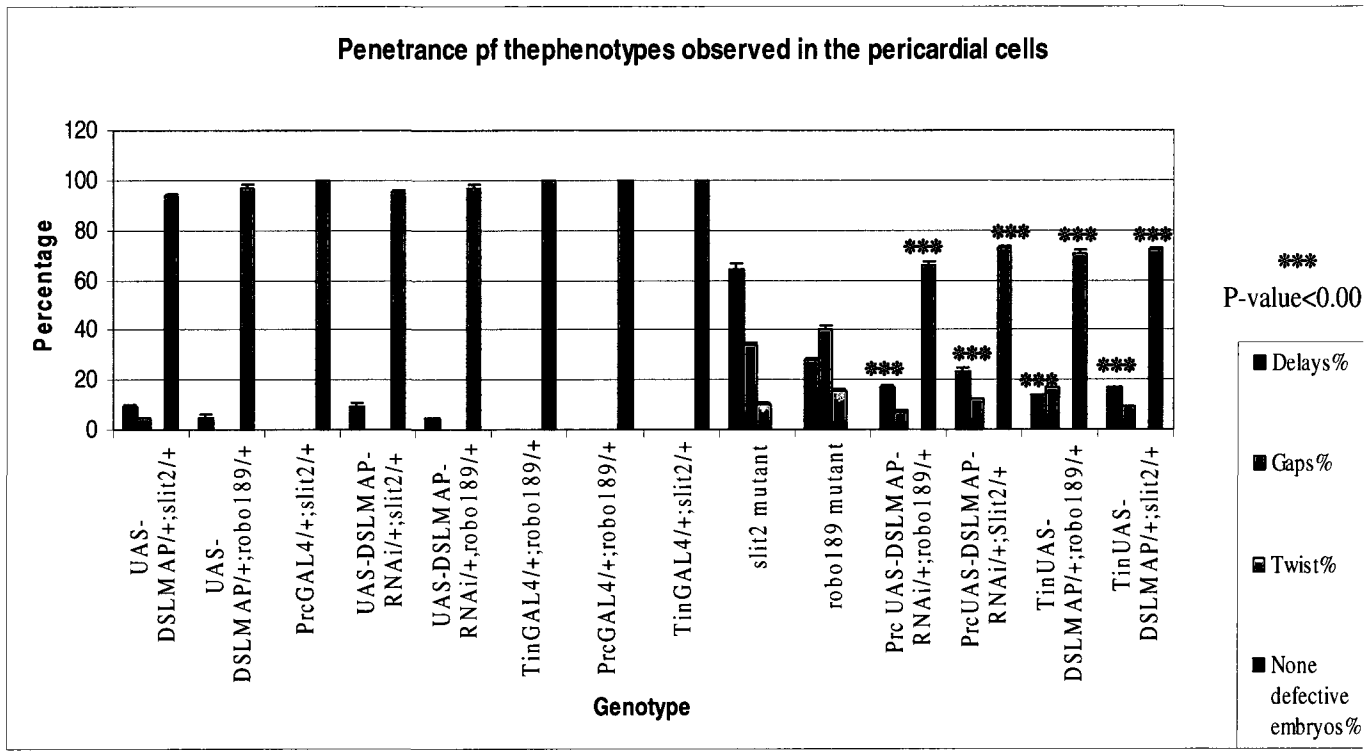


**B.**

| Phenotype / Genotype | P-value | | | |
|---|---|---|---|---|
| | Delayed migration | Gaps | Twist | Non defective embryos |
| Prc Gal4 UAS-DSLMAP-RNAi/+; *robo*$^{189}$/+ | 0.0176 | 0.0002 | 0.0001 | <0.0001 |
| Prc Gal4 UAS-DSLMAP-RNAi/+; *slit*$^{2}$/+ | 0.0004 | 0.0007 | <0.0001 | <0.0001 |
| TinGal4 UAS-DSLMAP/+; *robo*$^{189}$/+ | 0.0164 | 0.0005 | <0.0001 | < 0.0001 |
| TinGal4 UAS-DSLMAP/+; *slit*$^{2}$/+ | 0 .0001 | 0.0003 | 0.0005 | < 0.0001 |

The targeted pericardial down-regulation of *DSLMAP* in *slit*$^{2}$ mutants, led to a reduction in the defects seen in the PCs of *slit*$^{2}$ mutants alone, and the CBs were more organized compared to the CBs in *slit*$^{2}$ mutants alone. In addition, the pericardial expression of UAS-*DSLMAP*-RNAi transgene in *robo*$^{189}$ loss-of-functions mutants, showed a significant reduction in the defects seen in the PCs of *robo*$^{189}$ mutants alone. The CBs also had a significant reduction in the defects, compared to the defects seen in the CBs of *robo*$^{189}$ mutants alone.

Altogether, these data suggest that DSLMAP may play a role in guiding both the CBs and the PCs towards their destination, and it may genetically interact with the Slit/Robo pathway to form an organized heart tube.

# Discussion

*Drosophila* heart development is a complicated process which requires precise cell positioning and adhesion. During this process, the cardioblasts (CBs), and the PCs (PCs) align into rows, and migrate in an organized manner to the dorsal midline of the embryo, where they merge to form a linear heart tube (Rugendorff, 1994; Bodmer and Venkatesh, 1998). The CBs posses a contractile muscle property that pumps the hemolymph in an open circulatory system, and the PCs that flank the CBs on each side (Bodmer and Venkatesh, 1998; Bodmer and Frasch, 1999) may have a role in filtering and detoxifying the hemolymph of the fly (Miller, 1950). The similarity between *Drosophila* heart formation and vertebrate heart assembly at early stages of development (Bodmer and Venkatesh, 1998; Bodmer and Frasch, 1999), has led *Drosophila* to become an excellent model organism for studying the genetic mechanisms of heart tube formation, since most of these mechanisms are regulated by genetic networks that appear to be conserved from fruit flies to vertebrates (Ocorr *et al.,* 2007, Bier and Bodmer, 2007).

SLMAP, a tail anchored membrane protein was found to be expressed early in the mammalian heart (Guzzo *et al.*, 2004), and it may have an important role in cardiac development and function. *D*SLMAP, and its mammalian homologue share 28.6% identity over 721 amino acid residues with the SLMAP3 isoform; a higher percentage identity was noted in the forkhead-associated domain (55.9%) (M'omena Dawood thesis, 2006). Furthermore, it was demonstrated that *D*SLMAP has a ubiquitous expression during embryonic development of the fruit flies. The targeted de-regulation of *DSLMAP* using over-expression, and RNAi protocols in the CNS led to defective neuronal

development in *Drosophila*. In addition *DSLMAP* was also found to genetically interact with the Slit/Robo pathway, to maintain proper neuronal development (Dawood *et al.*, 2007).

The data here shows that *DSLMAP* has a ubiquitous expression including the heart tube, during different stages of embryonic development as illustrated by whole mount *in situ* hybridization. Further, double labeling with anti-*D*mef2 -which is specifically expressed in the CBs and the somatic muscles- and *in situ* hybridization with *DSLMAP* mRNA probes at different developmental stages, indicates that DSLMAP is expressed in CBs population of *Drosophila* heart from the beginning of heart tube formation. This expression pattern is similar to that observed for its mammalian homologue SLMAP, which was also expressed at early stages of development in cardiac tissue (Wigle *et al.*, 1997).

Changing the expression of *DSLMAP* in either CBs or PCs resulted in defects in heart tube development. Two different heart drivers were used; TinGAL4, PrcGAL4 to de-regulate *DSLMAP* specifically in CBs or PCs. Similar defects in heart tube development were noted when DSLMAP was de-regulated, these defects noted at different stages of heart development include: delayed cell migration, clustering of cells, gaps, and blisters in the midline alignment of cardiac cells. Instead of migrating dorsally to form a linear heart tube they either went inward, or outward, or aggregated together. These observations suggest that cardiac cells had undergone changes in cell-cell interactions, and become less adhered to each other, and perhaps had lost their ability for migration and guidance. The main defect was delayed cell migration associated with a delay in the CB cell rows as well as the PC rows. This would suggest that these two cell types may

interact with each other, and that both of them may require regulated levels of *DSLMAP* to maintain normal development of heart tube formation, and perhaps guiding these cells towards their final destination.

In wild-type embryos, there are normally 104 CBs that form two rows at the dorsal midline. However, in *DSLMAP* down-regulated embryos- at stage17, an average of (97 ±1.5) ($n$ = 18) CBs were noted. This change in CB numbers was not observed at stage 13, since both *DSLMAP* down-regulated embryos, and wild type embryos have the same number of cells. This suggests that this change in cell numbers occurs during development after stage 13. This may be a result of either cell loss due to cell death or perhaps changes in cell-cell interaction resulting in alterations in cell aggregation or cell fusion.

Spectrin is a protein that links the plasma membrane to the cytoskeleton. In *Drosophila* α-Spectrin is localized to the basal-lateral surface of the CBs and plays an important role in the determination of cell shape (Lee *et al.*, 1993). The visualization of the expression of α-spectrin in the cell membrane that surrounds the CBs showed that these cells had undergone a change in their shape during de-regulation of *DSLMAP.* In addition, in *DSLMAP* over-expression the cell membrane organization of CBs indicates that they have actually merged with adjacent cell membranes, and some of these cells were aggregated or fused together. Further, the CBs were seem to be fused to each other at early stage 14, compared to the wild type were the CBs fuse in to a linear heart tube at the dorsal midline by stage 17 (Bodmer and Venkatesh,1998). This suggests a role for DSLMAP in the CBs positioning, and perhaps adhesion during heart tube formation.

It is notable that over expression of the mammalian homologue of DSLMAP was associated with defective myotube development, due to reduced myoblast fusion of C2C12 myoblasts (Guzzo *et al.*, 2004, B). Furthermore, the membrane targeting or the FHA domain in SLMAP was not found to impact the effects on myotube development or myoblast fusion. The regulated levels and the temporal induction of endogenous SLMAP isoforms were concluded to be critical for muscle development, While, protein-interaction studies demonstrated that SLMAP can interact with it self, and can form homodimers *in vivo* (Guzzo *et al.*, 2004, A). Structural analysis of *DSLMAP* shows that it possesses a coiled-coil region, a FHA domain, and a TM domain. The coiled-coil regions are implicated in protein-protein interactions (Blazek *et al.*, 2005). In addition, the coiled-coil motif has also been demonstrated to be involved in intra-molecular interactions with the FHA domain (Lee *et al.*, 2004). Accordingly, the de-regulation of *DSLMAP* may affect the protein-protein interactions mediated by the coiled-coil region, and the intermolecular interactions mediated through the FHA domain leading to defective heart tube formation.

To address whether *DSLMAP* interacts genetically with the Slit/Robo pathway, the phenotypes generated by *DSLMAP* over-expression, and down-regulation were compared with those of *Slit* and *Robo* de-regulation in a cardiac specific manner. The data revealed that over-expression of *DSLMAP* has the same phenotypes as those observed in *Slit* over-expression, while down-regulation of *DSLMAP* has the same phenotypes as those of *Robo* down-regulation. These phenotypes were observed at different stages of embryonic heart development. In addition, Slit and Robo localization had changed, where Slit and Robo were not localized in the lumen between the CBs when *DSLMAP* expression was

altered. This indicates that de-regulated *DSLMAP* expression may result in Slit and Robo mislocalization in the cytoplasm, and prevent their proper targeting or secretion.

The expression of *DSLMAP* and Slit in the CBs implies that these proteins could interact with each other, while both DSLAMP and Robo are expressed in CBs and PCs and thus these proteins may interact in these cell types (Li *et al.*, 2005; Macmullin and Jacob, 2006).

Genetic interactions of DSLMAP with UAS-Slit, and UAS-Robo-RNAi transgenes revealed that the over-expression of DSLMAP in the CBs of Robo down-regulated embryos, reduced the number of defective embryos, and less embryos showed delayed migration defects in the CBs. Similar data was obtained when DSLMAP was over-expressed in the CBs of UAS-Slit transgene. Further, down-regulation of DSLMAP in the PCs of UAS-Robo-RNAi transgene, increased the number of non defective embryos, and reduced migration defects. Similar data was obtained in targeted down-regulation of DSLMAP in the PCs of UAS-Slit transgene. Altogether, these data suggest that DSLMAP may have a role in guiding cardiac cells migration the same as Slit and Robo, and may genetically interact with them to maintain normal heart tube development.

Furthermore, $slit^{2}$ and $robo^{189}$ loss of function mutants showed defects in cardiac cells alignment, and migration, which were observed at various stages throughout heart development. These defects include: delayed cell migration, large gaps, blisters in the midline alignment of cardiac cells, and clustering of cells. These data suggest a continuous requirement for regulated levels of Slit and Robo to maintain a normal cardiac cell alignment and migration, much in the same way as the requirement for DSLMAP expression. Since the targeted *DSLMAP* expression within the CBs, and the PCs was

found to partially reverse the heart tube defects observed in the *slit*$^{2}$ and *robo*$^{189}$ mutants. It is conceivable that DSLMAP may interact with the Slit/Robo pathway during *Drosophila* heart development.

Structural analysis of Slit and Robo showed that Slit is composed of four LRR domain (D1-D4) at the N-terminus, and six EGF repeats, then a laminin G-like domain, and a cysteine knot at the C-terminus; while Robo receptor consist of five immunoglobulin (Ig) repeats, and three fibronectin type III repeats, and polyproline stretch, the D2 of the LRR domain in Slit binds to the Ig-1 domain in Robo, and this binding will initiate the Slit/Robo signal (Chen *et al.*, 2001; Morlot, 2007, Hohenester, 2008).

Slit-Robo signaling was found to require Heparan sulfate (HS) which consist of a variably sulfated repeating disaccharide unit, (Lee and Chien, 2004). The disaccharide units in HS are connected to membrane associated proteins or secreted proteins to form the HS proteoglycans (HSPGs) (Hohenester, 2008). In *Drosophila* HSPG syndecan was found to control both the efficiency and distribution of Slit (Johnson *et al.*, 2004). While in the mammals the HSPG glypican-1 was able to recognize the cleavage products of Slit2 and it act as a receptor for the human Slit2 (Ronca et al., 2001). Studies suggest that HSPGs binds to D2 LRR in Slit and to the Ig1-Ig2 in Robo and this binding is required for the slit-Robo signaling (Hohenester, 2008)

It is suggested that the Slit-Robo signaling is transmitted through the cell membrane by the use of the changes in the oligomeric status of Robo, because Robo ectodomains are similar to those of cell adhesion molecules (CAMs), and Robos in fact mediate homophilic binding (Hivert, 2002). Abelson tyrosine kinase (Abl) is a downstream target of Robo signaling (Bashaw *et al.*, 2000), and it was found that it has a significant role in

controlling the interactions of N-cadherin with Robo (Rhee et al., 2002). Abl interacts with several effectors one of which is capulet (CAP) and CLASP that plays a role in controlling cytoskeletal dynamics (Chédotal, 2008) (Fig. 37). It is thought that Abl is not responsible for all the activity downstream of Robo (Garbe et al., 2004), but there is a number of adaptors that bind to the cytosolic domain of Robo and their activity in some way is controlled by Slit (Hohenester, 2008). Further, it was found that the Slit–Robo Rho GTPase-activating protein 1(srGAP1) binds to the proline-rich CC3 motif of Robo 1 in the mammalian system. The Slit induced srGAP1-Robo1 interaction results in inactivated cell division via Cdc42 (Wong *et al.*, 2001). In addition there is adaptor protein Dreadlocks Dock/Nck that binds to CC3 and also to CC2. Slit stimulation recruits Son of sevenless (Sos), and the p21-activated serine-threonine kinase (pak), cause an increase activity in the Rho GTPase Rac which will lead to axon replusion (Fan *et al.*, 2003, Yang and Bashaw, 2006) (Fig. 37).

Previous studies in our lab had shown that DSLMAP genetically interacts with the Robo/Rac pathway in *Drosophila* CNS, and DSLMAP may play a role in axonal guidance (Dawood *et al.*, 2007). DSLMAP possess a coiled-coil region that is involved in protein-protein interactions which appears similar in function to that of the Lucien Rich Repeat found in Slit.

While it seems clear that Slit and Robo have a significant role in the development of the *Drosophila* heart and CNS, and in guiding cell alignment and adhesion (Li *et al.*, 2005,) question of: how DSLMAP may interact with the Slit/Robo pathway needs to be addressed. Since our data implies that there might be genetic interactions between

## Figure 37. Slit and Robo signaling and axon repulsion

HSPG binds to Slit D2 and Ig1-Ig2 of Robo receptor, and is required for the Slit and Robo signalling, which is transmitted through the cell membrane, where the proline-rich motif downstream the Robo receptor interacts with different adaptor proteins; among these proteins Dock, which binds to both CC2, and CC3, and mediate the action of both Sos and PAK which in turn affect the Rac GTPase, and Pack will lead to actin filament reorganization which causes the repulsion signal. Abl also binds to CC3 in addition to CC1 and mediate the action of several effectors two of which were recognized, which are CAP that inhibit actin polymerization and CLASP that inhibit microtubule polymerization. (Adapted and modified Chédotal, 2008, Hohenester, 2008).

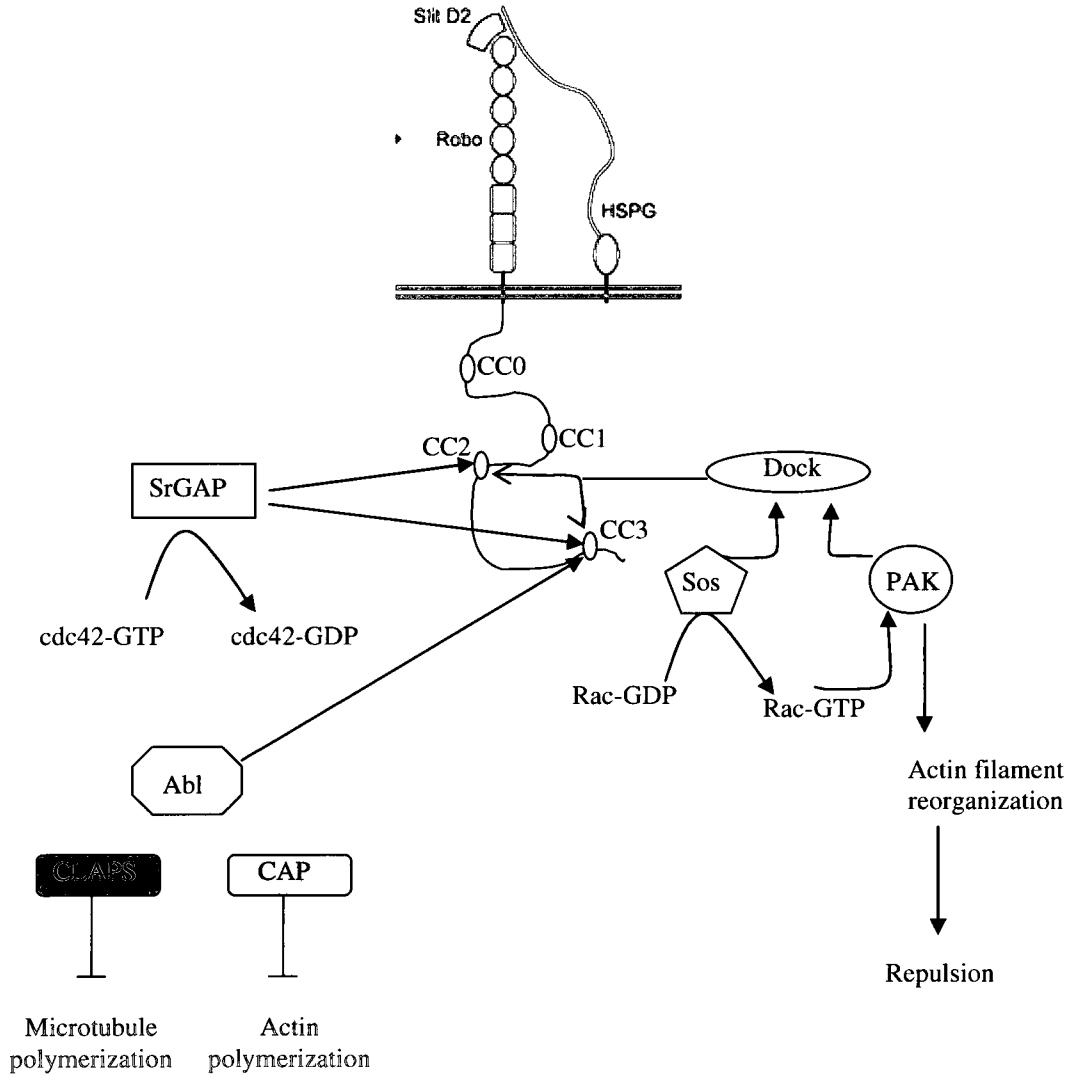
Slit D2
Robo
HSPG
CC0
CC1
CC2
CC3
SrGAP
Dock
Sos
PAK
cdc42-GTP
cdc42-GDP
Rac-GDP
Rac-GTP
Abl
Actin filament reorganization
CLAPS
CAP
Repulsion
Microtubule polymerization
Actin polymerization

DSLMAP and both Slit/Robo pathway, and based on the structural features of DSLMAP we propose that DSLMAP may work as an adaptor protein, where the TM domain may bind to HSPG which binds to Slit D2 and to Robo Ig1-Ig2, since the disaccraides units in HS are connected to membrane associated proteins or to secreted proteins (Hohenester, 2008), or through binding the coiled-coil region with one of proline-rich motif since the Slit-Robo signal is transmitted through theses motifs to other adapter protein like Dock. The FHA which is phosphopeptide signalling domain could interact with the adaptor protein Dock) which is affected by Rac GTPase that regulates PAK and Sos via Dock which binds to both CC2 and CC3 down stream Robo receptor (Fig. 38).

In summary, *D*SLMAP is a novel component expressed during heart tube development in CBs and PCs in *Drosophila*. Further, defects in heart tube development during the targeted deregulation of DSLMAP expression in the CBs or pericardial cell strongly implies a critical role for this molecule in normal heart development. The potential genetic interaction with the slit/robo pathway which is known to regulate cell guidance, migration, and adhesion suggests that DSLMAP may impact this pathway via its unique structural features encompassing membrane targeting, coiled-regions and the FHA domain. Further studies on the molecular interactions of DSLMAP will reveal weather it can signal downstream of the slit/Robo complex. .

**Figure 38. Putative molecular interaction of DSLMAP with the Slit/Robo pathway**

Schematic representation shows suggested molecular interaction of DSLMAP with Slit, and Robo during their signal transduction through the cell membrane. DSLMAP may interact with both Slit and Robo by either binding the Tm domain at the C-terminus with HSPG, which also binds to Slit D2 and to Ig1-Ig2 of Robo, or via the coiled-coil region which may bind to one of the proline-rich motif, or by affecting the Rac pathway via the adaptor protein Dock which in turn binds to CC2 and CC3 downstream of the Robo, and mediate the affect of both Sos and PAK on filament reorganization which lead to repulsion.

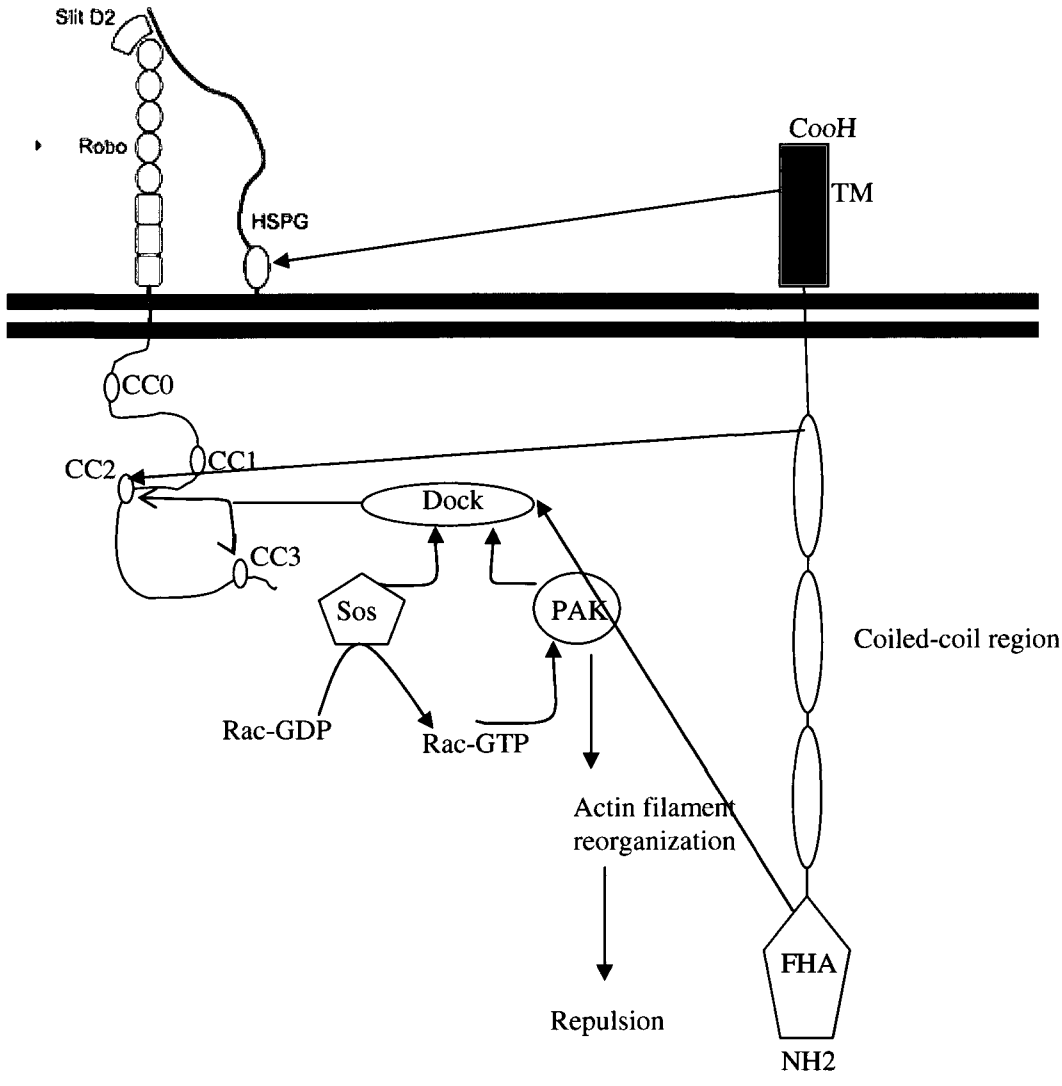
Slit D2
Robo
HSPG
CooH
TM
CC0
CC1
CC2
CC3
Dock
Sos
PAK
Coiled-coil region
Rac-GDP
Rac-GTP
Actin filament
reorganization
Repulsion
FHA
NH2

DSLMAP

# References


Anderson, R. H., Wilkinson, J. L., and Becker, A. E. 1978. The bulbus cordis—A misunderstood region of the developing human heart: Its significance to the classification of congenital cardiac malformations. *In* "Birth Defects: Original Article Series," Vol.14, No. 7, pp. 1–28.

Ashe, H.L. 2005. BMP signalling synergy and feedback create a step gradient. *Curr. Biol.* 15, R375–R377.

Azpiazu N and Frasch M.1993. *tinman* and *bagpipe*: two homeobox genes that determine cell fates in the dorsal mesoderm of *Drosophila*. *Genes Dev* 7: 1325-1340.

Byers, JT., Guzzo RM, Salih M, Moore ED, and Tuana BS. 2009. Hydrophobic profiles of the tail anchors in SLMAP dictate subcellular targeting., *BMC Cell Biology* 10:48

Berg, C. A. and Eisenberg, L. M. .1999. WNT11 promotes cardiac tissue formation of early mesoderm. *Dev. Dyn.* 216,45 -58.

Bodmer R. 1993. The gene *tinman* is required for specification of the heart and visceral muscles in Drosophila. *Development.*; 118:1301–1306.

Bodmer R. 1995. Heart development in *Drosophila* and its relationship to vertebrate systems.*Trends in Cardiovascular Medicine.*;5:21–27.

Bodmer R. and Venkatesh, T.V., 1998. Heart development in *Drosophila* and vertebrates: conservation of molecular mechanisms. *Dev. Genet.* 22, pp. 1–4.

Bodmer R. and Frasch M. 1999. Genetic determination of the *Drosophila* heart development.*Heart Development*, Academic Press, New York, pp. 65–90.

Bodmer, R.; Wessells, RJ. Johnson, EC.; Dowse, H. 2005. Heart development and function. *Comprehensive Molecular Insect Science.* 1–7. Vol.2. Elsevier; pp. 199–250.

Bolker, J. A. 1995. Model systems in developmental biology, *Bio assay* 17(5), 451-455.

Bour, B.A. O'Brien, M.A. Lockwood, W.L. Goldstein, E.S. Bodmer, R. Taghert, P.H. Abmayr, S.M. Nguyen, H.T. 1995. *Drosophila* MEF2, a transcription factor that is essential for myogenesis. *Genes Dev.* 9, pp. 730–741

Brand, Perrimon. 1993. Targeted gene expression as a means of altering cell fates and generating dominant phenotypes. *Development.* Jun; 118(2):401-15.

Chien KR, Olson EN. 2002. Converging pathways and principles in heart development and disease: *Cell.*2:153–62

Chen, J. N. and Fishman, M. C. 1996. Zebrafish *tinman* homolog demarcates the heart field and initiates myocardial differentiation. *Development* 122, 3809-3816.

Chi, N.C., Shaw, R.M., De Val, S., Kang, G., Jan, L.Y., Black, B.L., and Stainier, D.Y.R. 2008. Foxn4 directly regulates *tbx2b* expression and atrioventricular canal formation. *Genes & Dev.* 10.1101

Clancy DJ, Gems D, Harshman LG, Oldham S, Stocker H, Hafen E. 2001. Extension of life-span by loss of CHICO, a *Drosophila* insulin receptor substrate protein. *Science.*; 5514:104–106

Cleaver, O. B., Patterson, K. D. and Krieg, P. A. 1996. Overexpression of the *tinman*-related genes *XNkx-2.5* and *XNkx-2.3* in *Xenopus* embryos results in myocardial hyperplasia. *Development* 122, 3549-3556.

Cripps RM and Olson EN. 2002. Control of cardiac development by an evolutionarily conserved transcriptional network. *Dev Biol.* 1:14–28

Chisholm and M Tessier-Lavigne. 1999. Conservation and divergence of axon guidance mechanisms *Curr. Opin. Neurobiol.* 9; pp. 603–615.
Dawood, M., Sonnenfeld, S., Tuana, BS. 2007. The *Drosophila* sarcolemmal membrane associated protein (*D*SLMAP) cooperates with Robo and *D*Rac1 to regulates repulsive CNS axon guidance. Abstract. The genetic society of Canada 38, 2, pp42

Dale.L, Howes.M Prices G. and Smoth J.C.1992. Bone morphogenetic protein 4: a ventralizing factor in early Xenopus development. *Development.* 115, 573–585)

Donovan, J., Kordylewska, A., Jan, Y. N. & Utset, M. F. 2002. Tetralogy of Fallot and other congenital heart defects in *Hey2* mutant mice. *Curr. Biol.* 12, 1605–1610.

Duffy, J. B. 2002. Gal4 system in Drosophila a fly genetics swiss army knife. *Genesis;* 34:1-15.

Durocher D. and Nemer M. 1998. Combinatorial interactions regulating cardiac transcription. *Dev Genet* 22: 250-2

Eisenberg, L. M. and Eisenberg, C. A. 2006. Wnt signal transduction and the formation of the myocardium. *Dev. Biol.* 293,305 -315

Cohen.E.D. and Morrisey E. 2008. a house with many rooms how theheart get it chamberes with foxn4.*Genes and Devel.* 22: 706-710

Hohenester Erhard. 2008. Structural insight into Slit–Robo signalling. *Biochemical Society Transactions* 36, (251–256)

Fernandis, A. Z., Ganju, R. K. 2001. Slit: a roadblock for chemotaxis *Sci. STKE* 91

Frasch, M. 1995. Induction of visceral and cardiac mesoderm by ectodermal Dpp in the early Drosophila embryo. *Nature374*, 464–467

Fischer, A., Schumacher, N., Maier, M., Sendtner, M.& Gessler, M. 2004. The Notch target genes *Hey1* and *Hey2* are required for embryonic vascular development. *Genes Dev.* 18, 901–911

Fleming RJ. 1998. Structural conservation of Notch receptors and ligands.*Semin Cell Dev Biol.*; 9:599–607

Flannery, C. M. 1997. Models in biology, American Biology, 59(Apr), 244-248.

Francois V, Bier E. 1995. Xenopus chordin and Drosophila short gastrulation genes encode homologous proteins functioning in dorsal ventral axis formation. *Cell,* 80: 19-20.

Gessler, M. Knobeloch, K. P., Helisch, A., Schumacher, A., Rohde, E., Fischer, A., Leimeister,C. 2002. Mouse gridlock: no aortic coarctation or deficiency, but fatal cardiacdefects in *Hey2–/–* mice. *Curr. Biol.* 12, 1601–1604

Gisselbrecht, S., Skeath, J. B., Doe, C. Q. and Michelson, A. M. 1996. Heartless encodes a fibroblast growth factor receptor (DFR1/DFGF-R2) involved in the directional migration of early mesodermal cells in the *Drosophila* embryo. *Genes Dev.* 10, 3003-3017.

Guzzo RM, Sevinc S, Salih M, and Tuana BS. 2004. A novel isoform of sarcolemmal membrane associated protein (SLMAP) is a component of the microtubule organizing centre. *Cell Sci* 117: 2271–2281.

Guzzo RM, Wigle JT, Salih M, Moore ED, and Tuana BS. 2004. The tail-regulated expression and temporal induction of the tail-anchored membrane protein SLMAP is critical for myoblast fusion. *Biochem* 381:599–608.

Harrelson, Z., Kelly, R.G., Goldin, S.N., Gibson-Brown, J.J., Bollag, R.J., Silver, L.M., and Papaioannou, V.E. 2004.Tbx2 is essential for patterning the atrioventricular canaland for morphogenesis of the outflow tract during heart development. *Development,* 131; 5041–5052.

Halfon,M.S., Carmena, A. S. Gisselbrecht, C.M. Sackerson, F. Jimenez and M.K. Baylies 2000. Ras pathway specificity is determined by the integration of multiple signal-activated and tissue-restricted transcription factors, *Cell* 103 pp. 63–74.

http://www.pitt.edu /~biohome/Dept/Frame/drosophila.htm.

http://genome.wellcome ac.uk/ doc_WTD020807.htm

http/:www.fly move .com

http://www.sciencedaily.com/releases/2008

Han Z, Bodmer R. 2003. Myogenic cells fates are antagonized by Notch only inasymmetric lineages of the *Drosophila* heart, with or without cell division. *Development*;130:3039–51.

Iso, T., Kedes, L. & Hamamori. Y. 2003. HES and HERP families: multiple effectors of the Notch signaling pathway. *Cell. Physiol*

Iso, T., Chung, G., Hamamori, Y. & Kedes, L. 2002. HERP1 is a cell type-specific primary target of Notch. *J. Biol.Chem.* 277, 6598–6607.

Jagla, K., Frasch, M., Jagla, T., Dretzen, G., Bellard, F., and Bellard, M. 1997. Ladybird, a new component of the cardiogenic pathway in Drosophila required for diversification of heart precursors. *Development,* 3471–34

Kokubo, H., Miyagawa-Tomita, S., Nakazawa, M., Saga, Y. & Johnson, R. L. 2005. Mouse *Hesr1* and *Hesr2* genes are redundantly required to mediate Notch signaling in the developing cardiovascular system. *Dev. Biol.* 278, 301–309.

Kramer, C. D. 1986. The classroom animal - fruit flies. *scince and children*, 30-33

Kramer, J.M., Staveley, B.E. 2003. GAL4 causes developmental defects and apoptosis when expressed in the developing eye of *Drosophila melanogaster. Genet Mol Res.* 2(1):43-47.

Kokubo, H., Miyagawa-Tomita, S., Tomimatsu, H., Nakazawa, M., Saga, Y., Johnson, R.L. 2004. Targeted disruption of *hesr2* resultsin atrioventricular valve anomalies that lead to heartdysfunction..*Circ. Res.* 95, 540–547.

Knirr S, Frasch M. 2001. Molecular integration of inductive and mesodermintrinsicinputs governs *even-skipped* enhancer activity in a subset of pericardial and dorsal muscle progenitors. *Dev Biol*; 238:13–26.

Komuro, I. and Izumo, S. 1993. Csx: A murine homeobox-containing gene specifically expressed in the developing heart. *Proc. Natl. Acad. Sci. USA*; 90, 8145-8149.

Karen Ocorr, Takeshi Akasaka, and Rolf Bodmer. 2007. Age-related Cardiac Disease Model of *Drosophila. Dev.*, 128 (1) 112-116.

Kokubo, H., Lun, Y. & Johnson, R. L. 1999. Identification and expression of a novel family of bHLH cDNAsrelated to *Drosophila* Hairy and Enhancer of Split. *Biochem. Biophys. Res. Commun.* 260,459–465

Lee, J.K., R.S. Coyne, R.R. Dubreuil, L.S. Goldstein, and D. Branton. 1993.Cell shapeand interaction defects in a-spectrin mutants of *Drosophila melanogaster. Cell Biol.* 123:1797–1809.

Lavery.D, Martin.J, Turnbull.Y, and Hoppler .S. 2008. Wnt6 signaling regulates heart muscle development during organogenesis. *Dev.Biol* 15; 323(2): 177–188.

Langdon,T., Hayward, P., Brennan, K., Phil, P., Vincent, Z., Adrian, F., Tina., Balayo, Marteinez, A.A. 2006. Notch receptor encodes two structurally separable functions in *Drosophila.Developmental dynamics* vol. 235, n°4, pp. 998-1013.

Lanot, R., Zachary, D., Holder, F. and Meister, M. 2001. Postembryonic hematopoiesis in *Drosophila.Dev. Biol.* 230,243 -257.

Lawrence P.A., Bodmer R. and Vincent J.P..1995. Segmental patterning of heart precursors in *Drosophila, Development* 121 pp. 4303–4308.

Lee H.H. and Frasch M.. 2000.Wingless effects mesoderm patterning and ectoderm segmentation events via induction of its downstream target *sloppy paired, Development* 127 pp. 5497–5508.

Lints, T. J., Parsons, L. M., Hartley, L., Lyons, I. and Harvey, R. P. 1993. *Nkx-2.5*: a novel murine homeobox gene expressed in early heart progenitor cells and their myogenic descendants. *Development* 119, 419-431.

Liberatore C, Searcy-Schrick R, Vincent E, Yutzey K. 2002. Nkx-2.5 gene induction in mice is mediated by a Smad consensus regulatory region. *Dev Biol*; 244:243–256.104.

Lien C, McAnally J, Richardson J, Olson E. 2002.Cardiacspecific activity ofan Nkx2–5 enhancer requires an evolutionarily conserved Smad binding site. *Dev Biol.*; 244:257–266.

Lyons, I., Parsons, L. M., Hartley, L., Li, R., Andrews, J. E., Tobb, L. And Harvey, R. P. 1995. Myogenic and morphogenetic defects in the heart tubes of murine embryos lacking the homeo box gene *Nkx2-5. Genes Dev.*9, 1654-1666.

Murakami, M., Zhuang W.Z., Moodien L.K. 2008. Michael Simons, Fibroblast Growth Factor Inhibition in Mice Impair Cardiac Function and Promote Development of Heart Failure*Circulation*; 118:S_484.

Molina M.R. and Cripps R.M.. 2001. Ostia, the inflow tracts of the *Drosophila* heart, develop from a genetically distinct subset of cardial cells, *Development* 109, pp. 51–59.

Marvin MJ, Di Rocco G, Gardiner A, Bush SM, Lassar AB. 2001.Inhibition of Wnt activity induces heart formation from posterior mesoderm. *Genes Dev.* 15:316–327.113.

Miller.A 1950.The Internal Anatomy and Histology of the Imago of *Drosophila* Melanogaste- *Biology of Drosophila*; pp 1-4.

M'omena A.Dawood. 2006. Studies on the molecular and functional analysis of tail anchored membrane associated protein (SLMAP). Univesity of Ottawa.

Moorman, A. F. M., de Boer, P. A. J., Ruijter, J. M., Hagoort, J.,Franco, D., and Lamers, W. H. 1999. Radio-isotopic in situ hybridization on tissue sections: Practical aspects and quantification.*In* "Methods in Molecular Biology," Vol 137, "Developmental Bi ology Protocols" (R. S. Tuan and C. W. Lo, Eds.), Vol.III, Chap. 11, pp. 97–115

Mumm JS, Kopan R. 2000. Notch signaling: from the outside in. *Dev* Bil;228:151–65.

Nader, M., Westendorp, B., Leenen, F HH., Tuana BS. 2008. SLMAP overexpression in mouse heart remodels subcellular membranes involved in E-C couplinge. *FASEB.* 22:386.6.

Nakagawa, O.,McFadden DG, Nakagawa M, Yanagisawa H, Hu T, Srivastava D, Olson EN. 2000. Members of the HRT family of basic helix–loop–helix proteins act as transcriptionalrepressors downstream of Notch signaling. *Proc. NatlAcad. Sci. USA* 97, 13655–13660.

Pandur, P., Lasche, M., Eisenberg, L. M. and Kuhl, M. 2002. Wnt-11 activation of a non-canonical Wnt signalling pathway is required for cardiogenesis. *Nature* 418,636 -641.

Prall OW, Elliott DA, Harvey RP. . 2002. Developmental paradigms in heart disease: insights *tinman. Ann Med*; 3:148–15

Park, M. Wu, X Golden,. K. Axelrod J.D. and Bodmer R.. 1996. The Wingless signaling pathway is directly involved in *Drosophila* heart development, *Dev Biol* 177

Park, M. Venkatesh T.V. and Bodmer R.. 1998. Dual role for the *zeste-white3/shaggy*-encoded kinase in mesoderm and heart development of *Drosophila*, *Dev Genet* 22 pp. 201–21104–116.

Pike, B.L., A., and heierhost, J. 2001. role of the N-terminal forkhead associated domain in the cell cycle *Biol.Chem.*276 (17), 14019-14026.

Park, M.,Wu, X., Golden, K., Axelrod, J. D., and Bodmer R.1996. The wingless signaling pathway is directly involved in Drosophila heart development. *Dev. Biol* 104–116.

Redkar A, Montgomery M, Litvin J. 2001. Fate map of early avian cardiac progenitor cells. *Development*; 128:2269–2279.

Reiter J, Verkade H, Stainier D.2001.mp2b and Oep promote early myocardialdifferentiation through their regulation of gata5. *Dev Biol.* 234:330–338.

Rugendorff, A., Younossi-Hartenstein, A. and Hartenstein, V. 1994. Embryonic origin and differentiation of the *Drosophila* heart. *Dev. Biol.* 203,266 -280.

Rosenblueth, A., & Wiener, N. 1945. The role of models in science. *Philosophy ofscince,* 12, 316-321.

Reifers F, Walsh E, Leger S, Stainier D, Brand M. 2000. Induction and differentiation of the zebrafish heart requires fibroblast growth factor 8*(fgf8/acerebellar).* *Development.*;127:2549–2561.

Ranganayakulu, G., Zhao, B., Dokidis, A., Molkentin, J.D., Olson, E.N., Schulz, R.A. 1995. A series of mutations in the D-MEF2 transcription factor reveal multiple functions in larval and adult myogenesis in Drosophila. Dev .Biol.171 (1): 169—181.

Rizki T.M. 1978. The circulatory system and associated cells and tissues. *The Genetics and Biology of Drosophila* vol. 2, pp. 397–452.

Rothberg, J.M., Jacobs, J.R., Goodman, C.S., Artavanis-Tsakonas, S., 1990. Slit: an extracellular protein necessary for development of midline gliaand commissural axon pathways contains both EGF and LRR domains. *Genes Dev.* 4, 2169–2187.

Sofer, W., & Tompkins, L. 1994. Genetics in the classroom - *drosophila* genetics in the classroom.Genetics, 136, 417-422.

J M Rothberg, J R Jacobs, C S Goodman, and S Artavanis-Tsakonas.1990. slit: an extracellular protein necessary for development of midline glia and commissural axon pathways contains both EGF and LRR domains. *Genes and Dev.* 4:2169-2187, ISSN 0890-9369.

Sakata, Y., Kamei, CN., Nakagami, H., Bronson, R., Liao, Jk., Chin, MT. 2002. entricular septal defect and cardiomyopathy in mice lacking the transcription factor CHF1/Hey2. *Proc. Natl Acad. Sci. USA* 99,16197–16202

Santiago-Martínez , E. , Soplop N.H., and Kramer S.G. . 2006 . Lateral positioning at the dorsal midline: Slit and Roundabout receptors guide *Drosophila* heart cell migration. *Proc. Natl. Acad. Sci. USA* . 103 : 12441 – 12446

Santiago-Martínez , E. , Soplop N.H. ,Patel.R and . Kramer S.G. 2008. Repulsion by Slit and Roundabout prevents Shotgun/E-cadherin – mediated cell adhesion during *Drosophila* heart tube lumen formation. *Cell Biol.* 182(2): 241–248.

Schultheiss TM, Burch JB, Lassar AB. 1997. role for bone morphogenetic proteins in the induction of cardiac myogenesis. *Genes Dev.*; 11:451–462.

Shinsuke Yuasa1, Keiichi Fukuda. 2008 Multiple roles for BMP signaling incardiac development, *Cell Dev* 10.1016

Schneider VA, Mercola M. 2001.Wnt antagonism initiates cardiogenesis in *Xenopus laevis*. *Genes Dev.*; 15:304–315.

Shishido, E., Higashijima, S., Emori, Y. and Saigo, K. 1993. Two FGF receptor homologues of *Drosophila* – one is expressed in mesodermal primordium in early embryos. *Development* 117, 751-761.

Srivastava D. 2006. Making or breaking the heart: from lineage determination tomorphogenesis, *Cell;* 6:1037–1048.

Sorrentino RP, Gajewski KM, Schulz RA. 2005.GATA factors in *Drosophila* heart and blood cell development,. Semin *Cell Dev Biol*; 16:107–16.

Terami, H., Hidaka, K., Katsumata, T., Iio, A. and Morisaki, T. 2001. Wnt11 facilitates embryonic stem cell differentiation to Nkx2.5-positive cardiomyocytes. *Biochem. Biophys. Res. Commun.* 325,968 -975.

Tonissen, K. F., Drysdale, T. A., Lints, T. J., Harvey, R. P. and Krieg, P. A. 1994. *XNkx-2.5*, a *Xenopus* gene related to *Nkx-2.5* and *tinman*: evidence for a conserved role in cardiac development. *Dev. Biol.* 162, 325-328.

Xu X, Yin Z, Hudson JB, Ferguson EL, Frasch M. 1998. Smad proteins act in combination with synergistic and antagonistic regulators to target Dpp responses to the Drosophila mesoderm. Genes Dev;12:2354–70.

Tao, Y, Schulz, R. A. 2007. Seminars in Cell & Developmental Biology. Heart development in *Drosophila* 3–15.

Yin Z, Frasch M. 1998. Regulation and function of *tinman* during dorsal mesoderm induction and heart specification in *Drosophila*. *Dev Genet.*;22:187–200.

Yin Z, Hudson JB, Ferguson EL, Frasch M. 1998. Smad proteins act in combination with synergistic and antagonistic regulators to target Dpp responses to the Drosophila mesoderm. *Genes Dev*;12:2354–70.

YIin.z Xu XL, Frasch M. 1997. Regulation of the Twist target gene tinman by modular cis-regulatory elements during early mesoderm development.*Dev*;124:4971–82.

Ward EJ, Skeath JB. 2000. Characterization of a novel subset of cardiac cells and their progenitors in the *Drosophila* embryo. *Development*.;127:4959–69.

Wigle, J.t.1997.Molecular cloning, characterization and expression of Tail-anchored membrane protein s from the myocardium *Ph.D.thesis* .University of Ottawa .pp.83n-87.

Wilson, R., Vogelsang, E., and Leptin, M. 2005. FGF signalling and the mechanism of mesoderm spreading in *Drosophila* embryos.,*Development* 132, 491-501.

Wigglesworth V.B. 1984, Insect Physiology, Chapman and Hall, London.

Walters M, Wayman G, Christian J. Bone. 2001. morphogenetic protein function is required for terminal differentiation of the heart but not for early expression of cardiac marker genes. *Mech Dev.*;100:263–273.

Wattenberg B., Lithgow. 2001. T. Targeting of C-terminal (tail)-anchored proteins: understanding how cytoplasmic activities are anchored to intracellular membranes. *Traffic.*; 2:66–71.

Zhao, L., Ranganayakulu, G., Paterson, B.M., Schultz, R.A. and Olson E.N.1995. Requirement of MADS domain transcription factor D-MEF2 for muscle formation in *Drosophila*. *Science* 267, pp. 688–693.

Zaffran, S., and Frasch, M. 2002. Early Signals in Cardiac Development. 2002. *Circulation*; 91:457.